

Measurement of the $t\bar{t}Z^-$ and $t\bar{t}W^-$ production cross sections in multilepton final states using 3.2 fb⁻¹ of pp collisions at $\sqrt{s} = 13$ TeV with the ATLAS detector

ATLAS Collaboration

DOI:

[10.1140/epjc/s10052-016-4574-y](https://doi.org/10.1140/epjc/s10052-016-4574-y)

License:

Creative Commons: Attribution (CC BY)

Document Version

Publisher's PDF, also known as Version of record

Citation for published version (Harvard):

ATLAS Collaboration 2017, 'Measurement of the $t\bar{t}Z^-$ and $t\bar{t}W^-$ production cross sections in multilepton final states using 3.2 fb⁻¹ of pp collisions at $\sqrt{s} = 13$ TeV with the ATLAS detector', *European Physical Journal C*, vol. 77, 40. <https://doi.org/10.1140/epjc/s10052-016-4574-y>

[Link to publication on Research at Birmingham portal](#)

General rights

Unless a licence is specified above, all rights (including copyright and moral rights) in this document are retained by the authors and/or the copyright holders. The express permission of the copyright holder must be obtained for any use of this material other than for purposes permitted by law.

- Users may freely distribute the URL that is used to identify this publication.
- Users may download and/or print one copy of the publication from the University of Birmingham research portal for the purpose of private study or non-commercial research.
- User may use extracts from the document in line with the concept of 'fair dealing' under the Copyright, Designs and Patents Act 1988 (?)
- Users may not further distribute the material nor use it for the purposes of commercial gain.

Where a licence is displayed above, please note the terms and conditions of the licence govern your use of this document.

When citing, please reference the published version.

Take down policy

While the University of Birmingham exercises care and attention in making items available there are rare occasions when an item has been uploaded in error or has been deemed to be commercially or otherwise sensitive.

If you believe that this is the case for this document, please contact UBIRA@lists.bham.ac.uk providing details and we will remove access to the work immediately and investigate.

Measurement of the $t\bar{t}Z$ and $t\bar{t}W$ production cross sections in multilepton final states using 3.2 fb^{-1} of pp collisions at $\sqrt{s} = 13\text{ TeV}$ with the ATLAS detector

ATLAS Collaboration*

CERN, 1211 Geneva 23, Switzerland

Received: 7 September 2016 / Accepted: 13 December 2016 / Published online: 20 January 2017

© CERN for the benefit of the ATLAS collaboration 2017. This article is published with open access at Springerlink.com

Abstract A measurement of the $t\bar{t}Z$ and $t\bar{t}W$ production cross sections in final states with either two same-charge muons, or three or four leptons (electrons or muons) is presented. The analysis uses a data sample of proton–proton collisions at $\sqrt{s} = 13\text{ TeV}$ recorded with the ATLAS detector at the Large Hadron Collider in 2015, corresponding to a total integrated luminosity of 3.2 fb^{-1} . The inclusive cross sections are extracted using likelihood fits to signal and control regions, resulting in $\sigma_{t\bar{t}Z} = 0.9 \pm 0.3\text{ pb}$ and $\sigma_{t\bar{t}W} = 1.5 \pm 0.8\text{ pb}$, in agreement with the Standard Model predictions.

1 Introduction

At the Large Hadron Collider (LHC), top quarks are copiously produced in quark–antiquark pairs ($t\bar{t}$). This process has been extensively studied in proton–proton collisions at 7 and 8 TeV, and recently at 13 TeV [1,2] centre-of-mass energy. Measurements of the associated production of $t\bar{t}$ with a Z boson ($t\bar{t}Z$) allow the extraction of information about the neutral-current coupling of the top quark. The production rate of a top-quark pair with a massive vector boson could be altered in the presence of physics beyond the Standard Model (SM), such as vector-like quarks [3,4], strongly coupled Higgs bosons [5] or technicolour [6–10], and therefore the measurements of $\sigma_{t\bar{t}Z}$ and $\sigma_{t\bar{t}W}$ are important checks of the validity of the SM at this new energy regime. The $t\bar{t}Z$ and $t\bar{t}W$ processes have been established by ATLAS [11] and CMS [12] using the Run-1 dataset at $\sqrt{s} = 8\text{ TeV}$, with measured cross sections compatible with the SM prediction and having uncertainties of $\sim 30\%$. At $\sqrt{s} = 13\text{ TeV}$, the SM cross sections of the $t\bar{t}Z$ and $t\bar{t}W$ processes increase by factors of 3.5 and 2.4, respectively, compared to $\sqrt{s} = 8\text{ TeV}$. The cross sections, computed at next-to-leading-order (NLO) QCD precision, using MADGRAPH5_aMC@NLO (referred

to in the following as MG5_aMC), are $\sigma_{t\bar{t}Z} = 0.84\text{ pb}$ and $\sigma_{t\bar{t}W} = 0.60\text{ pb}$ with an uncertainty of $\sim 12\%$ [13,14], primarily due to higher-order corrections, estimated by varying the renormalisation and factorisation scales.

This paper presents measurements of the $t\bar{t}Z$ and $t\bar{t}W$ cross sections using 3.2 fb^{-1} of proton–proton (pp) collision data at $\sqrt{s} = 13\text{ TeV}$ collected by the ATLAS detector in 2015. The final states of top-quark pairs produced in association with a Z or a W boson comprise up to four isolated, prompt leptons.¹ Decay modes with two same-sign (SS) charged muons, or three or four leptons are considered in this analysis. The analysis strategy follows the strategy adopted for the 8 TeV dataset [11], excluding the lower sensitivity SS dilepton channels. Table 1 lists the analysis channels and the targeted decay modes of the $t\bar{t}Z$ and $t\bar{t}W$ processes. Each channel is divided into multiple analysis regions in order to enhance the sensitivity to the signal. Simultaneous fits are performed to the signal regions and selected control regions in order to extract the cross sections for $t\bar{t}Z$ and $t\bar{t}W$ production. Additional validation regions are defined to check that the background estimate agrees with the data and are not used in the fit.

2 The ATLAS detector

The ATLAS detector [15] consists of four main subsystems: an inner tracking system, electromagnetic (EM) and hadronic calorimeters, and a muon spectrometer (MS). The inner detector (ID) consists of a high-granularity silicon pixel detector, including the newly installed Insertable B-Layer [16], which is the innermost layer of the tracking system, and a silicon microstrip tracker, together providing pre-

* e-mail: atlas.publications@cern.ch

¹ In this paper, lepton is used to denote electron or muon, and prompt lepton is used to denote a lepton produced in a Z or W boson or τ -lepton decay.

Table 1 List of $t\bar{t}W$ and $t\bar{t}Z$ decay modes and analysis channels targeting them

| Process | $t\bar{t}$ decay | Boson decay | Channel |
|-------------|------------------------------------|-----------------|-------------|
| $t\bar{t}W$ | $(\mu^\pm \nu b)(q\bar{q}b)$ | $\mu^\pm \nu$ | SS dimuon |
| | $(\ell^\pm \nu b)(\ell^\mp \nu b)$ | $\ell^\pm \nu$ | Trilepton |
| $t\bar{t}Z$ | $(\ell^\pm \nu b)(q\bar{q}b)$ | $\ell^+ \ell^-$ | Trilepton |
| | $(\ell^\pm \nu b)(\ell^\mp \nu b)$ | $\ell^+ \ell^-$ | Tetralepton |

cision tracking in the pseudorapidity² range $|\eta| < 2.5$ and of a transition radiation tracker covering $|\eta| < 2.0$. All the systems are immersed in a 2 T magnetic field provided by a superconducting solenoid. The EM sampling calorimeter uses lead and liquid argon (LAr) and is divided into barrel ($|\eta| < 1.475$) and endcap ($1.375 < |\eta| < 3.2$) regions. Hadron calorimetry is provided by a steel/scintillator-tile calorimeter, segmented into three barrel structures, in the range $|\eta| < 1.7$, and by two copper/LAr hadronic endcap calorimeters that cover the region $1.5 < |\eta| < 3.2$. The solid angle coverage is completed with forward copper/LAr and tungsten/LAr calorimeter modules, optimised for EM and hadronic measurements respectively, covering the region $3.1 < |\eta| < 4.9$. The muon spectrometer measures the deflection of muon tracks in the range $|\eta| < 2.7$ using multiple layers of high-precision tracking chambers located in toroidal magnetic fields. The field integral of the toroids ranges between 2.0 and 6.0 Tm for most of the detector. The muon spectrometer is also instrumented with separate trigger chambers covering $|\eta| < 2.4$. A two-level trigger system, using custom hardware followed by a software-based trigger level, is used to reduce the event rate to an average of around 1 kHz for offline storage.

3 Data and simulated event samples

The data were collected with the ATLAS detector during 2015 with a bunch spacing of 25 ns and a mean number of 14 pp interactions per bunch crossing (pile-up). With strict data-quality requirements, the integrated luminosity considered corresponds to 3.2 fb^{-1} with an uncertainty of 2.1% [17].

Monte Carlo simulation samples (MC) are used to model the expected signal and background distributions in the different control, validation and signal regions described below. The heavy-flavour decays involving b - and c -quarks, partic-

ularly important to this measurement, are modelled using the EVTGEN [18] program, except for processes modelled using the SHERPA generator. In all samples the top-quark mass is set to 172.5 GeV and the Higgs boson mass is set to 125 GeV. The response of the detector to stable³ particles is emulated by a dedicated simulation [19] based either fully on GEANT [20] or on a faster parameterisation [21] for the calorimeter response and GEANT for other detector systems. To account for additional pp interactions from the same and close-by bunch crossings, a set of minimum-bias interactions generated using PYTHIA v8.210 [22], referred to as PYTHIA 8 in the following, with the A2 [23] set of tuned MC parameters (A2 tune) is superimposed on the hard-scattering events. In order to reproduce the same pile-up levels present in the data, the distribution of the number of additional pp interactions in the MC samples is reweighted to match the one in the data. All samples are processed through the same reconstruction software as the data. Simulated events are corrected so that the object identification, reconstruction and trigger efficiencies, energy scales and energy resolutions match those determined from data control samples.

The associated production of a top-quark pair with one or two vector bosons is generated at leading order (LO) with MG5_aMC interfaced to PYTHIA 8, with up to two ($t\bar{t}W$), one ($t\bar{t}Z$) or no ($t\bar{t}WW$) extra partons included in the matrix elements. The γ^* contribution and the Z/γ^* interference are included in the $t\bar{t}Z$ samples. The A14 [24] set of tuned MC parameters (A14 tune) is used together with the NNPDF2.3LO parton distribution function (PDF) set [25]. The samples are normalised using cross sections computed at NLO in QCD [26].

The t -channel production of a single top quark in association with a Z boson (tZ) is generated using MG5_aMC interfaced with PYTHIA v6.427 [27], referred to as PYTHIA 6 in the following, with the CTEQ6L1 PDF [28] set and the Perugia2012 [29] set of tuned MC parameters at NLO in QCD. The Z/γ^* interference is included, and the four-flavour scheme is used in the computation.

The Wt -channel production of a single top quark together with a Z boson (tWZ) is generated with MG5_aMC and showered with PYTHIA 8, using the NNPDF3.0NLO PDF set [30] and the A14 tune. The generation is performed at NLO in QCD using the five-flavour scheme. Diagrams containing a top-quark pair are removed to avoid overlap with the $t\bar{t}Z$ process.

Diboson processes with four charged leptons (4ℓ), three charged leptons and one neutrino ($\ell\ell\ell\nu$) or two charged leptons and two neutrinos ($\ell\ell\nu\nu$) are simulated using the SHERPA 2.1 generator [31]. The matrix elements include all diagrams with four electroweak vertices. They are calculated for up to one (4ℓ , $\ell\ell\nu\nu$) or no additional partons ($\ell\ell\ell\nu$) at

² ATLAS uses a right-handed coordinate system with its origin at the nominal interaction point (IP) in the centre of the detector and the z -axis along the beam pipe. The x -axis points from the IP to the centre of the LHC ring, and the y -axis points upward. Cylindrical coordinates (r , ϕ) are used in the transverse plane, ϕ being the azimuthal angle around the z -axis. The pseudorapidity is defined in terms of the polar angle θ as $\eta = -\ln \tan(\theta/2)$.

³ A particle is considered stable if $c\tau \geq 1 \text{ cm}$.

NLO and up to three partons at LO using the COMIX [32] and OPENLOOPS [33] matrix element generators and merged with the SHERPA parton shower using the ME+PS@NLO prescription [34]. The CT10nlo PDF set [35] is used in conjunction with a dedicated parton-shower tuning developed by the SHERPA authors. The NLO cross sections calculated by the generator are used to normalise diboson processes. Alternative diboson samples are simulated using the POWHEG-BOX v2 [36] generator, interfaced to the PYTHIA 8 parton shower model, and for which the CT10nlo PDF set is used in the matrix element, while the CTEQ6L1 PDF set is used for the parton shower along with the AZNLO [37] set of tuned MC parameters.

The production of three massive vector bosons with subsequent leptonic decays of all three bosons is modelled at LO with the SHERPA 2.1 generator and the CT10 PDF set [35]. Up to two additional partons are included in the matrix element at LO and the full NLO accuracy is used for the inclusive process.

Electroweak processes involving the vector-boson scattering (VBS) diagram and producing two same-sign leptons, two neutrinos and two partons are modelled using SHERPA 2.1 at LO accuracy and the CT10 PDF set. Processes of orders four and six in the electroweak coupling constant are considered, and up to one additional parton is included in the matrix element.

For the generation of $t\bar{t}$ events and Wt -channel single-top-quark events the POWHEG-BOX v2 generator is used with the CT10 PDF set. The parton shower and the underlying event are simulated using PYTHIA 6 with the CTEQ6L1 PDF set and the corresponding Perugia2012 tune. The $t\bar{t}$ samples are normalised to their next-to-next-to-leading-order (NNLO) cross-section predictions, including soft-gluon resummation to next-to-next-to-leading-log order, as calculated with the TOP++2.0 program (see Ref. [38] and references therein). For more efficient sample generation, the $t\bar{t}$ sample is produced by selecting only true dilepton events in the final state. Moreover, an additional dilepton $t\bar{t}$ sample requiring a b -hadron not coming from top-quark decays is generated after b -jet selection. Diagram removal is employed to remove the overlap between $t\bar{t}$ and Wt [39].

Samples of $t\bar{t}$ events produced in association with a Higgs boson ($t\bar{t}H$) are generated using NLO matrix elements in MG5_aMC with the CT10NLO PDF set and interfaced with PYTHIA 8 for the modelling of the parton shower. Higgs boson production via gluon–gluon fusion (ggF) and vector boson fusion (VBF) is generated using the POWHEG-BOX v2 generator with CT10 PDF set. The parton shower and underlying event are simulated using PYTHIA 8 with the CTEQ6L1 PDF set and AZNLO tune. Higgs boson production with a vector boson is generated at LO using PYTHIA 8 with the CTEQ6L1 PDF. All Higgs boson samples are normalised using theoretical calculations of Ref. [40].

Events containing Z or W bosons with associated jets, referred to as Z +jets and W +jets in the following, are simulated using the SHERPA 2.1 generator. Matrix elements are calculated for up to two partons at NLO and four partons at LO. The CT10 PDF set is used in conjunction with a dedicated parton-shower tuning developed by the SHERPA authors [31]. The Z/W +jets samples are normalised to the NNLO cross sections [41–44]. Alternative Z/W +jets samples are simulated using MG5_aMC at LO interfaced to the PYTHIA 8 parton shower model. The A14 tune is used together with the NNPDF2.3LO PDF set.

The SM production of three and four top quarks is generated at LO with MG5_aMC+PYTHIA 8, using the A14 tune together with the NNPDF2.3LO PDF set. The samples are normalised using cross sections computed at NLO [45,46].

4 Object reconstruction

The final states of interest in this analysis contain electrons, muons, jets, b -jets and missing transverse momentum.

Electron candidates [47] are reconstructed from energy deposits (clusters) in the EM calorimeter that are associated with reconstructed tracks in the inner detector. The electron identification relies on a likelihood-based selection [48,49]. Electrons are required to pass the “medium” likelihood identification requirements described in Ref. [49]. These include requirements on the shapes of the electromagnetic shower in the calorimeter as well as tracking and track-to-cluster matching quantities. The electrons are also required to have transverse momentum $p_T > 7$ GeV and $|\eta_{\text{cluster}}| < 2.47$, where η_{cluster} is the pseudorapidity of the calorimeter energy deposit associated with the electron candidate. Candidates in the EM calorimeter barrel/endcap transition region $1.37 < |\eta_{\text{cluster}}| < 1.52$ are excluded.

Muon candidates are reconstructed from a fit to track segments in the various layers of the muon spectrometer, matched with tracks identified in the inner detector. Muons are required to have $p_T > 7$ GeV and $|\eta| < 2.4$ and to pass the “medium” identification requirements defined in Ref. [50]. The medium requirement includes selections on the numbers of hits in the ID and MS as well as a compatibility requirement between momentum measurements in the ID and MS. It provides a high efficiency and purity of selected muons. Electron candidates sharing a track with a muon candidate are removed.

To reduce the non-prompt lepton background from hadron decays or jets misidentified as leptons (labelled as “fake leptons” throughout this paper), electron and muon candidates are required to be isolated. The total sum of track transverse momenta in a surrounding cone of size $\min(10 \text{ GeV}/p_T, r_{e,\mu})$, excluding the track of the candidate from the sum, is required to be less than 6% of the candidate p_T , where $r_e = 0.2$ and $r_\mu = 0.3$. In addition, the sum of the

cluster transverse energies in the calorimeter within a cone of size $\Delta R_\eta \equiv \sqrt{(\Delta\eta)^2 + (\Delta\phi)^2} = 0.2$ of any electron candidate, excluding energy deposits of the candidate itself, is required to be less than 6% of the candidate p_T .

For both electrons and muons, the longitudinal impact parameter of the associated track with respect to the primary vertex,⁴ z_0 , is required to satisfy $|z_0 \sin \theta| < 0.5$ mm. The significance of the transverse impact parameter d_0 is required to satisfy $|d_0|/\sigma(d_0) < 5$ for electrons and $|d_0|/\sigma(d_0) < 3$ for muons, where $\sigma(d_0)$ is the uncertainty in d_0 .

Jets are reconstructed using the anti- k_t algorithm [51,52] with radius parameter $R = 0.4$, starting from topological clusters in the calorimeters [53]. The effect of pile-up on jet energies is accounted for by a jet-area-based correction [54] and the energy resolution of the jets is improved by using global sequential corrections [55]. Jets are calibrated to the hadronic energy scale using E - and η -dependent calibration factors based on MC simulations, with in-situ corrections based on Run-1 data [56,57] and checked with early Run-2 data [58]. Jets are accepted if they fulfil the requirements $p_T > 25$ GeV and $|\eta| < 2.5$. To reduce the contribution from jets associated with pile-up, jets with $p_T < 60$ GeV and $|\eta| < 2.4$ are required to satisfy pile-up rejection criteria (JVT), based on a multivariate combination of track-based variables [59].

Jets are b -tagged as likely to contain b -hadrons using the MV2C20 algorithm, a multivariate discriminant making use of the long lifetime, large decay multiplicity, hard fragmentation and high mass of b -hadrons [60]. The average efficiency to correctly tag a b -jet is approximately 77%, as determined in simulated $t\bar{t}$ events, but it varies as a function of p_T and η . In simulation, the tagging algorithm gives a rejection factor of about 130 against light-quark and gluon jets, and about 4.5 against jets containing charm quarks [61]. The efficiency of b -tagging in simulation is corrected to that in data using a $t\bar{t}$ -based calibration using Run-1 data [62] and validated with Run-2 data [63].

The missing transverse momentum $\mathbf{p}_T^{\text{miss}}$, with magnitude E_T^{miss} , is a measure of the transverse momentum imbalance due to particles escaping detection. It is computed [64] as the negative sum of the transverse momenta of all electrons, muons and jets and an additional soft term. The soft term is constructed from all tracks that are associated with the primary vertex but not with any physics object. In this way, the E_T^{miss} is adjusted for the best calibration of the jets and the other identified physics objects above, while maintaining pile-up independence in the soft term [65,66].

To prevent double-counting of electron energy deposits as jets, the closest jet within $\Delta R_y = 0.2$ of a reconstructed electron is removed, where $\Delta R_y \equiv \sqrt{(\Delta y)^2 + (\Delta\phi)^2}$. If the nearest jet surviving the above selection is within $\Delta R_y = 0.4$ of an electron, the electron is discarded to ensure that selected electrons are sufficiently separated from nearby jet activity. To reduce the background from muons originating from heavy-flavour particle decays inside jets, muons are removed if they are separated from the nearest jet by $\Delta R_y < 0.4$. However, if this jet has fewer than three associated tracks, the muon is kept and the jet is removed instead; this avoids an inefficiency for high-energy muons undergoing significant energy loss in the calorimeter.

5 Event selection and background estimation

Only events collected using single-electron or single-muon triggers are accepted. The trigger thresholds, $p_T > 24$ GeV for electrons and $p_T > 20$ GeV for muons, are set to be almost fully efficient for reconstructed leptons with $p_T > 25$ GeV. Events are required to have at least one reconstructed primary vertex. In all selections considered, at least one reconstructed lepton with $p_T > 25$ GeV is required to match ($\Delta R_\eta < 0.15$) a lepton with the same flavour reconstructed by the trigger algorithm. Three channels are defined based on the number of reconstructed leptons, which are sorted according to their transverse momentum in decreasing order.

Background events containing well-identified prompt leptons are modelled by simulation. The normalisations for the WZ and ZZ processes are taken from data control regions and included in the fit. The yields in these data control regions are extrapolated to the signal regions using simulation. Systematic uncertainties in the extrapolation are taken into account in the overall uncertainty in the background estimate.

Background sources involving one or more fake leptons are modelled using data events from control regions. For the same-sign dimuon (2μ -SS) analysis and the trilepton analysis the fake-lepton background is estimated using the matrix method [67], where any combination of fake leptons among the selected leptons is considered. However, compared to Ref. [67], the real- and fake-lepton efficiencies used by the matrix method are estimated in a different way in this measurement. The lepton efficiencies are measured by applying the matrix method in control regions, where the lepton efficiencies are extracted in a likelihood fit as free parameters using the matrix method as model, assuming Poisson statistics, and assuming that events with two fake leptons are negligible. In this way the parameters are by construction the actual parameters of the matrix model itself, instead of relying on external lepton efficiency measurements, which are not guaranteed to be fully consistent with the matrix model. The control regions are defined in dilepton events, separately for b -tagged and b -vetoed events

⁴ A primary vertex candidate is defined as a vertex with at least five associated tracks, consistent with the beam collision region. If more than one such vertex is found, the vertex candidate with the largest sum of squared transverse momenta of its associated tracks is taken as the primary vertex.

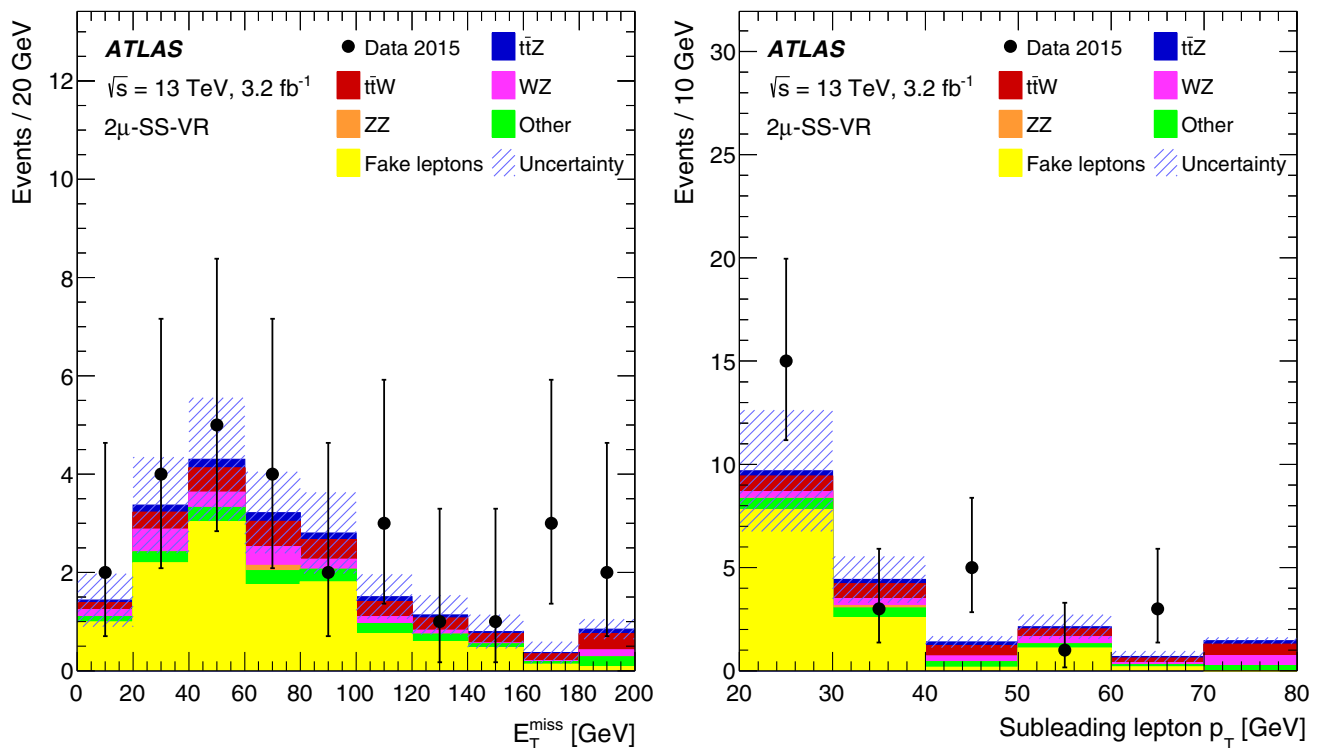


Fig. 1 The (left) E_T^{miss} and (right) subleading lepton p_T distributions shown for the b -tagged 2μ -SS channel where the signal region requirements on subleading lepton p_T , number of b -tags, and E_T^{miss} are relaxed. The shaded band represents the total uncertainty. The background

denoted ‘Other’ contains other SM processes producing two same-sign prompt leptons. The last bin in each of the distributions includes the overflow

to take into account the different fake-lepton efficiencies depending on whether the source is a light-flavour jet or a heavy-flavour jet. The real-lepton efficiencies are measured in inclusive opposite-sign events, and fake-lepton efficiencies in events with same-sign leptons and $E_T^{\text{miss}} > 40$ GeV (for b -tagged events $E_T^{\text{miss}} > 20$ GeV), after subtracting the estimated contribution from events with misidentification of the charge of a lepton (referred to as “charge-flip” in the following), and excluding the same-sign dimuon signal region. The charge-flip events are subtracted using simulation. The extracted fake-lepton efficiencies are found to be compatible with fake-lepton efficiencies from a fully data-driven procedure where the charge-flip events are estimated from data. For the tetralepton channel, the contribution from backgrounds containing fake leptons is estimated from simulation and corrected with scale factors determined in control regions.

The full selection requirements and the background evaluation strategies in the different channels are described below.

5.1 Same-sign dimuon analysis

The same-sign dimuon signal region targets the $t\bar{t}W$ process and has the highest sensitivity among all same-sign dilepton regions [11]. The main reason for this is that electrons have a much larger charge misidentification probability, inducing

a significant background from top-quark pairs. Events are required to have two muon candidates with the same charge and $p_T > 25$ GeV, $E_T^{\text{miss}} > 40$ GeV, the scalar sum of the p_T of selected leptons and jets, H_T , above 240 GeV, and at least two b -tagged jets. Events containing additional leptons (with $p_T > 7$ GeV) are vetoed.

The dominant background in the 2μ -SS region arises from events containing fake leptons, where the main source is $t\bar{t}$ events. Backgrounds from the production of prompt leptons with correctly identified charge come primarily from WZ production, but the relative contribution of this background is small compared to the fake-lepton background. The charge-flip background is negligible in this signal region, as the probability of misidentifying the charge of a muon in the relevant p_T range is negligible. For the validation of the fake-lepton background estimate a region is defined based on the signal region selection but omitting the E_T^{miss} requirement, reducing the p_T threshold of the subleading lepton to 20 GeV and requiring at least one b -tagged jet. The distributions of E_T^{miss} and subleading lepton p_T in this validation region (2μ -SS-VR) are shown in Fig. 1. The expected numbers of events in the 2μ -SS signal region are shown in Table 4. Nine events are observed in data for this signal region.

Table 2 Summary of event selections in the trilepton signal regions

| Variable | 3 ℓ -Z-1b4j | 3 ℓ -Z-2b3j | 3 ℓ -Z-2b4j | 3 ℓ -noZ-2b |
|-----------------------------|------------------|------------------|------------------|-----------------------|
| Leading leptons p_T | >25 GeV | >25 GeV | >25 GeV | >25 GeV |
| Other leptons' p_T | >20 GeV | >20 GeV | >20 GeV | >20 GeV |
| Sum of leptons' charges | ± 1 | ± 1 | ± 1 | ± 1 |
| OSSF $ m_{\ell\ell} - m_Z $ | <10 GeV | <10 GeV | <10 GeV | >10 GeV |
| n_{jets} | ≥ 4 | 3 | ≥ 4 | ≥ 2 and ≤ 4 |
| $n_{b\text{-jets}}$ | 1 | ≥ 2 | ≥ 2 | ≥ 2 |

5.2 Trilepton analysis

Four signal regions with exactly three leptons are considered. The first three are sensitive to $t\bar{t}Z$; each of these requires an opposite-sign same-flavour (OSSF) pair of leptons whose invariant mass is within 10 GeV of the Z boson mass. The signal regions are categorised by their jet and b -jet multiplicities and have different signal-to-background ratios. In the 3 ℓ -Z-1b4j region, at least four jets are required, exactly one of which is b -tagged. In the 3 ℓ -Z-2b3j region, exactly three jets with at least two b -tagged jets are required. In the 3 ℓ -Z-2b4j region, at least four jets are required, of which at least two are b -tagged.

In the 3 ℓ -noZ-2b region at least two and at most four jets are required, of which at least two are b -tagged, no OSSF

lepton pair is allowed in the Z boson mass window, and the sum of the lepton charges must be ± 1 . This region primarily targets the $t\bar{t}W$ process but also has a sizeable $t\bar{t}Z$ contribution.

The signal region definitions for the trilepton channel are summarised in Table 2, while the expected numbers of events in the signal regions are shown in Table 4. The dominant backgrounds in the 3 ℓ -Z-1b4j, 3 ℓ -Z-2b3j and 3 ℓ -Z-2b4j signal regions arise from Z+jets production with a fake lepton, diboson production and the production of a single top quark in association with a Z boson.

A control region is used to constrain the normalisation of the WZ background in data. Exactly three leptons are required, at least one pair of which must be an OSSF pair with an invariant mass within 10 GeV of the Z boson mass.

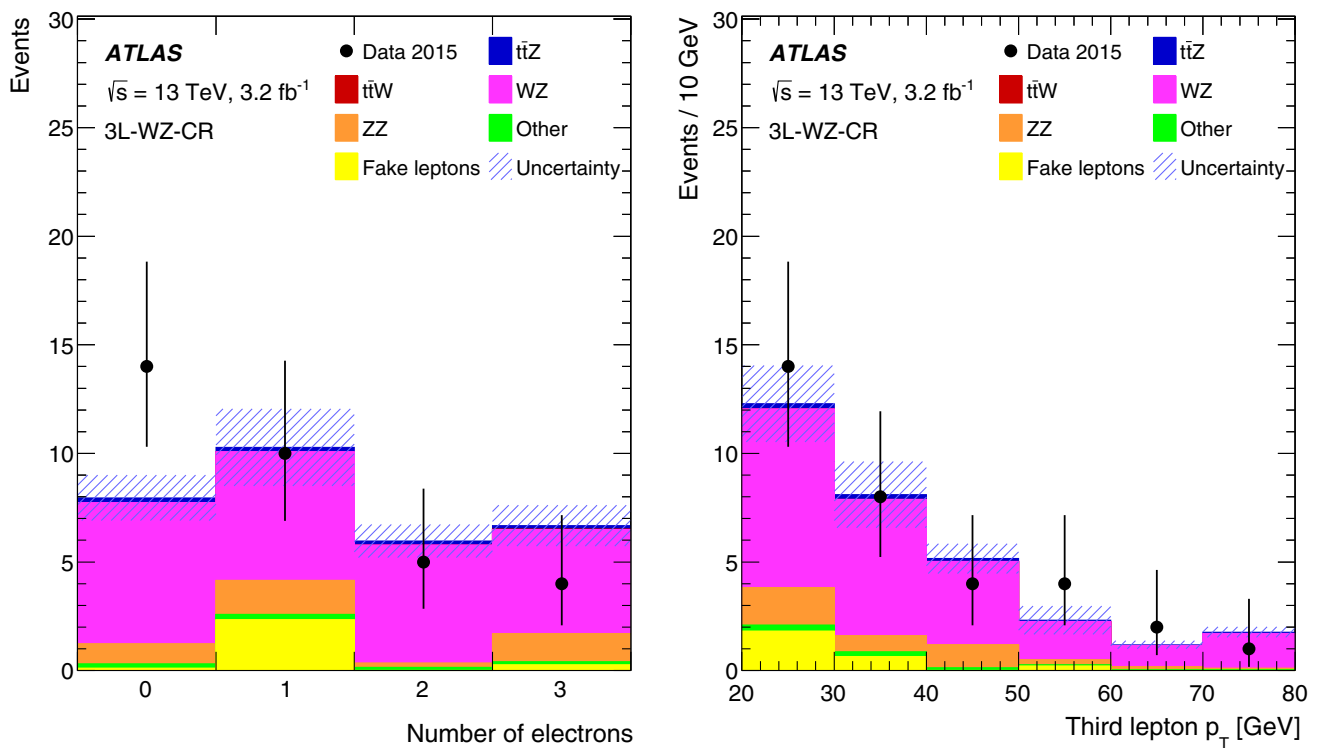


Fig. 2 Distributions of (left) the number of electrons and (right) the third-lepton p_T in the 3 ℓ -WZ-CR control region before the fit. The background denoted ‘Other’ contains other SM processes producing

three prompt leptons. The shaded band represents the total uncertainty. The last bin of the distribution shown in the right panel includes the overflow

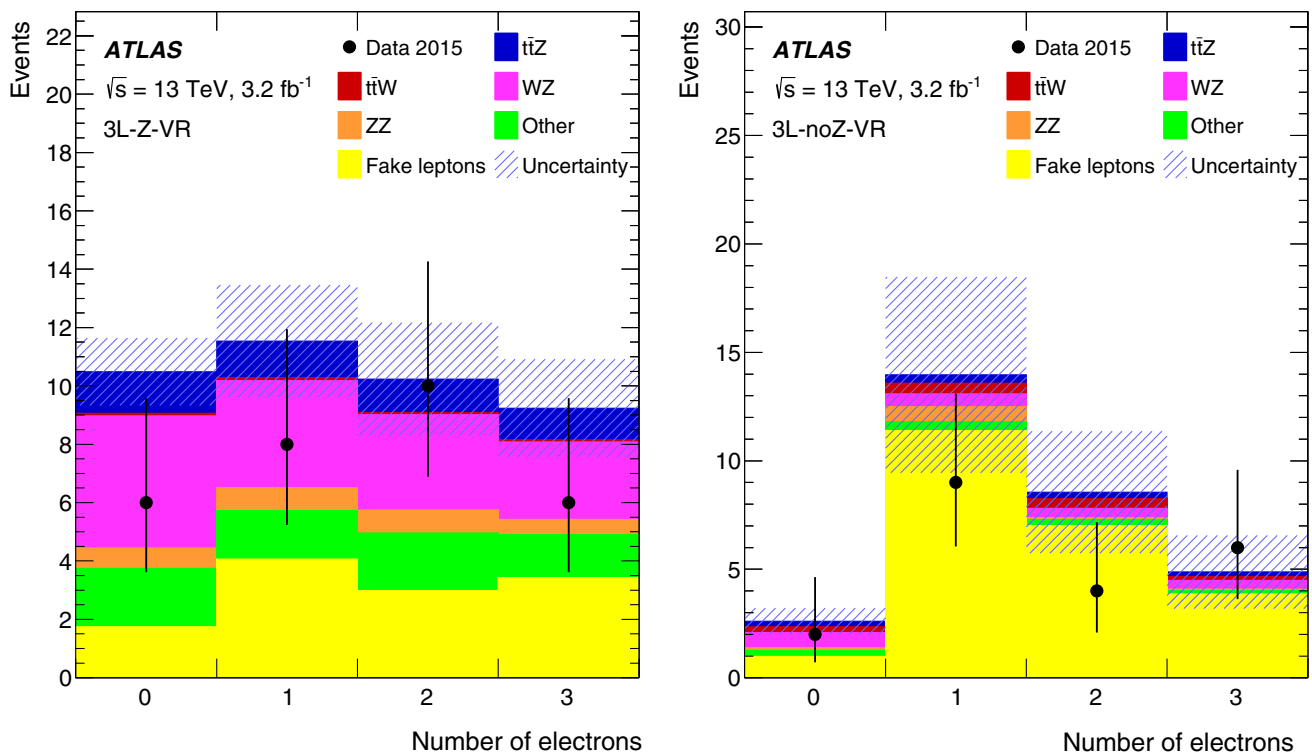


Fig. 3 Distributions of the number of electrons in the (left) 3L-Z-VR and (right) 3L-noZ-VR validation regions, shown before the fit. The background denoted ‘Other’ contains other SM processes producing three prompt leptons. The shaded band represents the total uncertainty

There must be exactly three jets, none of which pass the b -tagging requirement. With these requirements, the expected $t\bar{t}Z$ signal contribution is roughly 1% of the total number of events. This region is referred to as 3L-WZ-CR and it is included in the fit. Distributions comparing data and SM prediction are shown in Fig. 2.

Two background validation regions are defined for the trilepton channel. In the first region, 3L-Z-VR, the presence of two OSSF leptons with an invariant mass within 10 GeV of the mass of the Z boson is required. The region requires the events to have at most three jets where exactly one is b -tagged, or exactly two jets where both jets are b -tagged. The main backgrounds are WZ production and Z +jets events with fake leptons. In the second region, 3L-noZ-VR, events with such a pair of leptons are vetoed. This region requires the events to have at most three jets where exactly one is b -tagged, and it is dominated by the fake-lepton background from top-quark pair production. Neither validation region is used in the fit. The distributions of the number of electrons in each of the two validation regions are shown in Fig. 3, demonstrating that data and background modelling are in good agreement within statistical uncertainties.

In total, 29 events are observed in the four signal regions. Distributions of the number of jets, number of b -tagged jets, missing transverse momentum and transverse momentum of the third lepton are shown in Fig. 4.

5.3 Tetralepton analysis

The tetralepton channel targets the $t\bar{t}Z$ process for the case where both W bosons resulting from top-quark decays and the Z boson decay leptonically. Events with two pairs of opposite-sign leptons are selected, and at least one pair must be of same flavour. The OSSF lepton pair with reconstructed invariant mass closest to m_Z is attributed to the Z boson decay and denoted in the following by Z_1 . The two remaining leptons are used to define Z_2 . Four signal regions are defined according to the relative flavour of the two Z_2 leptons, different flavour (DF) or same flavour (SF), and the number of b -tagged jets: one, or at least two (1b, 2b). The signal regions are thus 4L-DF-1b, 4L-DF-2b, 4L-SF-1b and 4L-SF-2b.

To suppress events with fake leptons in the 1- b -tag multiplicity regions, additional requirements on the scalar sum of the transverse momenta of the third and fourth leptons (p_{T34}) are imposed. In the 4L-SF-1b and 4L-DF-1b regions, events are required to satisfy $p_{T34} > 25$ GeV and $p_{T34} > 35$ GeV, respectively. In all regions, the invariant mass of any two reconstructed OS leptons is required to be larger than 10 GeV. The signal region definitions for the tetralepton channel are summarised in Table 3.

A control region used to constrain the ZZ normalisation, referred to as 4L-ZZ-CR, is included in the fit and is defined to have exactly four reconstructed leptons, a Z_2 pair with

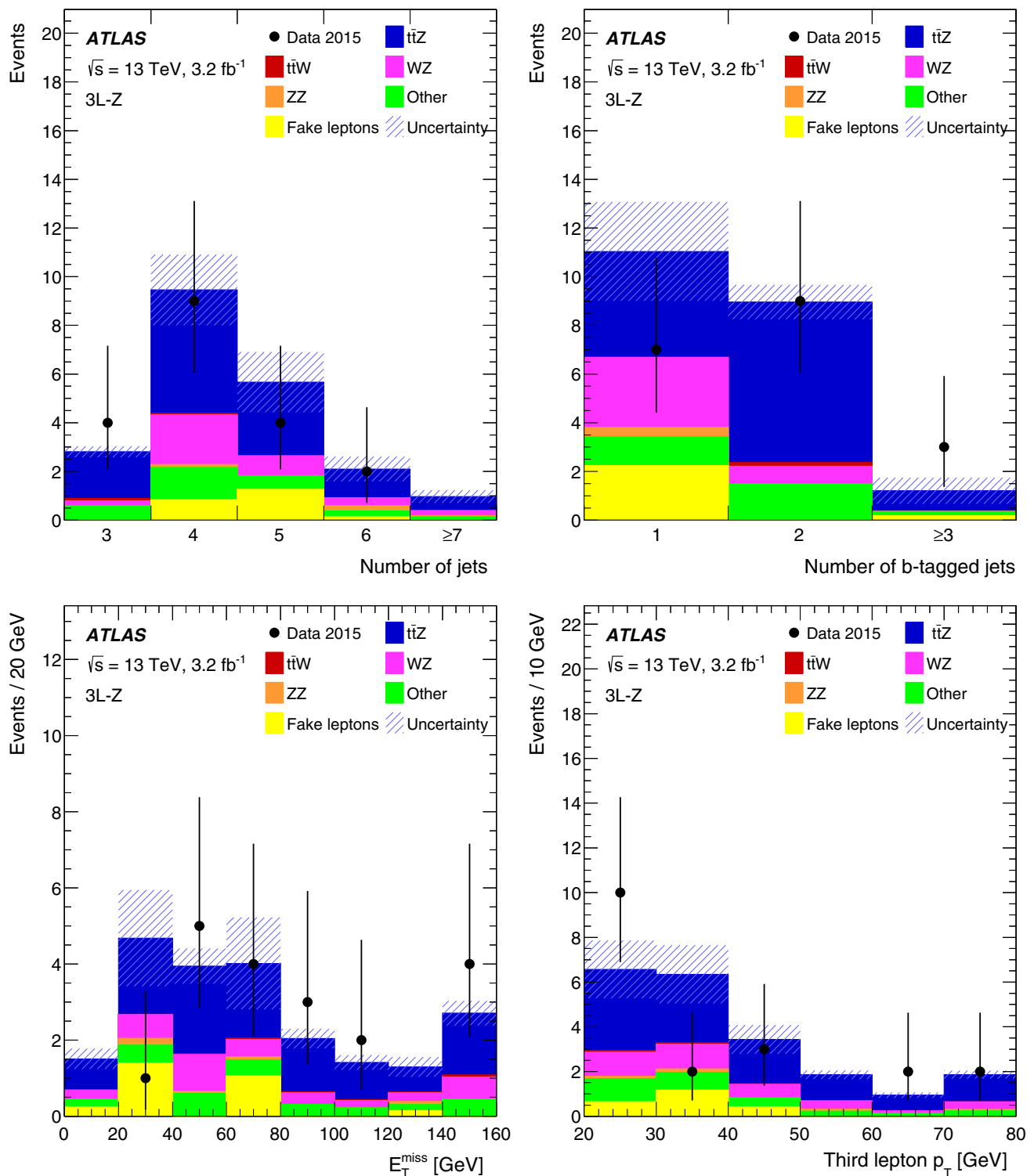


Fig. 4 Distributions of (*top left*) the number of jets, (*top right*) the number of b -tagged jets, (*bottom left*) the missing transverse momentum and (*bottom right*) the third-lepton p_T , for events contained in any of the three signal regions 3ℓ -Z-1b4j, 3ℓ -Z-2b3j or 3ℓ -Z-2b4j. The distribu-

tions are shown before the fit. The background denoted ‘Other’ contains other SM processes producing three prompt leptons. The shaded band represents the total uncertainty. The last bin in each of the distributions shown in the *bottom panels* includes the overflow

OSSF leptons, the value of both m_{Z_1} and m_{Z_2} within 10 GeV of the mass of the Z boson, and $E_T^{\text{miss}} < 40$ GeV. The leading lepton p_T , the invariant mass of the Z_2 lepton pair, the

missing transverse momentum and the jet multiplicity in this control region are shown in Fig. 5, and good agreement is seen between data and prediction.

Table 3 Definitions of the four signal regions in the tetralepton channel. All leptons are required to satisfy $p_T > 7$ GeV and at least one lepton with $p_T > 25$ GeV is required to be trigger matched. The invariant mass of any two reconstructed OS leptons is required to be larger than 10 GeV

| Region | Z_2 leptons | p_{T34} | $ m_{Z_2} - m_Z $ | E_T^{miss} | $n_{b\text{-tags}}$ |
|-----------------|--------------------------------|-----------|--|--|---------------------|
| 4 ℓ -DF-1b | $e^\pm \mu^\mp$ | >35 GeV | — | — | 1 |
| 4 ℓ -DF-2b | $e^\pm \mu^\mp$ | — | — | — | ≥ 2 |
| 4 ℓ -SF-1b | $e^\pm e^\mp, \mu^\pm \mu^\mp$ | >25 GeV | $\begin{cases} >10 \text{ GeV} \\ <10 \text{ GeV} \end{cases}$ | $\begin{cases} >40 \text{ GeV} \\ >80 \text{ GeV} \end{cases}$ | 1 |
| 4 ℓ -SF-2b | $e^\pm e^\mp, \mu^\pm \mu^\mp$ | — | $\begin{cases} >10 \text{ GeV} \\ <10 \text{ GeV} \end{cases}$ | $\begin{cases} - \\ >40 \text{ GeV} \end{cases}$ | ≥ 2 |

The contribution from backgrounds containing fake leptons is estimated from simulation and corrected with scale factors determined in two control regions: one region enriched in $t\bar{t}$ events and thus in heavy-flavour jets, and one region enriched in Z +jets events, and thus in light-flavour jets. The scale factors are calibrated separately for electron and muon fake-lepton candidates. The scale factors are applied to all MC simulation events with fewer than four prompt leptons according to the number and the flavour of the fake leptons. The $t\bar{t}$ scale factors are applied to MC processes with real top quarks, while for all other processes the Z +jets scale factors are applied. Different generators are used when determining the scale factors and when applying them. It is verified that the uncertainties in the scale factors include the differences between these generators.

The expected yields in the signal and control regions in the tetralepton channel are shown in Table 4. Five events are observed in the four signal regions. Figure 6 shows the data superimposed to the expected distributions for all four signal regions combined. Overall the acceptance times efficiency for the $t\bar{t}Z$ and $t\bar{t}W$ processes is 6‰ and 2‰, respectively.

6 Systematic uncertainties

The normalisation of signal and background in each channel can be affected by several sources of systematic uncertainty. These are described in the following subsections.

6.1 Luminosity

The uncertainty in the integrated luminosity in the 2015 dataset is 2.1%. It is derived, following a methodology similar to that detailed in Ref. [68], from a calibration of the luminosity scale using x - y beam-separation scans performed in August 2015. This systematic uncertainty is applied to all processes modelled using Monte Carlo simulations.

6.2 Uncertainties associated with reconstructed objects

Uncertainties associated with the lepton selection arise from imperfect knowledge of the trigger, reconstruction, identification and isolation efficiencies, and lepton momentum scale and resolution [47–50, 69]. The uncertainty in the electron identification efficiency is the largest systematic uncertainty in the trilepton channel and among the most important ones in the tetralepton channel.

Uncertainties associated with the jet selection arise from the jet energy scale (JES), the JVT requirement and the jet energy resolution (JER). Their estimations are based on Run-1 data and checked with early Run-2 data. The JES and its uncertainty are derived by combining information from test-beam data, collision data and simulation [70]. JES uncertainty components arising from the in-situ calibration and the jet flavour composition are among the dominant uncertainties in the 2μ -SS and trilepton channels. The uncertainties in the JER and JVT have a significant effect at low jet p_T . The JER uncertainty results in the second largest uncertainty in the trilepton channel.

The efficiency of the flavour-tagging algorithm is measured for each jet flavour using control samples in data and in simulation. From these measurements, correction factors are defined to correct the tagging rates in the simulation. In the case of b -jets, correction factors and their uncertainties are estimated based on observed and simulated b -tagging rates in $t\bar{t}$ dilepton events [62]. In the case of c -jets, they are derived based on jets with identified D^* mesons [71]. In the case of light-flavour jets, correction factors are derived using dijet events [71]. Sources of uncertainty affecting the b - and c -tagging efficiencies are considered as a function of jet p_T , including bin-to-bin correlations [62]. An additional uncertainty is assigned to account for the extrapolation of the b -tagging efficiency measurement from the p_T region used to determine the scale factors to regions with higher p_T . For the efficiency to tag light-flavour jets, the dependence of the uncertainty on the jet p_T and η is considered. These systematic uncertainties are taken as uncorrelated between b -jets, c -jets, and light-flavour jets.

The treatment of the uncertainties associated with reconstructed objects is common to all three channels, and thus these are considered as correlated among different regions.

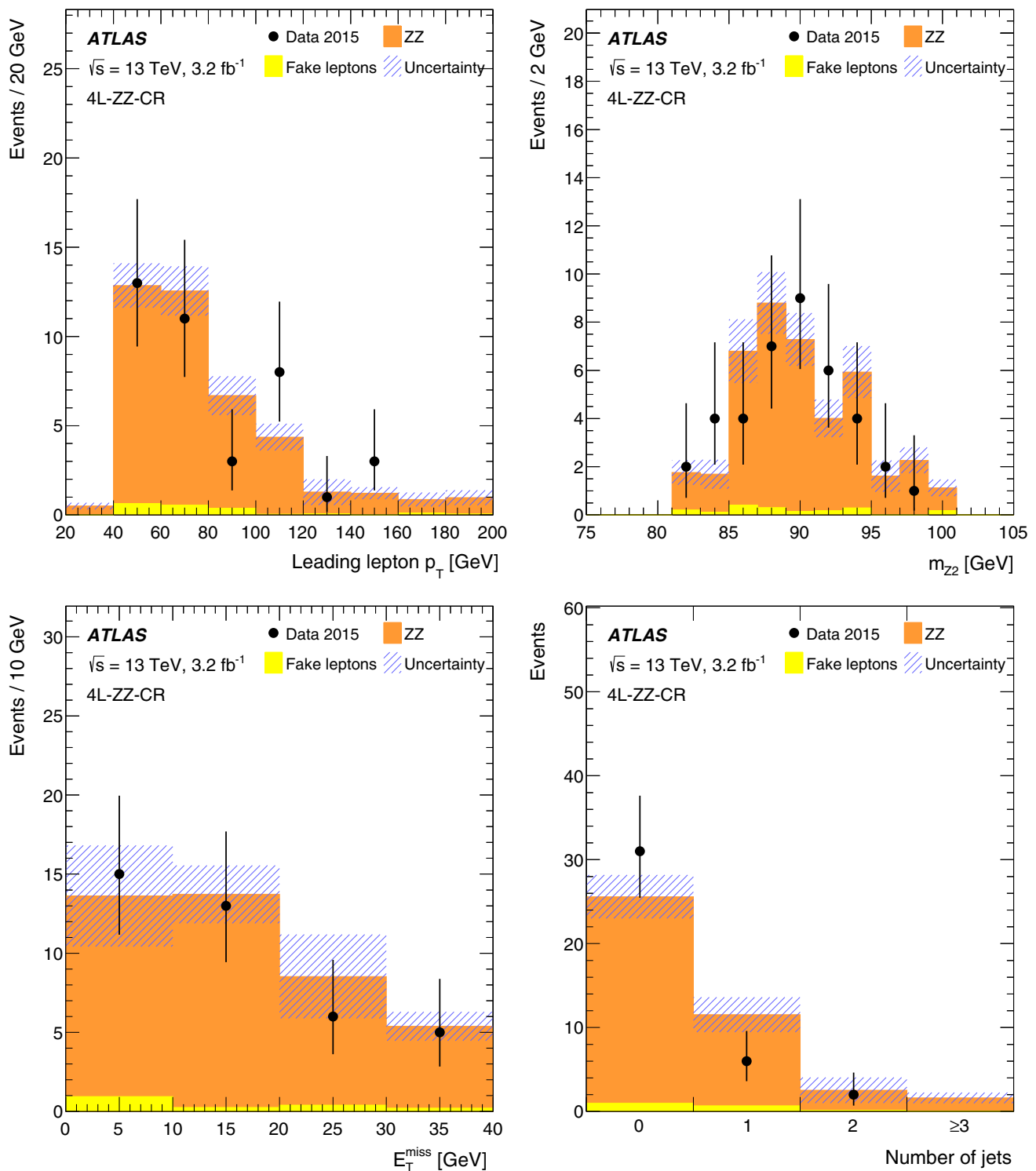


Fig. 5 (Top left) Leading lepton p_T , (top right) m_{Z_2} , (bottom left) missing transverse momentum and (bottom right) jet multiplicity distributions in the 4L-ZZ-CR control region. The distributions are shown before

the fit. The shaded band represents the total uncertainty. The last bin of the distribution shown in the top left panel includes the overflow

Table 4 Expected event yields for signal and backgrounds, and the observed data in all control and signal regions used in the fit to extract the $t\bar{t}Z$ and $t\bar{t}W$ cross sections. The quoted uncertainties in the expected event yields represent systematic uncertainties including MC statistical

uncertainties. The tZ , tWZ , $t\bar{t}H$, three- and four-top-quark processes are denoted $t + X$. The WZ , ZZ , $H \rightarrow ZZ$ (ggF and VBF), HW and HZ and VBS processes are denoted ‘Bosons’

| Region | $t + X$ | Bosons | Fake leptons | Total bkg. | $t\bar{t}W$ | $t\bar{t}Z$ | Data |
|------------------|-------------------|---------------------|-------------------|-----------------|-------------------|-------------------|------|
| 3 ℓ -WZ-CR | 0.52 ± 0.13 | 26.9 ± 2.2 | 2.2 ± 1.8 | 29.5 ± 2.8 | 0.015 ± 0.004 | 0.80 ± 0.13 | 33 |
| 4 ℓ -ZZ-CR | <0.001 | 39.5 ± 2.6 | 1.8 ± 0.6 | 41.2 ± 2.7 | <0.001 | 0.026 ± 0.007 | 39 |
| 2 μ -SS | 0.94 ± 0.08 | 0.12 ± 0.05 | 1.5 ± 1.3 | 2.5 ± 1.3 | 2.32 ± 0.33 | 0.70 ± 0.10 | 9 |
| 3 ℓ -Z-2b4j | 1.08 ± 0.25 | 0.5 ± 0.4 | <0.001 | 1.6 ± 0.5 | 0.065 ± 0.013 | 5.5 ± 0.7 | 8 |
| 3 ℓ -Z-1b4j | 1.14 ± 0.24 | 3.3 ± 2.2 | 2.2 ± 1.7 | 6.7 ± 2.8 | 0.036 ± 0.011 | 4.3 ± 0.6 | 7 |
| 3 ℓ -Z-2b3j | 0.58 ± 0.19 | 0.22 ± 0.18 | <0.001 | 0.80 ± 0.26 | 0.083 ± 0.014 | 1.93 ± 0.28 | 4 |
| 3 ℓ -noZ-2b | 0.95 ± 0.11 | 0.14 ± 0.12 | 3.6 ± 2.2 | 4.7 ± 2.2 | 1.59 ± 0.28 | 1.45 ± 0.20 | 10 |
| 4 ℓ -SF-1b | 0.212 ± 0.032 | 0.09 ± 0.07 | 0.113 ± 0.022 | 0.42 ± 0.08 | <0.001 | 0.66 ± 0.09 | 1 |
| 4 ℓ -SF-2b | 0.121 ± 0.021 | 0.07 ± 0.06 | 0.062 ± 0.012 | 0.25 ± 0.07 | <0.001 | 0.63 ± 0.09 | 1 |
| 4 ℓ -DF-1b | 0.25 ± 0.04 | 0.0131 ± 0.0032 | 0.114 ± 0.019 | 0.37 ± 0.04 | <0.001 | 0.75 ± 0.10 | 2 |
| 4 ℓ -DF-2b | 0.16 ± 0.05 | <0.001 | 0.063 ± 0.013 | 0.23 ± 0.05 | <0.001 | 0.64 ± 0.09 | 1 |

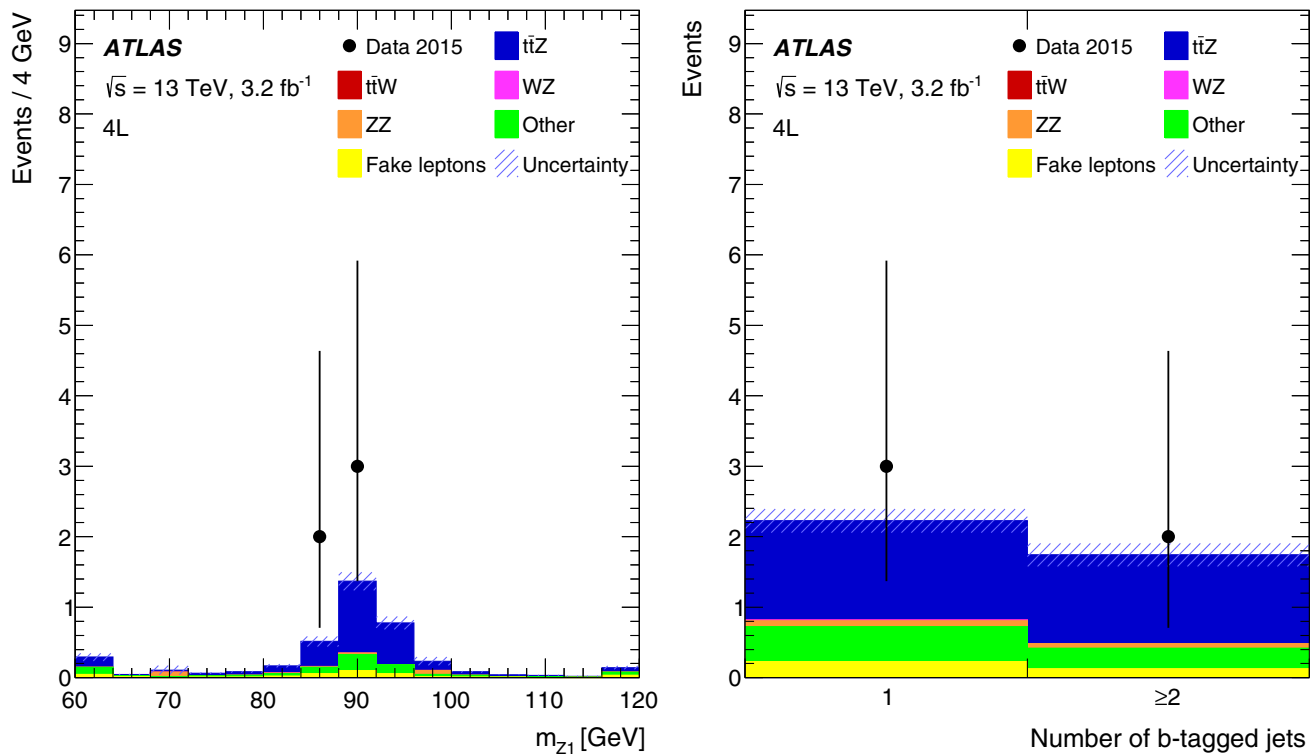


Fig. 6 Distributions (*left*) of the invariant mass of the OSSF lepton pair closest to the Z boson mass, m_{Z_1} , and (*right*) of the number of b -tagged jets, for events in the tetralepton signal regions. The distributions are shown before the fit. The background denoted ‘Other’ contains

other SM processes producing four prompt leptons. The shaded band represents the total uncertainty. The first and last bin of the distribution shown in the *left panel* include the underflow and overflow, respectively

6.3 Uncertainties in signal modelling

From the nominal MG5_aMC+PYTHIA 8 (A14 tune) configuration, two parameters are varied to investigate uncertainties from the modelling of the $t\bar{t}Z$ and $t\bar{t}W$ processes: the renormalisation (μ_R) and factorisation (μ_F) scales. A

simultaneous variation of $\mu_R = \mu_F$ by factors 2.0 and 0.5 is performed. In addition, the effects of a set of variations in the tune parameters (A14 eigentune variations), sensitive to initial- and final-state radiation, multiple parton interactions and colour reconnection, are evaluated. Studies performed at particle level show that the largest impact comes

from variations in initial-state radiation [26]. The systematic uncertainty due to the choice of generator for the $t\bar{t}Z$ and $t\bar{t}W$ signals is estimated by comparing the nominal sample with one generated with SHERPA v2.2. The SHERPA sample uses the LO matrix element with up to one (two) additional parton(s) included in the matrix element calculation for $t\bar{t}Z$ ($t\bar{t}W$) and merged with the SHERPA parton shower [72] using the ME+PS@LO prescription. The NNPDF3.0NLO PDF set is used in conjunction with a dedicated parton shower tune developed by the SHERPA authors. Signal modelling uncertainties are treated as correlated among channels.

6.4 Uncertainties in background modelling

In the trilepton and 2μ -SS channels, the diboson background is dominated by WZ production, while ZZ production is dominant in the tetralepton channel. While the inclusive cross sections for these processes are known to better than 10%, they contribute to the background in these channels if additional b -jets and other jets are produced and thus have a significantly larger uncertainty.

In the trilepton and 2μ -SS channels, the normalisation of the WZ background is treated as a free parameter in the fit used to extract the $t\bar{t}Z$ and $t\bar{t}W$ signals. The uncertainty in the extrapolation of the WZ background estimate from the control region to signal regions with specific jet and b -tag multiplicities is evaluated by comparing predictions obtained by varying the renormalisation, factorisation and resummation scales used in MC generation. The uncertainties vary across the different regions and an overall uncertainty of -50% and $+100\%$ is used.

The normalisation of the ZZ background is treated as a free parameter in the fit used to extract the $t\bar{t}Z$ and $t\bar{t}W$ signals. In the tetralepton channel, several uncertainties in the ZZ background estimate are considered. They arise from the extrapolation from the 4ℓ -ZZ-CR control region (corresponding to on-shell ZZ production) to the signal region (with off-shell ZZ background) and from the extrapolation from the control region without jets to the signal region with at least one jet. They are found to be 30% and 20%, respectively. An additional uncertainty of 10–30% is assigned to the normalisation of the heavy-flavour content of the ZZ background, based on a data-to-simulation comparison of events with one Z boson and additional jets and cross-checked with a comparison between different ZZ simulations [11].

The uncertainty in the $t\bar{t}H$ background is evaluated by varying the factorisation and renormalisation scales up and down by a factor of two with respect to the nominal value, $H_T/2$, where H_T is defined as the scalar sum of the transverse masses $\sqrt{p_T^2 + m^2}$ of all final state particles.

For the tZ background, an overall normalisation uncertainty of 50% is assumed. An additional uncertainty affecting

the distribution of this background as a function of jet and b -jet multiplicity is evaluated by varying the factorisation and renormalisation scales, as well as the amount of radiation in the Perugia2012 parton-shower tune.

An uncertainty of $+10\%$ and -22% is assigned to the tWZ background cross section. The uncertainty is asymmetric due to an alternative estimate of the interference effect between this process and the $t\bar{t}Z$ production. The shape uncertainty is evaluated by varying the factorisation and renormalisation scales up and down by a factor of two with respect to the nominal value $H_T/2$.

For other prompt-lepton backgrounds, uncertainties of 20% are assigned to the normalisations of the WH and ZH processes, based on calculations from Ref. [73]. An uncertainty of 50% is considered for triboson and same-sign WW processes.

The fake-lepton background uncertainty is evaluated as follows. The uncertainty due to the matrix method is estimated by propagating the statistical uncertainty on the measurement of the fake-lepton efficiencies. Additionally, a 20% uncertainty is added to the subtracted charge-flip yields estimated as the difference between data-driven charge-flips and simulation, and the E_T^{miss} requirement used to enhance the single-fake-lepton fraction is varied by 20 GeV. The main sources of fake muons are decays of light-flavour or heavy-flavour hadrons inside jets. For the 2μ -SS region, the flavour composition of the jets faking leptons is assumed to be unknown. To cover this uncertainty, the central values of the fake-lepton efficiencies extracted from the b -veto and the b -tag control regions are used, with the efficiency difference assigned as an extra uncertainty. For the tetralepton channel, fake-lepton systematic uncertainties are covered by the scale-factor uncertainties used to calibrate the simulated fake-lepton yield in the control regions. Within a fake-lepton estimation method, all systematic uncertainties are considered to be correlated among analysis channels and regions. Thus 2μ -SS and trilepton fake-lepton systematic uncertainties that use the matrix method are not correlated with the tetralepton systematic uncertainties. The expected uncertainties in the fake-lepton backgrounds relative to the total backgrounds vary in each channel and signal region: 50% for the 2μ -SS region, 25–50% for the trilepton channel and 5–10% for the tetralepton channel.

7 Results

In order to extract the $t\bar{t}Z$ and $t\bar{t}W$ cross sections, nine signal regions (2μ -SS, 3ℓ -Z-1b4j, 3ℓ -Z-2b3j, 3ℓ -Z-2b4j, 3ℓ -noZ-2b, 4ℓ -DF-1b, 4ℓ -DF-2b, 4ℓ -SF-1b, 4ℓ -SF-2b) and two control regions (3ℓ -WZ-CR, 4ℓ -ZZ-CR) are simultaneously fitted. The 2μ -SS signal region is particularly sensitive to $t\bar{t}W$, the 3ℓ -noZ-2b signal region is sensitive to both, $t\bar{t}W$

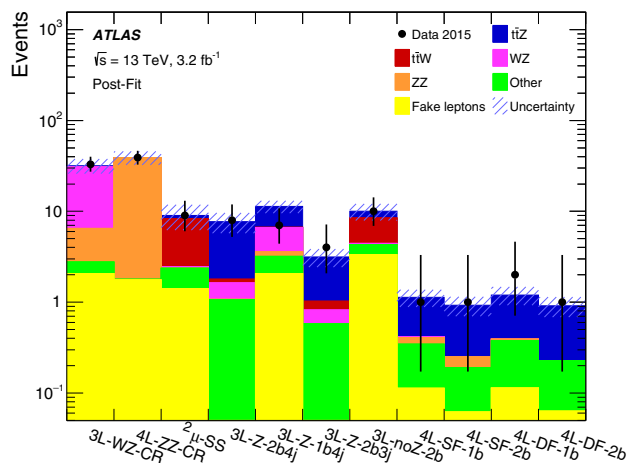


Fig. 7 Expected yields after the fit compared to data for the fit to extract $\sigma_{t\bar{t}Z}$ and $\sigma_{t\bar{t}W}$ in the signal regions and in the control regions used to constrain the WZ and ZZ backgrounds. The ‘Other’ background summarises all other backgrounds described in Sect. 3. The shaded band represents the total uncertainty

and $t\bar{t}Z$, while all other signal regions aim at the determination of the $t\bar{t}Z$ cross section. The cross sections $\sigma_{t\bar{t}Z}$ and $\sigma_{t\bar{t}W}$ are determined using a binned maximum-likelihood fit to the numbers of events in these regions. The fit is based on the profile-likelihood technique, where systematic uncertainties are allowed to vary as nuisance parameters and take on their best-fit values. None of the uncertainties are found to be significantly constrained or pulled from their initial values. The calculation of confidence intervals and hypothesis testing is performed using a modified frequentist method as implemented in RooStats [74, 75].

A summary of the fit to all regions used to measure the $t\bar{t}Z$ and $t\bar{t}W$ production cross sections are shown in Fig. 7. The normalisation corrections for the WZ and ZZ backgrounds with respect to the Standard Model predictions are obtained from the fits as described in Sect. 5 and found to be compatible with unity: 1.11 ± 0.30 for the WZ background and 0.94 ± 0.17 for the ZZ background.

The results of the fit are $\sigma_{t\bar{t}Z} = 0.92 \pm 0.29$ (stat.) ± 0.10 (syst.) pb and $\sigma_{t\bar{t}W} = 1.50 \pm 0.72$ (stat.) ± 0.33 (syst.) pb with a correlation of -0.13 and are shown in Fig. 8. The fit yields significances of 3.9σ and 2.2σ over the background-only hypothesis for the $t\bar{t}Z$ and $t\bar{t}W$ processes, respectively. The expected significances are 3.4σ for $t\bar{t}Z$ and 1.0σ for $t\bar{t}W$ production. The significance values are computed using the asymptotic approximation described in Ref. [76]. In the two channels most sensitive to the $t\bar{t}W$ signal the observed relative number of events with two positively or two negatively charged leptons is compatible with expectation. In the 3ℓ -noZ-2b channel the observed distribution of the number of events with a given amount of electrons and muons match expectation, as well.

Table 5 shows the leading and total uncertainties in the measured $t\bar{t}Z$ and $t\bar{t}W$ cross sections. In estimating the

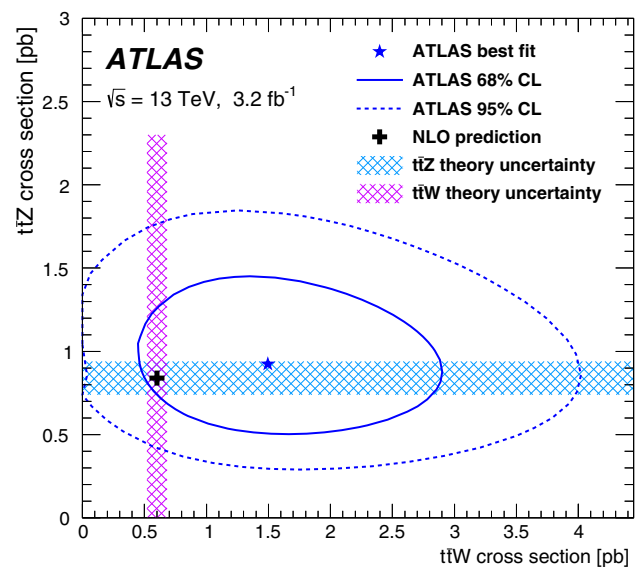


Fig. 8 The result of the simultaneous fit to the $t\bar{t}Z$ and $t\bar{t}W$ cross sections along with the 68 and 95% confidence level (CL) contours. The shaded areas correspond to the theoretical uncertainties in the Standard Model predictions, and include renormalisation and factorisation scale uncertainties as well as PDF uncertainties including α_S variations

Table 5 List of dominant and total uncertainties in the measured cross sections of the $t\bar{t}Z$ and $t\bar{t}W$ processes from the fit. All uncertainties are symmetrised

| Uncertainty | $\sigma_{t\bar{t}Z}(\%)$ | $\sigma_{t\bar{t}W}(\%)$ |
|-------------------------------|--------------------------|--------------------------|
| Luminosity | 2.6 | 3.1 |
| Reconstructed objects | 8.3 | 9.3 |
| Backgrounds from simulation | 5.3 | 3.1 |
| Fake leptons and charge misID | 3.0 | 19 |
| Signal modelling | 2.3 | 4.2 |
| Total systematic | 11 | 22 |
| Statistical | 31 | 48 |
| Total | 32 | 53 |

uncertainties for $t\bar{t}Z$ ($t\bar{t}W$), the cross section for $t\bar{t}W$ ($t\bar{t}Z$) is fixed to its Standard Model value. For both processes, the precision of the measurement is dominated by statistical uncertainties. For the $t\bar{t}Z$ determination, the different sources contribute with similar size to the total systematic uncertainty. For the $t\bar{t}W$ determination, the dominant systematic uncertainty source is the limited amount of data available for the estimation of the fake leptons.

8 Conclusion

Measurements of the production cross sections of a top-quark pair in association with a Z or W boson using 3.2 fb^{-1} of

data collected by the ATLAS detector in $\sqrt{s} = 13$ TeV pp collisions at the LHC are presented. Final states with either two same-charge muons, or three or four leptons are analysed. From a simultaneous fit to nine signal regions and two control regions, the $t\bar{t}Z$ and $t\bar{t}W$ production cross sections are determined to be $\sigma_{t\bar{t}Z} = 0.9 \pm 0.3$ pb and $\sigma_{t\bar{t}W} = 1.5 \pm 0.8$ pb. Both measurements are consistent with the NLO QCD theoretical calculations, $\sigma_{t\bar{t}Z} = 0.84 \pm 0.09$ pb and $\sigma_{t\bar{t}W} = 0.60 \pm 0.08$ pb.

Acknowledgements We thank CERN for the very successful operation of the LHC, as well as the support staff from our institutions without whom ATLAS could not be operated efficiently.

We acknowledge the support of ANPCyT, Argentina; YerPhI, Armenia; ARC, Australia; BMWFW and FWF, Austria; ANAS, Azerbaijan; SSTC, Belarus; CNPq and FAPESP, Brazil; NSERC, NRC and CFI, Canada; CERN; CONICYT, Chile; CAS, MOST and NSFC, China; COLCIENCIAS, Colombia; MSMT CR, MPO CR and VSC CR, Czech Republic; DNRF and DNSRC, Denmark; IN2P3-CNRS, CEA-DSM/IRFU, France; GNSF, Georgia; BMBF, HGF, and MPG, Germany; GSRT, Greece; RGC, Hong Kong SAR, China; ISF, I-CORE and Benoziyo Center, Israel; INFN, Italy; MEXT and JSPS, Japan; CNRST, Morocco; FOM and NWO, Netherlands; RCN, Norway; MNiSW and NCN, Poland; FCT, Portugal; MNE/IFA, Romania; MES of Russia and NRC KI, Russian Federation; JINR; MESTD, Serbia; MSSR, Slovakia; ARRS and MIZŠ, Slovenia; DST/NRF, South Africa; MINECO, Spain; SRC and Wallenberg Foundation, Sweden; SERI, SNSF and Cantons of Bern and Geneva, Switzerland; MOST, Taiwan; TAEK, Turkey; STFC, United Kingdom; DOE and NSF, United States of America. In addition, individual groups and members have received support from BCKDF, the Canada Council, CANARIE, CRC, Compute Canada, FQRNT, and the Ontario Innovation Trust, Canada; EPLANET, ERC, FP7, Horizon 2020 and Marie Skłodowska-Curie Actions, European Union; Investissements d'Avenir Labex and Idex, ANR, Région Auvergne and Fondation Partager le Savoir, France; DFG and AvH Foundation, Germany; Herakleitos, Thales and Aristeia programmes co-financed by EU-ESF and the Greek NSRF; BSF, GIF and Minerva, Israel; BRF, Norway; Generalitat de Catalunya, Generalitat Valenciana, Spain; the Royal Society and Leverhulme Trust, United Kingdom.

The crucial computing support from all WLCG partners is acknowledged gratefully, in particular from CERN, the ATLAS Tier-1 facilities at TRIUMF (Canada), NDGF (Denmark, Norway, Sweden), CC-IN2P3 (France), KIT/GridKA (Germany), INFN-CNAF (Italy), NL-T1 (Netherlands), PIC (Spain), ASGC (Taiwan), RAL (UK) and BNL (USA), the Tier-2 facilities worldwide and large non-WLCG resource providers. Major contributors of computing resources are listed in Ref. [77].

Open Access This article is distributed under the terms of the Creative Commons Attribution 4.0 International License (<http://creativecommons.org/licenses/by/4.0/>), which permits unrestricted use, distribution, and reproduction in any medium, provided you give appropriate credit to the original author(s) and the source, provide a link to the Creative Commons license, and indicate if changes were made. Funded by SCOAP³.

References

1. ATLAS Collaboration, Measurement of the $t\bar{t}$ production cross-section using $e\mu$ events with b -tagged jets in pp collisions at $\sqrt{s} = 13$ TeV with the ATLAS detector. Phys. Lett. B **761**, 136 (2016). doi:[10.1016/j.physletb.2016.08.019](https://doi.org/10.1016/j.physletb.2016.08.019), arXiv:[1606.02699](https://arxiv.org/abs/1606.02699) [hep-ex]
2. CMS Collaboration, Measurement of the top quark pair production cross section in proton-proton collisions at $\sqrt{s} = 13$ TeV. Phys. Rev. Lett. **116**, 052002 (2016). doi:[10.1103/PhysRevLett.116.052002](https://doi.org/10.1103/PhysRevLett.116.052002), arXiv:[1510.05302](https://arxiv.org/abs/1510.05302) [hep-ex]
3. J.A. Aguilar-Saavedra, Identifying top partners at LHC. JHEP **11**, 030 (2009). doi:[10.1088/1126-6708/2009/11/030](https://doi.org/10.1088/1126-6708/2009/11/030), arXiv:[0907.3155](https://arxiv.org/abs/0907.3155) [hep-ph]
4. J.A. Aguilar-Saavedra et al., Handbook of vectorlike quarks: mixing and single production. Phys. Rev. D **88**, 094010 (2013). doi:[10.1103/PhysRevD.88.094010](https://doi.org/10.1103/PhysRevD.88.094010), arXiv:[1306.0572](https://arxiv.org/abs/1306.0572) [hep-ph]
5. M. Perelstein, Little Higgs models and their phenomenology. Prog. Part. Nucl. Phys. **58**, 247 (2007). doi:[10.1016/j.pnpnp.2006.04.001](https://doi.org/10.1016/j.pnpnp.2006.04.001), arXiv:[hep-ph/0512128](https://arxiv.org/abs/hep-ph/0512128)
6. R.S. Chivukula, S.B. Selipsky, E.H. Simmons, Nonoblique effects in the $Zb\bar{b}$ vertex from ETC dynamics. Phys. Rev. Lett. **69**, 575 (1992). doi:[10.1103/PhysRevLett.69.575](https://doi.org/10.1103/PhysRevLett.69.575), arXiv:[hep-ph/9204214](https://arxiv.org/abs/hep-ph/9204214)
7. R.S. Chivukula, E.H. Simmons, J. Terning, A heavy top quark and the $Zb\bar{b}$ vertex in noncommuting extended technicolor. Phys. Lett. B **331**, 383 (1994). doi:[10.1016/0370-2693\(94\)91068-5](https://doi.org/10.1016/0370-2693(94)91068-5), arXiv:[hep-ph/9404209](https://arxiv.org/abs/hep-ph/9404209)
8. K. Hagiwara, N. Kitazawa, Extended technicolor contribution to the $Zb\bar{b}$ vertex. Phys. Rev. D **52**, 5374 (1995). doi:[10.1103/PhysRevD.52.5374](https://doi.org/10.1103/PhysRevD.52.5374), arXiv:[hep-ph/9504332](https://arxiv.org/abs/hep-ph/9504332)
9. U. Mahanta, Noncommuting ETC corrections to $Zt\bar{t}$ vertex. Phys. Rev. D **55**, 5848 (1997). doi:[10.1103/PhysRevD.55.5848](https://doi.org/10.1103/PhysRevD.55.5848), arXiv:[hep-ph/9611289](https://arxiv.org/abs/hep-ph/9611289)
10. U. Mahanta, Probing noncommuting ETC effects by $e^+e^- \rightarrow t\bar{t}$ at NLC. Phys. Rev. D **56**, 402 (1997). doi:[10.1103/PhysRevD.56.402](https://doi.org/10.1103/PhysRevD.56.402)
11. ATLAS Collaboration, Measurement of the $t\bar{t}W$ and $t\bar{t}Z$ production cross sections in pp collisions at $\sqrt{s} = 8$ TeV with the ATLAS detector. JHEP **11**, 172 (2015). doi:[10.1007/JHEP11\(2015\)172](https://doi.org/10.1007/JHEP11(2015)172), arXiv:[1509.05276](https://arxiv.org/abs/1509.05276) [hep-ex]
12. CMS Collaboration, Observation of top quark pairs produced in association with a vector boson in pp collisions at $\sqrt{s} = 8$ TeV. JHEP **01**, 096 (2016). doi:[10.1007/JHEP01\(2016\)096](https://doi.org/10.1007/JHEP01(2016)096), arXiv:[1510.01131](https://arxiv.org/abs/1510.01131) [hep-ex]
13. S. Frixione et al., Electroweak and QCD corrections to top-pair hadroproduction in association with heavy bosons. JHEP **06**, 184 (2015). doi:[10.1007/JHEP06\(2015\)184](https://doi.org/10.1007/JHEP06(2015)184), arXiv:[1504.03446](https://arxiv.org/abs/1504.03446) [hep-ph]
14. J. Alwall et al., The automated computation of tree-level and next-to-leading order differential cross sections, and their matching to parton shower simulations. JHEP **07**, 079 (2014). doi:[10.1007/JHEP07\(2014\)079](https://doi.org/10.1007/JHEP07(2014)079), arXiv:[1405.0301](https://arxiv.org/abs/1405.0301) [hep-ph]
15. ATLAS Collaboration, The ATLAS experiment at the CERN Large Hadron Collider. JINST **3**, S08003 (2008). doi:[10.1088/1748-0221/3/08/S08003](https://doi.org/10.1088/1748-0221/3/08/S08003)
16. ATLAS Collaboration, ATLAS Insertable B-Layer Technical Design Report, ATLAS-TDR-19,2010. <http://cds.cern.ch/record/1291633>, ATLAS Insertable B-Layer Technical Design Report Addendum, ATLAS-TDR-19-ADD-1,2012. <http://cds.cern.ch/record/1451888>
17. ATLAS Collaboration, Luminosity determination in pp collisions at $\sqrt{s} = 8$ TeV using the ATLAS detector at the LHC. Eur. Phys. J. C **76**, 653 (2016). doi:[10.1140/epjc/s10052-016-4466-1](https://doi.org/10.1140/epjc/s10052-016-4466-1), arXiv:[1608.03953](https://arxiv.org/abs/1608.03953) [hep-ex]
18. D.J. Lange, The EvtGen particle decay simulation package. Nucl. Instrum. Meth. A **462**, 152 (2001). doi:[10.1016/S0168-9002\(01\)00089-4](https://doi.org/10.1016/S0168-9002(01)00089-4)
19. ATLAS Collaboration, The ATLAS simulation infrastructure. Eur. Phys. J. C **70**, 823 (2010). doi:[10.1140/epjc/s10052-010-1429-9](https://doi.org/10.1140/epjc/s10052-010-1429-9), arXiv:[1005.4568](https://arxiv.org/abs/1005.4568) [hep-ex]

20. S. Agostinelli et al., GEANT4—a simulation toolkit. Nucl. Instrum. Meth. A **506**, 250 (2003). doi:[10.1016/S0168-9002\(03\)01368-8](https://doi.org/10.1016/S0168-9002(03)01368-8)
21. ATLAS Collaboration, The simulation principle and performance of the ATLAS fast calorimeter simulation FastCaloSim, ATL-PHYS-PUB-2010-013 (2010). <http://cds.cern.ch/record/1300517>
22. T. Sjöstrand et al., An introduction to PYTHIA 8.2. Comput. Phys. Commun. **191**, 159 (2015). doi:[10.1016/j.cpc.2015.01.024](https://doi.org/10.1016/j.cpc.2015.01.024). arXiv:[1410.3012](https://arxiv.org/abs/1410.3012) [hep-ph]
23. ATLAS Collaboration, Further ATLAS tunes of PYTHIA 6 and PYTHIA 8, ATL-PHYS-PUB-2011-014 (2011). <http://cds.cern.ch/record/1400677>
24. ATLAS Collaboration, ATLAS PYTHIA 8 tunes to 7 TeV data, ATL-PHYS-PUB-2014-021 (2014). <http://cdsweb.cern.ch/record/1966419>
25. R.D. Ball et al., Parton distributions with LHC data. Nucl. Phys. B **867**, 244 (2013). doi:[10.1016/j.nuclphysb.2012.10.003](https://doi.org/10.1016/j.nuclphysb.2012.10.003). arXiv:[1207.1303](https://arxiv.org/abs/1207.1303) [hep-ph]
26. ATLAS Collaboration, Modelling of the $t\bar{t}H$ and $t\bar{t}V$ ($V = W, Z$) processes for $\sqrt{s} = 13$ TeV ATLAS analyses, ATL-PHYS-PUB-2016-005 (2016). <http://cds.cern.ch/record/2120826>
27. T. Sjöstrand, S. Mrenna, P.Z. Skands, PYTHIA 6.4 Physics and Manual. JHEP **05**, 026 (2006). doi:[10.1088/1126-6708/2006/05/026](https://doi.org/10.1088/1126-6708/2006/05/026), arXiv:[hep-ph/0603175](https://arxiv.org/abs/hep-ph/0603175)
28. J. Pumplin et al., New generation of parton distributions with uncertainties from global QCD analysis. JHEP **07**, 012 (2002). doi:[10.1088/1126-6708/2002/07/012](https://doi.org/10.1088/1126-6708/2002/07/012). arXiv:[hep-ph/0201195](https://arxiv.org/abs/hep-ph/0201195)
29. P.Z. Skands, Tuning Monte Carlo generators: the Perugia tunes. Phys. Rev. D **82**, 074018 (2010). doi:[10.1103/PhysRevD.82.074018](https://doi.org/10.1103/PhysRevD.82.074018). arXiv:[1005.3457](https://arxiv.org/abs/1005.3457) [hep-ph]
30. R.D. Ball et al., Parton distributions for the LHC Run II. JHEP **04**, 040 (2015). doi:[10.1007/JHEP04\(2015\)040](https://doi.org/10.1007/JHEP04(2015)040). arXiv:[1410.8849](https://arxiv.org/abs/1410.8849) [hep-ph]
31. T. Gleisberg et al., Event generation with SHERPA 1.1. JHEP **02**, 007 (2009). doi:[10.1088/1126-6708/2009/02/007](https://doi.org/10.1088/1126-6708/2009/02/007), arXiv:[0811.4622](https://arxiv.org/abs/0811.4622) [hep-ph]
32. T. Gleisberg, S. Höche, Comix, a new matrix element generator. JHEP **12**, 039 (2008). doi:[10.1088/1126-6708/2008/12/039](https://doi.org/10.1088/1126-6708/2008/12/039). arXiv:[0808.3674](https://arxiv.org/abs/0808.3674) [hep-ph]
33. F. Cascioli, P. Maierhofer, S. Pozzorini, Scattering amplitudes with open loops. Phys. Rev. Lett. **108**, 111601 (2012). doi:[10.1103/PhysRevLett.108.111601](https://doi.org/10.1103/PhysRevLett.108.111601). arXiv:[1111.5206](https://arxiv.org/abs/1111.5206) [hep-ph]
34. S. Höche et al., QCD matrix elements + parton showers: the NLO case. JHEP **04**, 027 (2013). doi:[10.1007/JHEP04\(2013\)027](https://doi.org/10.1007/JHEP04(2013)027). arXiv:[1207.5030](https://arxiv.org/abs/1207.5030) [hep-ph]
35. H.-L. Lai et al., New parton distributions for collider physics. Phys. Rev. D **82**, 074024 (2010). doi:[10.1103/PhysRevD.82.074024](https://doi.org/10.1103/PhysRevD.82.074024). arXiv:[1007.2241](https://arxiv.org/abs/1007.2241)
36. S. Alioli et al., A general framework for implementing NLO calculations in shower Monte Carlo programs: the POWHEG BOX. JHEP **06**, 043 (2010). doi:[10.1007/JHEP06043](https://doi.org/10.1007/JHEP06043). arXiv:[1002.2581](https://arxiv.org/abs/1002.2581) [hep-ph]
37. ATLAS Collaboration, Measurement of the Z/γ^* boson transverse momentum distribution in pp collisions at $\sqrt{s} = 7$ TeV with the ATLAS detector. JHEP **09**, 145 (2014). doi:[10.1007/JHEP09\(2014\)145](https://doi.org/10.1007/JHEP09(2014)145), arXiv:[1406.3660](https://arxiv.org/abs/1406.3660) [hep-ex]
38. M. Czakon, A. Mitov, Top++: a program for the calculation of the top-pair cross-section at hadron colliders. Comput. Phys. Commun. **185**, 2930 (2014). doi:[10.1016/j.cpc.2014.06.021](https://doi.org/10.1016/j.cpc.2014.06.021). arXiv:[1112.5675](https://arxiv.org/abs/1112.5675) [hep-ph]
39. E. Re, Single-top Wt-channel production matched with parton showers using the POWHEG method. Eur. Phys. J. C **71**, 1547 (2011). doi:[10.1140/epjc/s10052-011-1547-z](https://doi.org/10.1140/epjc/s10052-011-1547-z). arXiv:[1009.2450](https://arxiv.org/abs/1009.2450) [hep-ph]
40. D. de Florian et al., Handbook of LHC Higgs cross sections: 4. Deciphering the nature of the Higgs sector (2016). arXiv:[1610.07922](https://arxiv.org/abs/1610.07922) [hep-ph]
41. C. Anastasiou et al., High precision QCD at hadron colliders: Electroweak gauge boson rapidity distributions at NNLO. Phys. Rev. D **69**, 094008 (2004). doi:[10.1103/PhysRevD.69.094008](https://doi.org/10.1103/PhysRevD.69.094008). arXiv:[hep-ph/0312266](https://arxiv.org/abs/hep-ph/0312266)
42. R. Gavin et al., FEWZ 2.0: A code for hadronic Z production at next-to-next-to-leading order. Comput. Phys. Commun. **182**, 2388 (2011). doi:[10.1016/j.cpc.2011.06.008](https://doi.org/10.1016/j.cpc.2011.06.008). arXiv:[1011.3540](https://arxiv.org/abs/1011.3540) [hep-ph]
43. R. Gavin et al., W Physics at the LHC with FEWZ 2.1. Comput. Phys. Commun. **184**, 208 (2013). doi:[10.1016/j.cpc.2012.09.005](https://doi.org/10.1016/j.cpc.2012.09.005). arXiv:[1201.5896](https://arxiv.org/abs/1201.5896) [hep-ph]
44. Y. Li, F. Petriello, Combining QCD and electroweak corrections to dilepton production in FEWZ. Phys. Rev. D **86**, 094034 (2012). doi:[10.1103/PhysRevD.86.094034](https://doi.org/10.1103/PhysRevD.86.094034). arXiv:[1208.5967](https://arxiv.org/abs/1208.5967) [hep-ph]
45. V. Barger, W.-Y. Keung, B. Yencho, Triple-top signal of new physics at the LHC. Phys. Lett. B **687**, 70 (2010). doi:[10.1016/j.physletb.2010.03.001](https://doi.org/10.1016/j.physletb.2010.03.001). arXiv:[1001.0221](https://arxiv.org/abs/1001.0221) [hep-ph]
46. G. Bevilacqua, M. Worek, Constraining BSM Physics at the LHC: four top final states with NLO accuracy in perturbative QCD. JHEP **07**, 111 (2012). doi:[10.1007/JHEP07\(2012\)111](https://doi.org/10.1007/JHEP07(2012)111). arXiv:[1206.3064](https://arxiv.org/abs/1206.3064) [hep-ph]
47. ATLAS Collaboration, Electron reconstruction and identification efficiency measurements with the ATLAS detector using the 2011 LHC proton–proton collision data. Eur. Phys. J. C **74**, 2941 (2014). doi:[10.1140/epjc/s10052-014-2941-0](https://doi.org/10.1140/epjc/s10052-014-2941-0), arXiv:[1404.2240](https://arxiv.org/abs/1404.2240) [hep-ex]
48. ATLAS Collaboration, Electron efficiency measurements with the ATLAS detector using the 2012 LHC proton–proton collision data, ATLAS-CONF-2014-032 (2014). <http://cdsweb.cern.ch/record/1706245>
49. ATLAS Collaboration, Electron identification measurements in ATLAS using $\sqrt{s} = 13$ TeV data with 50 ns bunch spacing, ATL-PHYS-PUB-2015-041 (2015). <http://cdsweb.cern.ch/record/2048202>
50. ATLAS Collaboration, Muon reconstruction performance of the ATLAS detector in proton–proton collision data at $\sqrt{s} = 13$ TeV. Eur. Phys. J. C **76**, 292 (2016). doi:[10.1140/epjc/s10052-016-4120-y](https://doi.org/10.1140/epjc/s10052-016-4120-y), arXiv:[1603.05598](https://arxiv.org/abs/1603.05598) [hep-ex]
51. M. Cacciari, G.P. Salam, G. Soyez, The anti- k_t jet clustering algorithm. JHEP **04**, 063 (2008). doi:[10.1088/1126-6708/2008/04/063](https://doi.org/10.1088/1126-6708/2008/04/063). arXiv:[0802.1189](https://arxiv.org/abs/0802.1189) [hep-ph]
52. M. Cacciari, G.P. Salam, Dispelling the N^3 myth for the k_t jet-finder. Phys. Lett. B **641**, 57 (2006). doi:[10.1016/j.physletb.2006.08.037](https://doi.org/10.1016/j.physletb.2006.08.037). arXiv:[hep-ph/0512210](https://arxiv.org/abs/hep-ph/0512210)
53. ATLAS Collaboration, Topological cell clustering in the ATLAS calorimeters and its performance in LHC Run 1, (2016), arXiv:[1603.02934](https://arxiv.org/abs/1603.02934) [hep-ex]
54. M. Cacciari, G.P. Salam, G. Soyez, The catchment area of jets. JHEP **04**, 005 (2008). doi:[10.1088/1126-6708/2008/04/005](https://doi.org/10.1088/1126-6708/2008/04/005). arXiv:[0802.1188](https://arxiv.org/abs/0802.1188) [hep-ph]
55. ATLAS Collaboration, Jet global sequential corrections with the ATLAS detector in proton–proton collisions at $\sqrt{s} = 8$ TeV, ATLAS-CONF-2015-002 (2015). <http://cdsweb.cern.ch/record/2001682>
56. ATLAS Collaboration, Jet energy measurement with the ATLAS detector in proton–proton collisions at $\sqrt{s} = 7$ TeV, Eur. Phys. J. C **73** (2013) 2304, doi:[10.1140/epjc/s10052-013-2304-2](https://doi.org/10.1140/epjc/s10052-013-2304-2), arXiv:[1112.6426](https://arxiv.org/abs/1112.6426) [hep-ex]
57. ATLAS Collaboration, Monte Carlo calibration and combination of in-situ measurements of jet energy scale, jet energy resolution and jet mass in ATLAS, ATLAS-CONF-2015-037 (2015). <http://cdsweb.cern.ch/record/2044941>
58. ATLAS Collaboration, Jet calibration and systematic uncertainties for jets reconstructed in the ATLAS detector at $\sqrt{s} = 13$ TeV, ATL-PHYS-PUB-2015-015 (2015). <http://cds.cern.ch/record/2037613>

59. ATLAS Collaboration, Performance of pile-up mitigation techniques for jets in pp collisions at $\sqrt{s} = 8$ TeV using the ATLAS detector. *Eur. Phys. J. C* **76**, 581 (2016). doi:[10.1140/epjc/s10052-016-4395-1](https://doi.org/10.1140/epjc/s10052-016-4395-1), arXiv:[1510.03823](https://arxiv.org/abs/1510.03823) [hep-ex]
60. ATLAS Collaboration, Performance of b -jet identification in the ATLAS experiment. *JINST* **11**, P04008 (2016). doi:[10.1088/1748-0221/11/04/P04008](https://doi.org/10.1088/1748-0221/11/04/P04008), arXiv:[1512.01094](https://arxiv.org/abs/1512.01094) [hep-ex]
61. ATLAS Collaboration, Expected performance of the ATLAS b -tagging algorithms in Run-2, ATL-PHYS-PUB-2015-022 (2015). <http://cdsweb.cern.ch/record/2037697>
62. ATLAS Collaboration, Calibration of b -tagging using dileptonic top pair events in a combinatorial likelihood approach with the ATLAS experiment, ATLAS-CONF-2014-004 (2014). <http://cdsweb.cern.ch/record/1664335>
63. ATLAS Collaboration, Commissioning of the ATLAS b -tagging algorithms using $t\bar{t}$ events in early Run-2 data, ATL-PHYS-PUB-2015-039 (2015). <http://cdsweb.cern.ch/record/2047871>
64. ATLAS Collaboration, Performance of missing transverse momentum reconstruction in proton–proton collisions at $\sqrt{s} = 7$ TeV with ATLAS. *Eur. Phys. J. C* **72**, 1844 (2012). doi:[10.1140/epjc/s10052-011-1844-6](https://doi.org/10.1140/epjc/s10052-011-1844-6), arXiv:[1108.5602](https://arxiv.org/abs/1108.5602) [hep-ex]
65. ATLAS Collaboration, Performance of missing transverse momentum reconstruction with the ATLAS detector in the first proton–proton collisions at $\sqrt{s} = 13$ TeV, ATL-PHYS-PUB-2015-027 (2015). <http://cdsweb.cern.ch/record/2037904>
66. ATLAS Collaboration, Expected performance of missing transverse momentum reconstruction for the ATLAS detector at $\sqrt{s} = 13$ TeV, ATL-PHYS-PUB-2015-023 (2015). <http://cdsweb.cern.ch/record/2037700>
67. ATLAS Collaboration, Measurement of the top quark-pair production cross section with ATLAS in pp collisions at $\sqrt{s} = 7$ TeV. *Eur. Phys. J. C* **71** (2011) 1577. doi:[10.1140/epjc/s10052-011-1577-6](https://doi.org/10.1140/epjc/s10052-011-1577-6), arXiv:[1012.1792](https://arxiv.org/abs/1012.1792) [hep-ex]
68. ATLAS Collaboration, Improved luminosity determination in pp collisions at $\sqrt{s} = 7$ TeV using the ATLAS detector at the LHC. *Eur. Phys. J. C* **73** (2013) 2518, doi:[10.1140/epjc/s10052-013-2518-3](https://doi.org/10.1140/epjc/s10052-013-2518-3), arXiv:[1302.4393](https://arxiv.org/abs/1302.4393) [hep-ex]
69. ATLAS Collaboration, Expected electron performance in the ATLAS experiment, ATL-PHYS-PUB-2011-006 (2011). <http://cdsweb.cern.ch/record/1345327>
70. ATLAS Collaboration, Jet energy measurement and its systematic uncertainty in proton–proton collisions at $\sqrt{s} = 7$ TeV with the ATLAS detector. *Eur. Phys. J. C* **75**, 17 (2015). doi:[10.1140/epjc/s10052-014-3190-y](https://doi.org/10.1140/epjc/s10052-014-3190-y), arXiv:[1406.0076](https://arxiv.org/abs/1406.0076) [hep-ex]
71. ATLAS Collaboration, Calibration of the performance of b -tagging for c and light-flavour jets in the 2012 ATLAS data, ATLAS-CONF-2014-046 (2014). <http://cdsweb.cern.ch/record/1741020>
72. S. Schumann, F. Krauss, A parton shower algorithm based on Catani–Seymour dipole factorisation. *JHEP* **03**, 038 (2008). doi:[10.1088/1126-6708/2008/03/038](https://doi.org/10.1088/1126-6708/2008/03/038), arXiv:[0709.1027](https://arxiv.org/abs/0709.1027) [hep-ph]
73. S. Heinemeyer et al., Handbook of LHC Higgs cross sections: 3. Higgs Properties. arXiv:[1307.1347](https://arxiv.org/abs/1307.1347) [hep-ph]
74. W. Verkerke, D. Kirkby, 'The RooFit toolkit for data modeling'. arXiv:[physics/0306116](https://arxiv.org/abs/physics/0306116)
75. W. Verkerke, D. Kirkby, RooFit Users Manual v2.91. <http://rootfit.sourceforge.net>
76. G. Cowan et al., Asymptotic formulae for likelihood-based tests of new physics. *Eur. Phys. J. C* **71** (2011) 1554 (Erratum: *C* **73** (2013) 2501, doi:[10.1140/epjc/s10052-011-1554-0](https://doi.org/10.1140/epjc/s10052-011-1554-0), [10.1140/epjc/s10052-013-2501-z](https://doi.org/10.1140/epjc/s10052-013-2501-z), arXiv:[1007.1727](https://arxiv.org/abs/1007.1727))
77. ATLAS Collaboration, ATLAS computing acknowledgements 2016–2017, ATL-GEN-PUB-2016-002 (2016). <http://cds.cern.ch/record/2202407>

ATLAS Collaboration

M. Aaboud^{137d}, G. Aad⁸⁸, B. Abbott¹¹⁵, J. Abdallah⁶⁶, O. Abdinov¹², B. Abeloos¹¹⁹, R. Aben¹⁰⁹, O. S. AbouZeid¹³⁹, N. L. Abraham¹⁵³, H. Abramowicz¹⁵⁷, H. Abreu¹⁵⁶, R. Abreu¹¹⁸, Y. Abulaiti^{150a,150b}, B. S. Acharya^{167a,167b,a}, L. Adamczyk^{40a}, D. L. Adams²⁷, J. Adelman¹¹⁰, S. Adomeit¹⁰², T. Adye¹³³, A. A. Affolder⁷⁷, T. Agatonovic-Jovin¹⁴, J. Agricola⁵⁶, J. A. Aguilar-Saavedra^{128a,128f}, S. P. Ahlen²⁴, F. Ahmadov^{68,b}, G. Aielli^{135a,135b}, H. Akerstedt^{150a,150b}, T. P. A. Åkesson⁸⁴, A. V. Akimov⁹⁸, G. L. Alberghi^{22a,22b}, J. Albert¹⁷², S. Albrand⁵⁷, M. J. Alconada Verzini⁷⁴, M. Aleksa³², I. N. Aleksandrov⁶⁸, C. Alexa^{28b}, G. Alexander¹⁵⁷, T. Alexopoulos¹⁰, M. Alhroob¹¹⁵, B. Ali¹³⁰, M. Aliev^{76a,76b}, G. Alimonti^{94a}, J. Alison³³, S. P. Alkire³⁷, B. M. M. Allbrooke¹⁵³, B. W. Allen¹¹⁸, P. P. Allport¹⁹, A. Aloisio^{106a,106b}, A. Alonso³⁸, F. Alonso⁷⁴, C. Alpigiani¹⁴⁰, M. Alstady⁸⁸, B. Alvarez Gonzalez³², D. Álvarez Piqueras¹⁷⁰, M. G. Alvigi^{106a,106b}, B. T. Amadio¹⁶, K. Amako⁶⁹, Y. Amaral Coutinho^{26a}, C. Amelung²⁵, D. Amidei⁹², S. P. Amor Dos Santos^{128a,128c}, A. Amorim^{128a,128b}, S. Amoroso³², G. Amundsen²⁵, C. Anastopoulos¹⁴³, L. S. Ancu⁵¹, N. Andari¹¹⁰, T. Andeen¹¹, C. F. Anders^{61b}, G. Anders³², J. K. Anders⁷⁷, K. J. Anderson³³, A. Andreazza^{94a,94b}, V. Andrei^{61a}, S. Angelidakis⁹, I. Angelozzi¹⁰⁹, P. Anger⁴⁶, A. Angerami³⁷, F. Anghinolfi³², A. V. Anisenkov^{111,c}, N. Anjos¹³, A. Annovi^{126a,126b}, C. Antel^{61a}, M. Antonelli⁴⁹, A. Antonov^{100,*}, F. Anulli^{134a}, M. Aoki⁶⁹, L. Aperio Bella¹⁹, G. Arabidze⁹³, Y. Arai⁶⁹, J. P. Araque^{128a}, A. T. H. Arce⁴⁷, F. A. Arduh⁷⁴, J.-F. Arguin⁹⁷, S. Argyropoulos⁶⁶, M. Arik^{20a}, A. J. Armbruster¹⁴⁷, L. J. Armitage⁷⁹, O. Arnaez³², H. Arnold⁵⁰, M. Arratia³⁰, O. Arslan²³, A. Artamonov⁹⁹, G. Artoni¹²², S. Artz⁸⁶, S. Asai¹⁵⁹, N. Asbah⁴⁴, A. Ashkenazi¹⁵⁷, B. Åsman^{150a,150b}, L. Asquith¹⁵³, K. Assamagan²⁷, R. Astalos^{148a}, M. Atkinson¹⁶⁹, N. B. Atlay¹⁴⁵, K. Augsten¹³⁰, G. Avolio³², B. Axen¹⁶, M. K. Ayoub¹¹⁹, G. Azuelos^{97,d}, M. A. Baak³², A. E. Baas^{61a}, M. J. Baca¹⁹, H. Bachacou¹³⁸, K. Bachas^{76a,76b}, M. Backes³², M. Backhaus³², P. Bagiacchi^{134a,134b}, P. Bagnaia^{134a,134b}, Y. Bai^{35a}, J. T. Baines¹³³, O. K. Baker¹⁷⁹, E. M. Baldin^{111,c}, P. Balek¹³¹, T. Balestri¹⁵², F. Balli¹³⁸, W. K. Balunas¹²⁴, E. Banas⁴¹, Sw. Banerjee^{176,e}, A. A. E. Bannoura¹⁷⁸, L. Barak³², E. L. Barberio⁹¹, D. Barberis^{52a,52b}, M. Barbero⁸⁸, T. Barillari¹⁰³, T. Barklow¹⁴⁷, N. Barlow³⁰, S. L. Barnes⁸⁷, B. M. Barnett¹³³, R. M. Barnett¹⁶, Z. Barnovska-Blenessy⁵, A. Baroncelli^{136a}, G. Barone²⁵, A. J. Barr¹²², L. Barranco Navarro¹⁷⁰, F. Barreiro⁸⁵, J. Barreiro Guimarães da Costa^{35a}, R. Bartoldus¹⁴⁷, A. E. Barton⁷⁵, P. Bartos^{148a}, A. Basalae¹²⁵, A. Bassalat^{119,f},

R. L. Bates⁵⁵, S. J. Batista¹⁶², J. R. Batley³⁰, M. Battaglia¹³⁹, M. Bauce^{134a,134b}, F. Bauer¹³⁸, H. S. Bawa^{147,g}, J. B. Beacham¹¹³, M. D. Beattie⁷⁵, T. Beau⁸³, P. H. Beauchemin¹⁶⁵, P. Bechtel²³, H. P. Beck^{18,h}, K. Becker¹²², M. Becker⁸⁶, M. Beckingham¹⁷³, C. Becot¹¹², A. J. Beddall^{20d}, A. Beddall^{20b}, V. A. Bednyakov⁶⁸, M. Bedognetti¹⁰⁹, C. P. Bee¹⁵², L. J. Beemster¹⁰⁹, T. A. Beermann³², M. Begel²⁷, J. K. Behr⁴⁴, C. Belanger-Champagne⁹⁰, A. S. Bell⁸¹, G. Bella¹⁵⁷, L. Bellagamba^{22a}, A. Bellerive³¹, M. Bellomo⁸⁹, K. Belotskiy¹⁰⁰, O. Beltramello³², N. L. Belyaev¹⁰⁰, O. Benary^{157,*}, D. Benchechrout^{137a}, M. Bender¹⁰², K. Bendtz^{150a,150b}, N. Benekos¹⁰, Y. Benhammou¹⁵⁷, E. Benhar Nocchioli¹⁷⁹, J. Benitez⁶⁶, D. P. Benjamin⁴⁷, J. R. Bensinger²⁵, S. Bentvelsen¹⁰⁹, L. Beresford¹²², M. Beretta⁴⁹, D. Berge¹⁰⁹, E. Bergeas Kuutmann¹⁶⁸, N. Berger⁵, J. Beringer¹⁶, S. Berlendis⁵⁷, N. R. Bernard⁸⁹, C. Bernius¹¹², F. U. Bernlochner²³, T. Berry⁸⁰, P. Berta¹³¹, C. Bertella⁸⁶, G. Bertoli^{150a,150b}, F. Bertolucci^{126a,126b}, I. A. Bertram⁷⁵, C. Bertsche⁴⁴, D. Bertsche¹¹⁵, G. J. Besjes³⁸, O. Bessidskaia Bylund^{150a,150b}, M. Bessner⁴⁴, N. Besson¹³⁸, C. Betancourt⁵⁰, S. Bethke¹⁰³, A. J. Bevan⁷⁹, W. Bhimji¹⁶, R. M. Bianchi¹²⁷, L. Bianchini²⁵, M. Bianco³², O. Biebel¹⁰², D. Biedermann¹⁷, R. Bielski⁸⁷, N. V. Biesuz^{126a,126b}, M. Biglietti^{136a}, J. Bilbao De Mendizabal⁵¹, H. Bilokon⁴⁹, M. Bindi⁵⁶, S. Binet¹¹⁹, A. Bingul^{20b}, C. Bini^{134a,134b}, S. Biondi^{22a,22b}, D. M. Bjergaard⁴⁷, C. W. Black¹⁵⁴, J. E. Black¹⁴⁷, K. M. Black²⁴, D. Blackburn¹⁴⁰, R. E. Blair⁶, J.-B. Blanchard¹³⁸, J. E. Blanco⁸⁰, T. Blazek^{148a}, I. Bloch⁴⁴, C. Blocker²⁵, W. Blum^{86,*}, U. Blumenschein⁵⁶, S. Blunier^{34a}, G. J. Bobbink¹⁰⁹, V. S. Bobrovnikov^{111,c}, S. S. Bocchetta⁸⁴, A. Bocci⁴⁷, C. Bock¹⁰², M. Boehler⁵⁰, D. Boerner¹⁷⁸, J. A. Bogaerts³², D. Bogavac¹⁴, A. G. Bogdanchikov¹¹¹, C. Bohm^{150a}, V. Boisvert⁸⁰, P. Bokan¹⁴, T. Bold^{40a}, A. S. Boldyrev^{167a,167c}, M. Bomben⁸³, M. Bona⁷⁹, M. Boonekamp¹³⁸, A. Borisov¹³², G. Borissov⁷⁵, J. Bortfeldt³², D. Bortoletto¹²², V. Bortolotto^{63a,63b,63c}, K. Bos¹⁰⁹, D. Boscherini^{22a}, M. Bosman¹³, J. D. Bossio Sola²⁹, J. Boudreau¹²⁷, J. Bouffard², E. V. Bouhova-Thacker⁷⁵, D. Boumediene³⁶, C. Bourdarios¹¹⁹, S. K. Boutle⁵⁵, A. Boveia³², J. Boyd³², I. R. Boyko⁶⁸, J. Bracinik¹⁹, A. Brandt⁸, G. Brandt⁵⁶, O. Brandt^{61a}, U. Bratzler¹⁶⁰, B. Brau⁸⁹, J. E. Brau¹¹⁸, H. M. Braun^{178,*}, W. D. Breaden Madden⁵⁵, K. Brendlinger¹²⁴, A. J. Brennan⁹¹, L. Brenner¹⁰⁹, R. Brenner¹⁶⁸, S. Bressler¹⁷⁵, T. M. Bristow⁴⁸, D. Britton⁵⁵, D. Britzger⁴⁴, F. M. Brochu³⁰, I. Brock²³, R. Brock⁹³, G. Brooijmans³⁷, T. Brooks⁸⁰, W. K. Brooks^{34b}, J. Brosamer¹⁶, E. Brost¹¹⁸, J. H. Broughton¹⁹, P. A. Bruckman de Renstrom⁴¹, D. Bruncko^{148b}, R. Bruneliere⁵⁰, A. Bruni^{22a}, G. Bruni^{22a}, L. S. Bruni¹⁰⁹, B. H. Brunt³⁰, M. Bruschi^{22a}, N. Bruscinò²³, P. Bryant³³, L. Bryngemark⁸⁴, T. Buanes¹⁵, Q. Buat¹⁴⁶, P. Buchholz¹⁴⁵, A. G. Buckley⁵⁵, I. A. Budagov⁶⁸, F. Buehrer⁵⁰, M. K. Bugge¹²¹, O. Bulekov¹⁰⁰, D. Bullock⁸, H. Burckhart³², S. Burdin⁷⁷, C. D. Burgard⁵⁰, B. Burghgrave¹¹⁰, K. Burka⁴¹, S. Burke¹³³, I. Burmeister⁴⁵, J. T. P. Burr¹²², E. Busato³⁶, D. Büscher⁵⁰, V. Büscher⁸⁶, P. Bussey⁵⁵, J. M. Butler²⁴, C. M. Buttar⁵⁵, J. M. Butterworth⁸¹, P. Butti¹⁰⁹, W. Buttinger²⁷, A. Buzatu⁵⁵, A. R. Buzykaev^{111,c}, S. Cabrera Urbán¹⁷⁰, D. Caforio¹³⁰, V. M. Cairo^{39a,39b}, O. Cakir^{4a}, N. Calace⁵¹, P. Calafiura¹⁶, A. Calandri⁸⁸, G. Calderini⁸³, P. Calfayan¹⁰², L. P. Caloba^{26a}, S. Calvente Lopez⁸⁵, D. Calvet³⁶, S. Calvet³⁶, T. P. Calvet⁸⁸, R. Camacho Toro³³, S. Camarda³², P. Camarri^{135a,135b}, D. Cameron¹²¹, R. Caminal Armadans¹⁶⁹, C. Camincher⁵⁷, S. Campana³², M. Campanelli⁸¹, A. Camplani^{94a,94b}, A. Campoverde¹⁴⁵, V. Canale^{106a,106b}, A. Canepa^{163a}, M. Cano Bret¹⁴², J. Cantero¹¹⁶, R. Cantrill^{128a}, T. Cao⁴², M. D. M. Capeans Garrido³², I. Caprini^{28b}, M. Caprini^{28b}, M. Capua^{39a,39b}, R. Caputo⁸⁶, R. M. Carbone³⁷, R. Cardarelli^{135a}, F. Cardillo⁵⁰, I. Carli¹³¹, T. Carli³², G. Carlino^{106a}, L. Carminati^{94a,94b}, S. Caron¹⁰⁸, E. Carquin^{34b}, G. D. Carrillo-Montoya³², J. R. Carter³⁰, J. Carvalho^{128a,128c}, D. Casadei¹⁹, M. P. Casado^{13,i}, M. Casolino¹³, D. W. Casper¹⁶⁶, E. Castaneda-Miranda^{149a}, R. Castellijn¹⁰⁹, A. Castelli¹⁰⁹, V. Castillo Gimenez¹⁷⁰, N. F. Castro^{128a,j}, A. Catinaccio³², J. R. Catmore¹²¹, A. Cattai³², J. Caudron⁸⁶, V. Cavaliere¹⁶⁹, E. Cavallaro¹³, D. Cavalli^{94a}, M. Cavalli-Sforza¹³, V. Cavasinni^{126a,126b}, F. Ceradini^{136a,136b}, L. Cerda Alberich¹⁷⁰, B. C. Cerio⁴⁷, A. S. Cerqueira^{26b}, A. Cerri¹⁵³, L. Cerrito⁷⁹, F. Cerutti¹⁶, M. Cerv³², A. Cervelli¹⁸, S. A. Cetin^{20c}, A. Chafaq^{137a}, D. Chakraborty¹¹⁰, S. K. Chan⁵⁹, Y. L. Chan^{63a}, P. Chang¹⁶⁹, J. D. Chapman³⁰, D. G. Charlton¹⁹, A. Chatterjee⁵¹, C. C. Chau¹⁶², C. A. Chavez Barajas¹⁵³, S. Che¹¹³, S. Cheatham⁷⁵, A. Chegwidan⁹³, S. Chekanov⁶, S. V. Chekulaev^{163a}, G. A. Chelkov^{68,k}, M. A. Chelstowska⁹², C. Chen⁶⁷, H. Chen²⁷, K. Chen¹⁵², S. Chen^{35b}, S. Chen¹⁵⁹, X. Chen^{35c}, Y. Chen⁷⁰, H. C. Cheng⁹², H. J. Cheng^{35a}, Y. Cheng³³, A. Cheplakov⁶⁸, E. Cheremushkina¹³², R. Cherkaoui El Moursli^{137e}, V. Chernyatin^{27,*}, E. Cheu⁷, L. Chevalier¹³⁸, V. Chiarella⁴⁹, G. Chiarelli^{126a,126b}, G. Chiodini^{76a}, A. S. Chisholm¹⁹, A. Chitan^{28b}, M. V. Chizhov⁶⁸, K. Choi⁶⁴, A. R. Chomont³⁶, S. Chouridou⁹, B. K. B. Chow¹⁰², V. Christodoulou⁸¹, D. Chromek-Burckhart³², J. Chudoba¹²⁹, A. J. Chuinard⁹⁰, J. J. Chwastowski⁴¹, L. Chytka¹¹⁷, G. Ciapetti^{134a,134b}, A. K. Ciftci^{4a}, D. Cinca⁴⁵, V. Cindro⁷⁸, I. A. Cioara²³, C. Ciocca^{22a,22b}, A. Ciocio¹⁶, F. Ciotto^{106a,106b}, Z. H. Citron¹⁷⁵, M. Citterio^{94a}, M. Ciubancan^{28b}, A. Clark⁵¹, B. L. Clark⁵⁹, M. R. Clark³⁷, P. J. Clark⁴⁸, R. N. Clarke¹⁶, C. Clement^{150a,150b}, Y. Coadou⁸⁸, M. Cobal^{167a,167c}, A. Coccaro⁵¹, J. Cochran⁶⁷, L. Coffey²⁵, L. Colasurdo¹⁰⁸, B. Cole³⁷, A. P. Colijn¹⁰⁹, J. Collot⁵⁷, T. Colombo³², G. Compostella¹⁰³, P. Conde Muiño^{128a,128b}, E. Coniavitis⁵⁰, S. H. Connell^{149b}, I. A. Connelly⁸⁰, V. Consorti⁵⁰, S. Constantinescu^{28b}, G. Conti³², F. Conventi^{106a,l}, M. Cooke¹⁶, B. D. Cooper⁸¹, A. M. Cooper-Sarkar¹²², K. J. R. Cormier¹⁶², T. Cornelissen¹⁷⁸, M. Corradi^{134a,134b}, F. Corriveau^{90,m}, A. Corso-Radu¹⁶⁶, A. Cortes-Gonzalez¹³, G. Cortiana¹⁰³, G. Costa^{94a}, M. J. Costa¹⁷⁰, D. Costanzo¹⁴³,

- G. Cottin³⁰, G. Cowan⁸⁰, B. E. Cox⁸⁷, K. Cranmer¹¹², S. J. Crawley⁵⁵, G. Cree³¹, S. Crépé-Renaudin⁵⁷, F. Crescioli⁸³, W. A. Cribbs^{150a,150b}, M. Crispin Ortuzar¹²², M. Cristinziani²³, V. Croft¹⁰⁸, G. Crosetti^{39a,39b}, T. Cuhadar Donszelmann¹⁴³, J. Cummings¹⁷⁹, M. Curatolo⁴⁹, J. Cúth⁸⁶, C. Cuthbert¹⁵⁴, H. Czirr¹⁴⁵, P. Czodrowski³, G. D'amen^{22a,22b}, S. D'Auria⁵⁵, M. D'Onofrio⁷⁷, M. J. Da Cunha Sargedas De Sousa^{128a,128b}, C. Da Via⁸⁷, W. Dabrowski^{40a}, T. Dado^{148a}, T. Dai⁹², O. Dale¹⁵, F. Dallaire⁹⁷, C. Dallapiccola⁸⁹, M. Dam³⁸, J. R. Dandoy³³, N. P. Dang⁵⁰, A. C. Daniells¹⁹, N. S. Dann⁸⁷, M. Danninger¹⁷¹, M. Dano Hoffmann¹³⁸, V. Dao⁵⁰, G. Darbo^{52a}, S. Darmora⁸, J. Dassoulas³, A. Dattagupta⁶⁴, W. Davey²³, C. David¹⁷², T. Davidek¹³¹, M. Davies¹⁵⁷, P. Davison⁸¹, E. Dawe⁹¹, I. Dawson¹⁴³, R. K. Daya-Ishmukhametova⁸⁹, K. De⁸, R. de Asmundis^{106a}, A. De Benedetti¹¹⁵, S. De Castro^{22a,22b}, S. De Cecco⁸³, N. De Groot¹⁰⁸, P. de Jong¹⁰⁹, H. De la Torre⁸⁵, F. De Lorenzi⁶⁷, A. De Maria⁵⁶, D. De Pedis^{134a}, A. De Salvo^{134a}, U. De Sanctis¹⁵³, A. De Santo¹⁵³, J. B. De Vivie De Regie¹¹⁹, W. J. Dearnaley⁷⁵, R. Debbé²⁷, C. Debenedetti¹³⁹, D. V. Dedovich⁶⁸, N. Dehghanian³, I. Deigaard¹⁰⁹, M. Del Gaudio^{39a,39b}, J. Del Peso⁸⁵, T. Del Prete^{126a,126b}, D. Delgove¹¹⁹, F. Deliot¹³⁸, C. M. Delitzsch⁵¹, M. Deliyergiyev⁷⁸, A. Dell'Acqua³², L. Dell'Asta²⁴, M. Dell'Orso^{126a,126b}, M. Della Pietra^{106a,1}, D. della Volpe⁵¹, M. Delmastro⁵, P. A. Delsart⁵⁷, D. A. DeMarco¹⁶², S. Demers¹⁷⁹, M. Demichev⁶⁸, A. Demilly⁸³, S. P. Denisov¹³², D. Denysiuk¹³⁸, D. Derendarz⁴¹, J. E. Derkaoui^{137d}, F. Derue⁸³, P. Dervan⁷⁷, K. Desch²³, C. Deterre⁴⁴, K. Dette⁴⁵, P. O. Deviveiros³², A. Dewhurst¹³³, S. Dhaliwal²⁵, A. Di Ciaccio^{135a,135b}, L. Di Ciaccio⁵, W. K. Di Clemente¹²⁴, C. Di Donato^{134a,134b}, A. Di Girolamo³², B. Di Girolamo³², B. Di Micco^{136a,136b}, R. Di Nardo³², A. Di Simone⁵⁰, R. Di Sipio¹⁶², D. Di Valentino³¹, C. Diaconu⁸⁸, M. Diamond¹⁶², F. A. Dias⁴⁸, M. A. Diaz^{34a}, E. B. Diehl⁹², J. Dietrich¹⁷, S. Diglio⁸⁸, A. Dimitrievska¹⁴, J. Dingfelder²³, P. Dita^{28b}, S. Dita^{28b}, F. Dittus³², F. Djama⁸⁸, T. Djobava^{53b}, J. I. Djuvsland^{61a}, M. A. B. do Vale^{26c}, D. Dobos³², M. Dobre^{28b}, C. Doglioni⁸⁴, T. Dohmae¹⁵⁹, J. Dolejsi¹³¹, Z. Dolezal¹³¹, B. A. Dolgoshein^{100,*}, M. Donadelli^{26d}, S. Donati^{126a,126b}, P. Dondero^{123a,123b}, J. Donini³⁶, J. Dopke¹³³, A. Doria^{106a}, M. T. Dova⁷⁴, A. T. Doyle⁵⁵, E. Drechsler⁵⁶, M. Dris¹⁰, Y. Du¹⁴¹, J. Duarte-Campderros¹⁵⁷, E. Duchovni¹⁷⁵, G. Duckeck¹⁰², O. A. Ducu^{97,n}, D. Duda¹⁰⁹, A. Dudarev³², E. M. Duffield¹⁶, L. Dufflot¹¹⁹, L. Duguid⁸⁰, M. Dührssen³², M. Dumancic¹⁷⁵, M. Dunford^{61a}, H. Duran Yildiz^{4a}, M. Düren⁵⁴, A. Durglishvili^{53b}, D. Duschinger⁴⁶, B. Dutta⁴⁴, M. Dyndal⁴⁴, C. Eckardt⁴⁴, K. M. Ecker¹⁰³, R. C. Edgar⁹², N. C. Edwards⁴⁸, T. Eifert³², G. Eigen¹⁵, K. Einsweiler¹⁶, T. Ekelof¹⁶⁸, M. El Kacimi^{137c}, V. Ellajosyula⁸⁸, M. Ellert¹⁶⁸, S. Elles⁵, F. Ellinghaus¹⁷⁸, A. A. Elliot¹⁷², N. Ellis³², J. Elmsheuser²⁷, M. Elsing³², D. Emelianov¹³³, Y. Enari¹⁵⁹, O. C. Endner⁸⁶, M. Endo¹²⁰, J. S. Ennis¹⁷³, J. Erdmann⁴⁵, A. Ereditato¹⁸, G. Ernis¹⁷⁸, J. Ernst², M. Ernst²⁷, S. Errede¹⁶⁹, E. Ertel⁸⁶, M. Escalier¹¹⁹, H. Esch⁴⁵, C. Escobar¹²⁷, B. Esposito⁴⁹, A. I. Etienne¹³⁸, E. Etzion¹⁵⁷, H. Evans⁶⁴, A. Ezhilov¹²⁵, F. Fabbri^{22a,22b}, L. Fabbri^{22a,22b}, G. Facini³³, R. M. Fakhrutdinov¹³², S. Falciano^{134a}, R. J. Falla⁸¹, J. Faltova³², Y. Fang^{35a}, M. Fanti^{94a,94b}, A. Farbin⁸, A. Farilla^{136a}, C. Farina¹²⁷, E. M. Farina^{123a,123b}, T. Farooque¹³, S. Farrell¹⁶, S. M. Farrington¹⁷³, P. Farthouat³², F. Fassi^{137e}, P. Fassnacht³², D. Fassouliotis⁹, M. Fauci Giannelli⁸⁰, A. Favareto^{52a,52b}, W. J. Fawcett¹²², L. Fayard¹¹⁹, O. L. Fedin^{125,o}, W. Fedorko¹⁷¹, S. Feigl¹²¹, L. Feligioni⁸⁸, C. Feng¹⁴¹, E. J. Feng³², H. Feng⁹², A. B. Fenyuk¹³², L. Feremenga⁸, P. Fernandez Martinez¹⁷⁰, S. Fernandez Perez¹³, J. Ferrando⁵⁵, A. Ferrari¹⁶⁸, P. Ferrari¹⁰⁹, R. Ferrari^{123a}, D. E. Ferreira de Lima^{61b}, A. Ferrer¹⁷⁰, D. Ferrere⁵¹, C. Ferretti⁹², A. Ferretto Parodi^{52a,52b}, F. Fiedler⁸⁶, A. Filipčić⁷⁸, M. Filipuzzi⁴⁴, F. Filthaut¹⁰⁸, M. Fincke-Keeler¹⁷², K. D. Finelli¹⁵⁴, M. C. N. Fiolhais^{128a,128c}, L. Fiorini¹⁷⁰, A. Firan⁴², A. Fischer², C. Fischer¹³, J. Fischer¹⁷⁸, W. C. Fisher⁹³, N. Flaschel⁴⁴, I. Fleck¹⁴⁵, P. Fleischmann⁹², G. T. Fletcher¹⁴³, R. R. M. Fletcher¹²⁴, T. Flick¹⁷⁸, A. Floderus⁸⁴, L. R. Flores Castillo^{63a}, M. J. Flowerdew¹⁰³, G. T. Forcolin⁸⁷, A. Formica¹³⁸, A. Forti⁸⁷, A. G. Foster¹⁹, D. Fournier¹¹⁹, H. Fox⁷⁵, S. Fracchia¹³, P. Francavilla⁸³, M. Franchini^{22a,22b}, D. Francis³², L. Franconi¹²¹, M. Franklin⁵⁹, M. Frate¹⁶⁶, M. Fraternali^{123a,123b}, D. Freeborn⁸¹, S. M. Fressard-Batraneanu³², F. Friedrich⁴⁶, D. Froidevaux³², J. A. Frost¹²², C. Fukunaga¹⁶⁰, E. Fullana Torregrosa⁸⁶, T. Fusayasu¹⁰⁴, J. Fuster¹⁷⁰, C. Gabaldon⁵⁷, O. Gabizon¹⁷⁸, A. Gabrielli^{22a,22b}, A. Gabrielli¹⁶, G. P. Gach^{40a}, S. Gadatsch³², S. Gadomski⁵¹, G. Gagliardi^{52a,52b}, L. G. Gagnon⁹⁷, P. Gagnon⁶⁴, C. Galea¹⁰⁸, B. Galhardo^{128a,128c}, E. J. Gallas¹²², B. J. Gallop¹³³, P. Gallus¹³⁰, G. Galster³⁸, K. K. Gan¹¹³, J. Gao⁶⁰, Y. Gao⁴⁸, Y. S. Gao^{147,g}, F. M. Garay Walls⁴⁸, C. García¹⁷⁰, J. E. García Navarro¹⁷⁰, M. Garcia-Sciveres¹⁶, R. W. Gardner³³, N. Garelli¹⁴⁷, V. Garonne¹²¹, A. Gascon Bravo⁴⁴, C. Gatti⁴⁹, A. Gaudiello^{52a,52b}, G. Gaudio^{123a}, B. Gaur¹⁴⁵, L. Gauthier⁹⁷, I. L. Gavrilenko⁹⁸, C. Gay¹⁷¹, G. Gaycken²³, E. N. Gazis¹⁰, Z. Gece¹⁷¹, C. N. P. Gee¹³³, Ch. Geich-Gimbel²³, M. Geisen⁸⁶, M. P. Geisler^{61a}, C. Gemme^{52a}, M. H. Genest⁵⁷, C. Geng^{60,p}, S. Gentile^{134a,134b}, S. George⁸⁰, D. Gerbaudo¹³, A. Gershon¹⁵⁷, S. Ghasemi¹⁴⁵, H. Ghazlane^{137b}, M. Ghneimat²³, B. Giacobbe^{22a}, S. Giagu^{134a,134b}, P. Giannetti^{126a,126b}, B. Gibbard²⁷, S. M. Gibson⁸⁰, M. Gignac¹⁷¹, M. Gilchriese¹⁶, T. P. S. Gillam³⁰, D. Gillberg³¹, G. Gilles¹⁷⁸, D. M. Gingrich^{3,d}, N. Giokaris⁹, M. P. Giordani^{167a,167c}, F. M. Giorgi^{22a}, F. M. Giorgi¹⁷, P. F. Giraud¹³⁸, P. Giromini⁵⁹, D. Giugni^{94a}, F. Giuliani¹²², C. Giuliani¹⁰³, M. Giulini^{61b}, B. K. Gjelsten¹²¹, S. Gkaitatzis¹⁵⁸, I. Gkialas¹⁵⁸, E. L. Gkougkousis¹¹⁹, L. K. Gladilin¹⁰¹, C. Glasman⁸⁵, J. Glatzer⁵⁰, P. C. F. Glaysheer⁴⁸, A. Glazov⁴⁴, M. Goblirsch-Kolb¹⁰³, J. Godlewski⁴¹, S. Goldfarb⁹¹, T. Golling⁵¹, D. Golubkov¹³², A. Gomes^{128a,128b,128d}, R. Gonçalves^{128a}, J. Goncalves Pinto Firmino Da Costa¹³⁸

G. Gonella⁵⁰, L. Gonella¹⁹, A. Gongadze⁶⁸, S. González de la Hoz¹⁷⁰, G. Gonzalez Parra¹³, S. Gonzalez-Sevilla⁵¹, L. Goossens³², P. A. Gorbounov⁹⁹, H. A. Gordon²⁷, I. Gorelov¹⁰⁷, B. Gorini³², E. Gorini^{76a,76b}, A. Gorišek⁷⁸, E. Gornicki⁴¹, A. T. Goshaw⁴⁷, C. Gössling⁴⁵, M. I. Gostkin⁶⁸, C. R. Goudet¹¹⁹, D. Goujdami^{137c}, A. G. Goussiou¹⁴⁰, N. Govender^{149b,q}, E. Gozani¹⁵⁶, L. Graber⁵⁶, I. Grabowska-Bold^{40a}, P. O. J. Gradin⁵⁷, P. Grafström^{22a,22b}, J. Gramling⁵¹, E. Gramstad¹²¹, S. Grancagnolo¹⁷, V. Gratchev¹²⁵, P. M. Gravila^{28e}, H. M. Gray³², E. Graziani^{136a}, Z. D. Greenwood^{82,r}, C. Grefe²³, K. Gregersen⁸¹, I. M. Gregor⁴⁴, P. Grenier¹⁴⁷, K. Grevtsov⁵, J. Griffiths⁸, A. A. Grillo¹³⁹, K. Grimm⁷⁵, S. Grinstein^{13,s}, Ph. Gris³⁶, J.-F. Grivaz¹¹⁹, S. Groh⁸⁶, J. P. Grohs⁴⁶, E. Gross¹⁷⁵, J. Grosse-Knetter⁵⁶, G. C. Grossi⁸², Z. J. Grout¹⁵³, L. Guan⁹², W. Guan¹⁷⁶, J. Guenther⁶⁵, F. Guescini⁵¹, D. Guest¹⁶⁶, O. Gueta¹⁵⁷, E. Guido^{52a,52b}, T. Guillemain⁵, S. Guindon², U. Gul⁵⁵, C. Gumpert³², J. Guo¹⁴², Y. Guo^{60,p}, S. Gupta¹²², G. Gustavino^{134a,134b}, P. Gutierrez¹¹⁵, N. G. Gutierrez Ortiz⁸¹, C. Gutsche⁴⁶, C. Guyot¹³⁸, C. Gwenlan¹²², C. B. Gwilliam⁷⁷, A. Haas¹¹², C. Haber¹⁶, H. K. Hadavand⁸, N. Haddad^{137e}, A. Hadeef⁸⁸, P. Haefner²³, S. Hageböck²³, Z. Hajduk⁴¹, H. Hakobyan^{180,*}, M. Haleem⁴⁴, J. Haley¹¹⁶, G. Halladjian⁹³, G. D. Hallelwell⁸⁸, K. Hamacher¹⁷⁸, P. Hamal¹¹⁷, K. Hamano¹⁷², A. Hamilton^{149a}, G. N. Hamity¹⁴³, P. G. Hamnett⁴⁴, L. Han⁶⁰, K. Hanagaki^{69,t}, K. Hanawa¹⁵⁹, M. Hance¹³⁹, B. Haney¹²⁴, P. Hanke^{61a}, R. Hanna¹³⁸, J. B. Hansen³⁸, J. D. Hansen³⁸, M. C. Hansen²³, P. H. Hansen³⁸, K. Hara¹⁶⁴, A. S. Hard¹⁷⁶, T. Harenberg¹⁷⁸, F. Hariri¹¹⁹, S. Harkusha⁹⁵, R. D. Harrington⁴⁸, P. F. Harrison¹⁷³, F. Hartjes¹⁰⁹, N. M. Hartmann¹⁰², M. Hasegawa⁷⁰, Y. Hasegawa¹⁴⁴, A. Hasib¹¹⁵, S. Hassani¹³⁸, S. Haug¹⁸, R. Hauser⁹³, L. Hauswald⁴⁶, M. Havranek¹²⁹, C. M. Hawkes¹⁹, R. J. Hawkins³², D. Hayden⁹³, C. P. Hays¹²², J. M. Hays⁷⁹, H. S. Hayward⁷⁷, S. J. Haywood¹³³, S. J. Head¹⁹, T. Heck⁸⁶, V. Hedberg⁸⁴, L. Heelan⁸, S. Heim¹²⁴, T. Heim¹⁶, B. Heinemann¹⁶, J. J. Heinrich¹⁰², L. Heinrich¹¹², C. Heinz⁵⁴, J. Hejbal¹²⁹, L. Helary²⁴, S. Hellman^{150a,150b}, C. Helsen³², J. Henderson¹²², R. C. W. Henderson⁷⁵, Y. Heng¹⁷⁶, S. Henkelmann¹⁷¹, A. M. Henriques Correia³², S. Henrot-Versille¹¹⁹, G. H. Herbert¹⁷, Y. Hernández Jiménez¹⁷⁰, G. Herten⁵⁰, R. Hertenberger¹⁰², L. Hervas³², G. G. Hesketh⁸¹, N. P. Hessey¹⁰⁹, J. W. Hetherly⁴², R. Hickling⁷⁹, E. Higón-Rodríguez¹⁷⁰, E. Hill¹⁷², J. C. Hill³⁰, K. H. Hiller⁴⁴, S. J. Hillier¹⁹, I. Hinchliffe¹⁶, E. Hines¹²⁴, R. R. Hinman¹⁶, M. Hirose⁵⁰, D. Hirschbuehl¹⁷⁸, J. Hobbs¹⁵², N. Hod^{163a}, M. C. Hodgkinson¹⁴³, P. Hodgson¹⁴³, A. Hoecker³², M. R. Hoferkamp¹⁰⁷, F. Hoenig¹⁰², D. Hohn²³, T. R. Holmes¹⁶, M. Homann⁴⁵, T. M. Hong¹²⁷, B. H. Hooberman¹⁶⁹, W. H. Hopkins¹¹⁸, Y. Hori¹⁰⁵, A. J. Horton¹⁴⁶, J.-Y. Hostachy⁵⁷, S. Hou¹⁵⁵, A. Hoummada^{137a}, J. Howarth⁴⁴, M. Hrabovsky¹¹⁷, I. Hristova¹⁷, J. Hrivnac¹¹⁹, T. Hryn'ova⁵, A. Hrynevich⁹⁶, C. Hsu^{149c}, P. J. Hsu^{155,u}, S.-C. Hsu¹⁴⁰, D. Hu³⁷, Q. Hu⁶⁰, Y. Huang⁴⁴, Z. Hubacek¹³⁰, F. Hubaut⁸⁸, F. Huegging²³, T. B. Huffman¹²², E. W. Hughes³⁷, G. Hughes⁷⁵, M. Huhtinen³², P. Huo¹⁵², N. Huseynov^{68,b}, J. Huston⁹³, J. Huth⁵⁹, G. Iacobucci⁵¹, G. Iakovidis²⁷, I. Ibragimov¹⁴⁵, L. Iconomidou-Fayard¹¹⁹, E. Ideal¹⁷⁹, Z. Idrissi^{137e}, P. Iengo³², O. Igonkina^{109,v}, T. Iizawa¹⁷⁴, Y. Ikegami⁶⁹, M. Ikeno⁶⁹, Y. Ilchenko^{11,w}, D. Iliadis¹⁵⁸, N. Ilic¹⁴⁷, T. Ince¹⁰³, G. Introzzi^{123a,123b}, P. Ioannou^{9,*}, M. Iodice^{136a}, K. Iordanidou³⁷, V. Ippolito⁵⁹, N. Ishijima¹²⁰, M. Ishino⁷¹, M. Ishitsuka¹⁶¹, R. Ishmukhametov¹¹³, C. Issever¹²², S. Istin^{20a}, F. Ito¹⁶⁴, J. M. Iturbe Ponce⁸⁷, R. Iuppa^{135a,135b}, W. Iwanski⁶⁵, H. Iwasaki⁶⁹, J. M. Izen⁴³, V. Izzo^{106a}, S. Jabbar³, B. Jackson¹²⁴, M. Jackson⁷⁷, P. Jackson¹, V. Jain², K. B. Jakobi⁸⁶, K. Jakobs⁵⁰, S. Jakobsen³², T. Jakoubek¹²⁹, D. O. Jamin¹¹⁶, D. K. Jana⁸², E. Jansen⁸¹, R. Jansky⁶⁵, J. Janssen²³, M. Janus⁵⁶, G. Jarlskog⁸⁴, N. Javadov^{68,b}, T. Javůrek⁵⁰, F. Jeanneau¹³⁸, L. Jeanty¹⁶, G.-Y. Jeng¹⁵⁴, D. Jennens⁹¹, P. Jenni^{50,x}, J. Jentzsch⁴⁵, C. Jeske¹⁷³, S. Jézéquel⁵, H. Ji¹⁷⁶, J. Jia¹⁵², H. Jiang⁶⁷, Y. Jiang⁶⁰, S. Jiggins⁸¹, J. Jimenez Pena¹⁷⁰, S. Jin^{35a}, A. Jinaru^{28b}, O. Jinnouchi¹⁶¹, P. Johansson¹⁴³, K. A. Johns⁷, W. J. Johnson¹⁴⁰, K. Jon-And^{150a,150b}, G. Jones¹⁷³, R. W. L. Jones⁷⁵, S. Jones⁷, T. J. Jones⁷⁷, J. Jongmanns^{61a}, P. M. Jorge^{128a,128b}, J. Jovicevic^{163a}, X. Ju¹⁷⁶, A. Juste Rozas^{13,s}, M. K. Köhler¹⁷⁵, A. Kaczmarzka⁴¹, M. Kado¹¹⁹, H. Kagan¹¹³, M. Kagan¹⁴⁷, S. J. Kahn⁸⁸, E. Kajomovitz⁴⁷, C. W. Kalderon¹²², A. Kaluza⁸⁶, S. Kama⁴², A. Kamenshchikov¹³², N. Kanaya¹⁵⁹, S. Kaneti³⁰, L. Kanjir⁷⁸, V. A. Kantserov¹⁰⁰, J. Kanzaki⁶⁹, B. Kaplan¹¹², L. S. Kaplan¹⁷⁶, A. Kapliy³³, D. Kar^{149c}, K. Karakostas¹⁰, A. Karamaoun³, N. Karastathis¹⁰, M. J. Kareem⁵⁶, E. Karentzos¹⁰, M. Karnevskiy⁸⁶, S. N. Karpov⁶⁸, Z. M. Karpova⁶⁸, K. Karthik¹¹², V. Kartvelishvili⁷⁵, A. N. Karyukhin¹³², K. Kasahara¹⁶⁴, L. Kashif¹⁷⁶, R. D. Kass¹¹³, A. Kastanas¹⁵, Y. Kataoka¹⁵⁹, C. Kato¹⁵⁹, A. Katre⁵¹, J. Katzy⁴⁴, K. Kawade¹⁰⁵, K. Kawagoe⁷³, T. Kawamoto¹⁵⁹, G. Kawamura⁵⁶, S. Kazama¹⁵⁹, V. F. Kazanin^{111,c}, R. Keeler¹⁷², R. Kehoe⁴², J. S. Keller⁴⁴, J. J. Kempster⁸⁰, H. Keoshkerian¹⁶², O. Kepka¹²⁹, B. P. Kerševan⁷⁸, S. Kersten¹⁷⁸, R. A. Keyes⁹⁰, M. Khader¹⁶⁹, F. Khalil-zada¹², A. Khanov¹¹⁶, A. G. Kharlamov^{111,c}, T. J. Khoo⁵¹, V. Khovanskii⁹⁹, E. Khramov⁶⁸, J. Khubua^{53b,y}, S. Kido⁷⁰, H. Y. Kim⁸, S. H. Kim¹⁶⁴, Y. K. Kim³³, N. Kimura¹⁵⁸, O. M. Kind¹⁷, B. T. King⁷⁷, M. King¹⁷⁰, S. B. King¹⁷¹, J. Kirk¹³³, A. E. Kiryunin¹⁰³, T. Kishimoto⁷⁰, D. Kisielewska^{40a}, F. Kiss⁵⁰, K. Kiuchi¹⁶⁴, O. Kivernyk¹³⁸, E. Kladiva^{148b}, M. H. Klein³⁷, M. Klein⁷⁷, U. Klein⁷⁷, K. Kleinknecht⁸⁶, P. Klimek¹¹⁰, A. Klimentov²⁷, R. Klingenberg⁴⁵, J. A. Klinger¹⁴³, T. Klioutchnikova³², E.-E. Kluge^{61a}, P. Kluit¹⁰⁹, S. Kluth¹⁰³, J. Knapik⁴¹, E. Kneringer⁶⁵, E. B. F. G. Knoops⁸⁸, A. Knue⁵⁵, A. Kobayashi¹⁵⁹, D. Kobayashi¹⁶¹, T. Kobayashi¹⁵⁹, M. Kobel⁴⁶, M. Kocian¹⁴⁷, P. Kodys¹³¹, T. Koffas³¹, E. Koffeman¹⁰⁹, T. Koi¹⁴⁷, H. Kolanoski¹⁷, M. Kolb^{61b}, I. Koletsou⁵, A. A. Komar^{98,*}, Y. Komori¹⁵⁹, T. Kondo⁶⁹, N. Kondrashova⁴⁴, K. Köneke⁵⁰, A. C. König¹⁰⁸,

- T. Kono^{69,z}, R. Konoplich^{112,aa}, N. Konstantinidis⁸¹, R. Kopeliansky⁶⁴, S. Koperny^{40a}, L. Köpke⁸⁶, A. K. Kopp⁵⁰, K. Korcyl⁴¹, K. Kordas¹⁵⁸, A. Korn⁸¹, A. A. Korol^{111,c}, I. Korolkov¹³, E. V. Korolkova¹⁴³, O. Kortner¹⁰³, S. Kortner¹⁰³, T. Kosek¹³¹, V. V. Kostyukhin²³, A. Kotwal⁴⁷, A. Kourkumeli-Charalampidi¹⁵⁸, C. Kourkumelis⁹, V. Kouskoura²⁷, A. B. Kowalewska⁴¹, R. Kowalewski¹⁷², T. Z. Kowalski^{40a}, C. Kozakai¹⁵⁹, W. Kozanecki¹³⁸, A. S. Kozhin¹³², V. A. Kramarenko¹⁰¹, G. Kramberger⁷⁸, D. Krasnopevtsev¹⁰⁰, M. W. Krasny⁸³, A. Krasznahorkay³², J. K. Kraus²³, A. Kravchenko²⁷, M. Kretz^{61c}, J. Kretzschmar⁷⁷, K. Kreutzfeldt⁵⁴, P. Krieger¹⁶², K. Krizka³³, K. Kroeninger⁴⁵, H. Kroha¹⁰³, J. Kroll¹²⁴, J. Kroseberg²³, J. Krstic¹⁴, U. Kruchonak⁶⁸, H. Krüger²³, N. Krumnack⁶⁷, A. Kruse¹⁷⁶, M. C. Kruse⁴⁷, M. Kruskal²⁴, T. Kubota⁹¹, H. Kucuk⁸¹, S. Kудay^{4b}, J. T. Kuechler¹⁷⁸, S. Kuehn⁵⁰, A. Kugel^{61c}, F. Kuger¹⁷⁷, A. Kuhl¹³⁹, T. Kuhl⁴⁴, V. Kukhtin⁶⁸, R. Kukla¹³⁸, Y. Kulchitsky⁹⁵, S. Kuleshov^{34b}, M. Kuna^{134a,134b}, T. Kunigo⁷¹, A. Kupco¹²⁹, H. Kurashige⁷⁰, Y. A. Kurochkin⁹⁵, V. Kus¹²⁹, E. S. Kuwertz¹⁷², M. Kuze¹⁶¹, J. Kvita¹¹⁷, T. Kwan¹⁷², D. Kyriazopoulos¹⁴³, A. La Rosa¹⁰³, J. L. La Rosa Navarro^{26d}, L. La Rotonda^{39a,39b}, C. Lacasta¹⁷⁰, F. Lacava^{134a,134b}, J. Lacey³¹, H. Lacker¹⁷, D. Lacour⁸³, V. R. Lacuesta¹⁷⁰, E. Ladygin⁶⁸, R. Lafaye⁵, B. Laforge⁸³, T. Lagouri¹⁷⁹, S. Lai⁵⁶, S. Lammers⁶⁴, W. Lampl⁷, E. Lançon¹³⁸, U. Landgraf⁵⁰, M. P. J. Landon⁷⁹, V. S. Lang^{61a}, J. C. Lange¹³, A. J. Lankford¹⁶⁶, F. Lanni²⁷, K. Lantzsch²³, A. Lanza^{123a}, S. Laplace⁸³, C. Lapoire³², J. F. Laporte¹³⁸, T. Lari^{94a}, F. Lasagni Manghi^{22a,22b}, M. Lassnig³², P. Laurelli⁴⁹, W. Lavrijsen¹⁶, A. T. Law¹³⁹, P. Laycock⁷⁷, T. Lazovich⁵⁹, M. Lazzaroni^{94a,94b}, B. Le⁹¹, O. Le Dortz⁸³, E. Le Guirrec⁸⁸, E. P. Le Quilleuc¹³⁸, M. LeBlanc¹⁷², T. LeCompte⁶, F. Ledroit-Guillon⁵⁷, C. A. Lee²⁷, S. C. Lee¹⁵⁵, L. Lee¹, G. Lefebvre⁸³, M. Lefebvre¹⁷², F. Legger¹⁰², C. Leggett¹⁶, A. Lehan⁷⁷, G. Lehmann Miotto³², X. Lei⁷, W. A. Leight³¹, A. Leisos^{158,ab}, A. G. Leister¹⁷⁹, M. A. L. Leite^{26d}, R. Leitner¹³¹, D. Lellouch¹⁷⁵, B. Lemmer⁵⁶, K. J. C. Leney⁸¹, T. Lenz²³, B. Lenzi³², R. Leone⁷, S. Leone^{126a,126b}, C. Leonidopoulos⁴⁸, S. Leontsinis¹⁰, G. Lerner¹⁵³, C. Leroy⁹⁷, A. A. J. Lesage¹³⁸, C. G. Lester³⁰, M. Levchenko¹²⁵, J. Levêque⁵, D. Levin⁹², L. J. Levinson¹⁷⁵, M. Levy¹⁹, D. Lewis⁷⁹, A. M. Leyko²³, M. Leyton⁴³, B. Li^{60,p}, H. Li¹⁵², H. L. Li³³, L. Li⁴⁷, L. Li¹⁴², Q. Li^{35a}, S. Li⁴⁷, X. Li⁸⁷, Y. Li¹⁴⁵, Z. Liang^{35a}, B. Liberti^{135a}, A. Liblong¹⁶², P. Lichard³², K. Lie¹⁶⁹, J. Liebal²³, W. Liebig¹⁵, A. Limosani¹⁵⁴, S. C. Lin^{155,ac}, T. H. Lin⁸⁶, B. E. Lindquist¹⁵², A. E. Lioni⁵¹, E. Lipeles¹²⁴, A. Lipniacka¹⁵, M. Lisovsky^{61b}, T. M. Liss¹⁶⁹, A. Lister¹⁷¹, A. M. Litke¹³⁹, B. Liu^{155,ad}, D. Liu¹⁵⁵, H. Liu⁹², H. Liu²⁷, J. Liu⁸⁸, J. B. Liu⁶⁰, K. Liu⁸⁸, L. Liu¹⁶⁹, M. Liu⁴⁷, M. Liu⁶⁰, Y. L. Liu⁶⁰, Y. Liu⁶⁰, M. Livan^{123a,123b}, A. Lleres⁵⁷, J. Llorente Merino^{35a}, S. L. Lloyd⁷⁹, F. Lo Sterzo¹⁵⁵, E. M. Lobodzinska⁴⁴, P. Loch⁷, W. S. Lockman¹³⁹, F. K. Loebinger⁸⁷, A. E. Loevschall-Jensen³⁸, K. M. Loew²⁵, A. Loginov^{179,*}, T. Lohse¹⁷, K. Lohwasser⁴⁴, M. Lokajicek¹²⁹, B. A. Long²⁴, J. D. Long¹⁶⁹, R. E. Long⁷⁵, L. Longo^{76a,76b}, K. A. Looper¹¹³, L. Lopes^{128a}, D. Lopez Mateos⁵⁹, B. Lopez Paredes¹⁴³, I. Lopez Paz¹³, A. Lopez Solis⁸³, J. Lorenz¹⁰², N. Lorenzo Martinez⁶⁴, M. Losada²¹, P. J. Lösel¹⁰², X. Lou^{35a}, A. Lounis¹¹⁹, J. Love⁶, P. A. Love⁷⁵, H. Lu^{63a}, N. Lu⁹², H. J. Lubatti¹⁴⁰, C. Luci^{134a,134b}, A. Lucotte⁵⁷, C. Luedtke⁵⁰, F. Luehring⁶⁴, W. Lukas⁶⁵, L. Luminari^{134a}, O. Lundberg^{150a,150b}, B. Lund-Jensen¹⁵¹, P. M. Luzzi⁸³, D. Lynn²⁷, R. Lysak¹²⁹, E. Lytken⁸⁴, V. Lyubushkin⁶⁸, H. Ma²⁷, L. L. Ma¹⁴¹, Y. Ma¹⁴¹, G. Maccarrone⁴⁹, A. Macchiolo¹⁰³, C. M. Macdonald¹⁴³, B. Maček⁷⁸, J. Machado Miguens^{124,128b}, D. Madaffari⁸⁸, R. Madar³⁶, H. J. Maddocks¹⁶⁸, W. F. Mader⁴⁶, A. Madsen⁴⁴, J. Maeda⁷⁰, S. Maeland¹⁵, T. Maeno²⁷, A. Maevskiy¹⁰¹, E. Magradze⁵⁶, J. Mahlstedt¹⁰⁹, C. Maiani¹¹⁹, C. Maidantchik^{26a}, A. A. Maier¹⁰³, T. Maier¹⁰², A. Maio^{128a,128b,128d}, S. Majewski¹¹⁸, Y. Makida⁶⁹, N. Makovec¹¹⁹, B. Malaescu⁸³, Pa. Malecki⁴¹, V. P. Maleev¹²⁵, F. Malek⁵⁷, U. Mallik⁶⁶, D. Malon⁶, C. Malone¹⁴⁷, S. Maltezos¹⁰, S. Malyukov³², J. Mamuzic¹⁷⁰, G. Mancini⁴⁹, B. Mandelli³², L. Mandelli^{94a}, I. Mandić⁷⁸, J. Maneira^{128a,128b}, L. Manhaes de Andrade Filho^{26b}, J. Manjarres Ramos^{163b}, A. Mann¹⁰², A. Manousos³², B. Mansoulie¹³⁸, J. D. Mansour^{35a}, R. Mantifel⁹⁰, M. Mantoani⁵⁶, S. Manzoni^{94a,94b}, L. Mapelli³², G. Marceca²⁹, L. March⁵¹, G. Marchiori⁸³, M. Marcisovsky¹²⁹, M. Marjanovic¹⁴, D. E. Marley⁹², F. Marroquim^{26a}, S. P. Marsden⁸⁷, Z. Marshall¹⁶, S. Marti-Garcia¹⁷⁰, B. Martin⁹³, T. A. Martin¹⁷³, V. J. Martin⁴⁸, B. Martin dit Latour¹⁵, M. Martinez^{13,s}, V. I. Martinez Outschoorn¹⁶⁹, S. Martin-Haugh¹³³, V. S. Martoiu^{28b}, A. C. Martyniuk⁸¹, M. Marx¹⁴⁰, A. Marzin³², L. Masetti⁸⁶, T. Mashimo¹⁵⁹, R. Mashinistov⁹⁸, J. Masik⁸⁷, A. L. Maslennikov^{111,c}, I. Massa^{22a,22b}, L. Massa^{22a,22b}, P. Mastrandrea⁵, A. Mastroberardino^{39a,39b}, T. Masubuchi¹⁵⁹, P. Mättig¹⁷⁸, J. Mattmann⁸⁶, J. Maurer^{28b}, S. J. Maxfield⁷⁷, D. A. Maximov^{111,c}, R. Mazini¹⁵⁵, S. M. Mazza^{94a,94b}, N. C. Mc Fadden¹⁰⁷, G. Mc Goldrick¹⁶², S. P. Mc Kee⁹², A. McCarn⁹², R. L. McCarthy¹⁵², T. G. McCarthy¹⁰³, L. I. McClymont⁸¹, E. F. McDonald⁹¹, K. W. McFarlane^{58,*}, J. A. Mcfayden⁸¹, G. Mchedlidze⁵⁶, S. J. McMahon¹³³, R. A. McPherson^{172,m}, M. Medinnis⁴⁴, S. Meehan¹⁴⁰, S. Mehlhase¹⁰², A. Mehta⁷⁷, K. Meier^{61a}, C. Meineck¹⁰², B. Meirose⁴³, D. Melini¹⁷⁰, B. R. Mellado Garcia^{149c}, M. Melo^{148a}, F. Meloni¹⁸, A. Mengarelli^{22a,22b}, S. Menke¹⁰³, E. Meoni¹⁶⁵, S. Mergelmeyer¹⁷, P. Mermod⁵¹, L. Merola^{106a,106b}, C. Meroni^{94a}, F. S. Merritt³³, A. Messina^{134a,134b}, J. Metcalfe⁶, A. S. Mete¹⁶⁶, C. Meyer⁸⁶, C. Meyer¹²⁴, J.-P. Meyer¹³⁸, J. Meyer¹⁰⁹, H. Meyer Zu Theenhausen^{61a}, F. Miano¹⁵³, R. P. Middleton¹³³, S. Miglioranzì^{52a,52b}, L. Mijović²³, G. Mikenberg¹⁷⁵, M. Mikestikova¹²⁹, M. Mikuz⁷⁸, M. Milesi⁹¹, A. Milic⁶⁵, D. W. Miller³³, C. Mills⁴⁸, A. Milov¹⁷⁵, D. A. Milstead^{150a,150b}, A. A. Minaenko¹³², Y. Minami¹⁵⁹, I. A. Minashvili⁶⁸, A. I. Mincer¹¹², B. Mindur^{40a}, M. Mineev⁶⁸, Y. Ming¹⁷⁶, L. M. Mir¹³, K. P. Mistry¹²⁴

- T. Mitani¹⁷⁴, J. Mitrevski¹⁰², V. A. Mitsou¹⁷⁰, A. Miucci⁵¹, P. S. Miyagawa¹⁴³, J. U. Mjörnmark⁸⁴, T. Moa^{150a,150b}, K. Mochizuki⁹⁷, S. Mohapatra³⁷, S. Molander^{150a,150b}, R. Moles-Valls²³, R. Monden⁷¹, M. C. Mondragon⁹³, K. Mönig⁴⁴, J. Monk³⁸, E. Monnier⁸⁸, A. Montalbano¹⁵², J. Montejo Berlingen³², F. Monticelli⁷⁴, S. Monzani^{94a,94b}, R. W. Moore³, N. Morange¹¹⁹, D. Moreno²¹, M. Moreno Llácer⁵⁶, P. Morettini^{52a}, S. Morgenstern³², D. Mori¹⁴⁶, T. Mori¹⁵⁹, M. Morii⁵⁹, M. Morinaga¹⁵⁹, V. Morisbak¹²¹, S. Moritz⁸⁶, A. K. Morley¹⁵⁴, G. Mornacchi³², J. D. Morris⁷⁹, S. S. Mortensen³⁸, L. Morvaj¹⁵², M. Mosidze^{53b}, J. Moss^{147,ae}, K. Motohashi¹⁶¹, R. Mount¹⁴⁷, E. Mountricha²⁷, S. V. Mouraviev^{98,*}, E. J. W. Moyse⁸⁹, S. Muanza⁸⁸, R. D. Mudd¹⁹, F. Mueller¹⁰³, J. Mueller¹²⁷, R. S. P. Mueller¹⁰², T. Mueller³⁰, D. Muenstermann⁷⁵, P. Mullen⁵⁵, G. A. Mullier¹⁸, F. J. Munoz Sanchez⁸⁷, J. A. Murillo Quijada¹⁹, W. J. Murray^{173,133}, H. Musheghyan⁵⁶, M. Muškinja⁷⁸, A. G. Myagkov^{132,af}, M. Myska¹³⁰, B. P. Nachman¹⁴⁷, O. Nackenhorst⁵¹, K. Nagai¹²², R. Nagai^{69,z}, K. Nagano⁶⁹, Y. Nagasaka⁶², K. Nagata¹⁶⁴, M. Nagel⁵⁰, E. Nagy⁸⁸, A. M. Nairz³², Y. Nakahama³², K. Nakamura⁶⁹, T. Nakamura¹⁵⁹, I. Nakano¹¹⁴, H. Namasivayam⁴³, R. F. Naranjo Garcia⁴⁴, R. Narayan¹¹, D. I. Narrias Villar^{61a}, I. Naryshkin¹²⁵, T. Naumann⁴⁴, G. Navarro²¹, R. Nayyar⁷, H. A. Neal⁹², P. Yu. Nechaeva⁹⁸, T. J. Neep⁸⁷, P. D. Nef¹⁴⁷, A. Negri^{123a,123b}, M. Negrini^{22a}, S. Nektarijevic¹⁰⁸, C. Nellist¹¹⁹, A. Nelson¹⁶⁶, S. Nemecek¹²⁹, P. Nemethy¹¹², A. A. Nepomuceno^{26a}, M. Nessi^{32,ag}, M. S. Neubauer¹⁶⁹, M. Neumann¹⁷⁸, R. M. Neves¹¹², P. Nevski²⁷, P. R. Newman¹⁹, D. H. Nguyen⁶, T. Nguyen Manh⁹⁷, R. B. Nickerson¹²², R. Nicolaidou¹³⁸, J. Nielsen¹³⁹, A. Nikiforov¹⁷, V. Nikolaenko^{132,af}, I. Nikolic-Audit⁸³, K. Nikolopoulos¹⁹, J. K. Nilsen¹²¹, P. Nilsson²⁷, Y. Ninomiya¹⁵⁹, A. Nisati^{134a}, R. Nisius¹⁰³, T. Nobe¹⁵⁹, L. Nodulman⁶, M. Nomachi¹²⁰, I. Nomidis³¹, T. Nooney⁷⁹, S. Norberg¹¹⁵, M. Nordberg³², N. Norjoharuddeen¹²², O. Novgorodova⁴⁶, S. Nowak¹⁰³, M. Nozaki⁶⁹, L. Nozka¹¹⁷, K. Ntekas¹⁰, E. Nurse⁸¹, F. Nuti⁹¹, F. O'grady⁷, D. C. O'Neil¹⁴⁶, A. A. O'Rourke⁴⁴, V. O'Shea⁵⁵, F. G. Oakham^{31,d}, H. Oberlack¹⁰³, T. Obermann²³, J. Ocariz⁸³, A. Ochi⁷⁰, I. Ochoa³⁷, J. P. Ochoa-Ricoux^{34a}, S. Oda⁷³, S. Odaka⁶⁹, H. Ogren⁶⁴, A. Oh⁸⁷, S. H. Oh⁴⁷, C. C. Ohm¹⁶, H. Ohman¹⁶⁸, H. Oide³², H. Okawa¹⁶⁴, Y. Okumura³³, T. Okuyama⁶⁹, A. Olariu^{28b}, L. F. Oleiro Seabra^{128a}, S. A. Olivares Pino⁴⁸, D. Oliveira Damazio²⁷, A. Olszewski⁴¹, J. Olszowska⁴¹, A. Onofre^{128a,128e}, K. Onogi¹⁰⁵, P. U. E. Onyisi^{11,w}, M. J. Oreglia³³, Y. Oren¹⁵⁷, D. Orestano^{136a,136b}, N. Orlando^{63b}, R. S. Orr¹⁶², B. Osculati^{52a,52b,*}, R. Ospanov⁸⁷, G. Otero y Garzon²⁹, H. Otono⁷³, M. Ouchrif^{137d}, F. Ould-Saada¹²¹, A. Ouraou¹³⁸, K. P. Oussoren¹⁰⁹, Q. Ouyang^{35a}, M. Owen⁵⁵, R. E. Owen¹⁹, V. E. Ozcan^{20a}, N. Ozturk⁸, K. Pachal¹⁴⁶, A. Pacheco Pages¹³, L. Pacheco Rodriguez¹³⁸, C. Padilla Aranda¹³, M. Pagáčová⁵⁰, S. Pagan Griso¹⁶, F. Paige²⁷, P. Pais⁸⁹, K. Pajchel¹²¹, G. Palacino^{163b}, S. Palazzo^{39a,39b}, S. Palestini³², M. Palka^{40b}, D. Pallin³⁶, A. Palma^{128a,128b}, E. St. Panagiotopoulou¹⁰, C. E. Pandini⁸³, J. G. Panduro Vazquez⁸⁰, P. Pani^{150a,150b}, S. Panitkin²⁷, D. Pantea^{28b}, L. Paolozzi⁵¹, Th. D. Papadopoulos¹⁰, K. Papageorgiou¹⁵⁸, A. Paramonov⁶, D. Paredes Hernandez¹⁷⁹, A. J. Parker⁷⁵, M. A. Parker³⁰, K. A. Parker¹⁴³, F. Parodi^{52a,52b}, J. A. Parsons³⁷, U. Parzefall⁵⁰, V. R. Pascuzzi¹⁶², E. Pasqualucci^{134a}, S. Passaggio^{52a}, Fr. Pastore⁸⁰, G. Pásztor^{31,ah}, S. Pataria¹⁷⁸, J. R. Pater⁸⁷, T. Pauly³², J. Pearce¹⁷², B. Pearson¹¹⁵, L. E. Pedersen³⁸, M. Pedersen¹²¹, S. Pedraza Lopez¹⁷⁰, R. Pedro^{128a,128b}, S. V. Peleganchuk^{111,c}, D. Pelikan¹⁶⁸, O. Penc¹²⁹, C. Peng^{35a}, H. Peng⁶⁰, J. Penwell⁶⁴, B. S. Peralva^{26b}, M. M. Perego¹³⁸, D. V. Perepelitsa²⁷, E. Perez Codina^{163a}, L. Perini^{94a,94b}, H. Pernegger³², S. Perrella^{106a,106b}, R. Peschke⁴⁴, V. D. Peshekhonov⁶⁸, K. Peters⁴⁴, R. F. Y. Peters⁸⁷, B. A. Petersen³², T. C. Petersen³⁸, E. Petit⁵⁷, A. Petridis¹, C. Petridou¹⁵⁸, P. Petroff¹¹⁹, E. Petrolo^{134a}, M. Petrov¹²², F. Petrucci^{136a,136b}, N. E. Pettersson⁸⁹, A. Peyaud¹³⁸, R. Pezoa^{34b}, P. W. Phillips¹³³, G. Piacquadio^{147,ai}, E. Pianori¹⁷³, A. Picazio⁸⁹, E. Piccaro⁷⁹, M. Piccinini^{22a,22b}, M. A. Pickering¹²², R. Piegaia²⁹, J. E. Pilcher³³, A. D. Pilkington⁸⁷, A. W. J. Pin⁸⁷, M. Pinamonti^{167a,167c,aj}, J. L. Pinfold³, A. Pingel³⁸, S. Pires⁸³, H. Pirumov⁴⁴, M. Pitt¹⁷⁵, L. Plazak^{148a}, M.-A. Pleier²⁷, V. Pleskot⁸⁶, E. Plotnikova⁶⁸, P. Plucinski⁹³, D. Pluth⁶⁷, R. Poettgen^{150a,150b}, L. Poggioli¹¹⁹, D. Pohl²³, G. Polesello^{123a}, A. Poley⁴⁴, A. Policicchio^{39a,39b}, R. Polifka¹⁶², A. Polini^{22a}, C. S. Pollard⁵⁵, V. Polychronakos²⁷, K. Pommès³², L. Pontecorvo^{134a}, B. G. Pope⁹³, G. A. Popeneciu^{28c}, D. S. Popovic¹⁴, A. Poppleton³², S. Pospisil¹³⁰, K. Potamianos¹⁶, I. N. Potrap⁶⁸, C. J. Potter³⁰, C. T. Potter¹¹⁸, G. Poulard³², J. Poveda³², V. Pozdnyakov⁶⁸, M. E. Pozo Astigarraga³², P. Pralavorio⁸⁸, A. Pranko¹⁶, S. Prell⁶⁷, D. Price⁸⁷, L. E. Price⁶, M. Primavera^{76a}, S. Prince⁹⁰, M. Proissl⁴⁸, K. Prokofiev^{63c}, F. Prokoshin^{34b}, S. Protopopescu²⁷, J. Proudfoot⁶, M. Przybycien^{40a}, D. Puddu^{136a,136b}, M. Purohit^{27,ak}, P. Puzo¹¹⁹, J. Qian⁹², G. Qin⁵⁵, Y. Qin⁸⁷, A. Quadt⁵⁶, W. B. Quayle^{167a,167b}, M. Queitsch-Maitland⁸⁷, D. Quilty⁵⁵, S. Raddum¹²¹, V. Radeka²⁷, V. Radescu^{61b}, S. K. Radhakrishnan¹⁵², P. Radloff¹¹⁸, P. Rados⁹¹, F. Ragusa^{94a,94b}, G. Rahal¹⁸¹, J. A. Raine⁸⁷, S. Rajagopalan²⁷, M. Rammensee³², C. Rangel-Smith¹⁶⁸, M. G. Ratti^{94a,94b}, F. Rauscher¹⁰², S. Rave⁸⁶, T. Ravenscroft⁵⁵, I. Ravinovich¹⁷⁵, M. Raymond³², A. L. Read¹²¹, N. P. Readioff⁷⁷, M. Reale^{76a,76b}, D. M. Rebuzzi^{123a,123b}, A. Redelbach¹⁷⁷, G. Redlinger²⁷, R. Reece¹³⁹, K. Reeves⁴³, L. Rehnisch¹⁷, J. Reichert¹²⁴, H. Reisig²⁹, C. Rembser³², H. Ren^{35a}, M. Rescigno^{134a}, S. Resconi^{94a}, O. L. Rezanova^{111,c}, P. Reznicek¹³¹, R. Rezvani⁹⁷, R. Richter¹⁰³, S. Richter⁸¹, E. Richter-Was^{40b}, O. Ricken²³, M. Ridel⁸³, P. Rieck¹⁷, C. J. Riegel¹⁷⁸, J. Rieger⁵⁶, O. Rifki¹¹⁵, M. Rijssenbeek¹⁵², A. Rimoldi^{123a,123b}, M. Rimoldi¹⁸, L. Rinaldi^{22a}, B. Ristić⁵¹, E. Ritsch³², I. Riu¹³, F. Rizatdinova¹¹⁶, E. Rizvi⁷⁹, C. Rizzi¹³, S. H. Robertson^{90,m}, A. Robichaud-Veronneau⁹⁰, D. Robinson³⁰, J. E. M. Robinson⁴⁴, A. Robson⁵⁵

C. Roda^{126a,126b}, Y. Rodina⁸⁸, A. Rodriguez Perez¹³, D. Rodriguez Rodriguez¹⁷⁰, S. Roe³², C. S. Rogan⁵⁹, O. Røhne¹²¹, A. Romaniouk¹⁰⁰, M. Romano^{22a,22b}, S. M. Romano Saez³⁶, E. Romero Adam¹⁷⁰, N. Rompotis¹⁴⁰, M. Ronzani⁵⁰, L. Roos⁸³, E. Ros¹⁷⁰, S. Rosati^{134a}, K. Rosbach⁵⁰, P. Rose¹³⁹, O. Rosenthal¹⁴⁵, N.-A. Rosien⁵⁶, V. Rossetti^{150a,150b}, E. Rossi^{106a,106b}, L. P. Rossi^{52a}, J. H. N. Rosten³⁰, R. Rosten¹⁴⁰, M. Rotaru^{28b}, I. Roth¹⁷⁵, J. Rothberg¹⁴⁰, D. Rousseau¹¹⁹, C. R. Royon¹³⁸, A. Rozanov⁸⁸, Y. Rozen¹⁵⁶, X. Ruan^{149c}, F. Rubbo¹⁴⁷, M. S. Rudolph¹⁶², F. Rühr⁵⁰, A. Ruiz-Martinez³¹, Z. Rurikova⁵⁰, N. A. Rusakovich⁶⁸, A. Ruschke¹⁰², H. L. Russell¹⁴⁰, J. P. Rutherford⁷, N. Ruthmann³², Y. F. Ryabov¹²⁵, M. Rybar¹⁶⁹, G. Rybkin¹¹⁹, S. Ryu⁶, A. Ryzhov¹³², G. F. Rzehorz⁵⁶, A. F. Saavedra¹⁵⁴, G. Sabato¹⁰⁹, S. Sacerdoti²⁹, H. F.-W. Sadrozinski¹³⁹, R. Sadykov⁶⁸, F. Safai Tehrani^{134a}, P. Saha¹¹⁰, M. Sahinsoy^{61a}, M. Saimpert¹³⁸, T. Saito¹⁵⁹, H. Sakamoto¹⁵⁹, Y. Sakurai¹⁷⁴, G. Salamanna^{136a,136b}, A. Salamon^{135a,135b}, J. E. Salazar Loyola^{34b}, D. Salek¹⁰⁹, P. H. Sales De Bruin¹⁴⁰, D. Salihagic¹⁰³, A. Salnikov¹⁴⁷, J. Salt¹⁷⁰, D. Salvatore^{39a,39b}, F. Salvatore¹⁵³, A. Salvucci^{63a}, A. Salzburger³², D. Sammel⁵⁰, D. Sampsonidis¹⁵⁸, A. Sanchez^{106a,106b}, J. Sánchez¹⁷⁰, V. Sanchez Martinez¹⁷⁰, H. Sandaker¹²¹, R. L. Sandbach⁷⁹, H. G. Sander⁸⁶, M. Sandhoff¹⁷⁸, C. Sandoval²¹, R. Sandstroem¹⁰³, D. P. C. Sankey¹³³, M. Sannino^{52a,52b}, A. Sansoni⁴⁹, C. Santoni³⁶, R. Santonico^{135a,135b}, H. Santos^{128a}, I. Santoyo Castillo¹⁵³, K. Sapp¹²⁷, A. Saproinov⁶⁸, J. G. Saraiva^{128a,128d}, B. Sarrazin²³, O. Sasaki⁶⁹, Y. Sasaki¹⁵⁹, K. Sato¹⁶⁴, G. Sauvage^{5,*}, E. Sauvan⁵, G. Savage⁸⁰, P. Savard^{162,d}, C. Sawyer¹³³, L. Sawyer^{82,r}, J. Saxon³³, C. Sbarra^{22a}, A. Sbrizzi^{22a,22b}, T. Scanlon⁸¹, D. A. Scannicchio¹⁶⁶, M. Scarcella¹⁵⁴, V. Scarfone^{39a,39b}, J. Schaarschmidt¹⁷⁵, P. Schacht¹⁰³, B. M. Schachtner¹⁰², D. Schaefer³², R. Schaefer⁴⁴, J. Schaeffer⁸⁶, S. Schaepe²³, S. Schaetzel^{61b}, U. Schäfer⁸⁶, A. C. Schaffer¹¹⁹, D. Schaile¹⁰², R. D. Schamberger¹⁵², V. Scharf^{61a}, V. A. Schegelsky¹²⁵, D. Scheirich¹³¹, M. Schernau¹⁶⁶, C. Schiavi^{52a,52b}, S. Schier¹³⁹, C. Schillo⁵⁰, M. Schioppa^{39a,39b}, S. Schlenker³², K. R. Schmidt-Sommerfeld¹⁰³, K. Schmieden³², C. Schmitt⁸⁶, S. Schmitt⁴⁴, S. Schmitz⁸⁶, B. Schneider^{163a}, U. Schnoor⁵⁰, L. Schoeffel¹³⁸, A. Schoening^{61b}, B. D. Schoenrock⁹³, E. Schopf²³, M. Schott⁸⁶, J. Schovancova⁸, S. Schramm⁵¹, M. Schreyer¹⁷⁷, N. Schuh⁸⁶, A. Schulte⁸⁶, M. J. Schultens²³, H.-C. Schultz-Coulon^{61a}, H. Schulz¹⁷, M. Schumacher⁵⁰, B. A. Schumm¹³⁹, Ph. Schune¹³⁸, A. Schwartzman¹⁴⁷, T. A. Schwarz⁹², Ph. Schwegler¹⁰³, H. Schweiger⁸⁷, Ph. Schwemling¹³⁸, R. Schwienhorst⁹³, J. Schwindling¹³⁸, T. Schwindt²³, G. Sciolla²⁵, F. Scuri^{126a,126b}, F. Scutti⁹¹, J. Searcy⁹², P. Seema²³, S. C. Seidel¹⁰⁷, A. Seiden¹³⁹, F. Seifert¹³⁰, J. M. Seixas^{26a}, G. Sekhniaidze^{106a}, K. Sekhon⁹², S. J. Sekula⁴², D. M. Seliverstov^{125,*}, N. Semprini-Cesari^{22a,22b}, C. Serfon¹²¹, L. Serin¹¹⁹, L. Serkin^{167a,167b}, M. Sessa^{136a,136b}, R. Seuster¹⁷², H. Severini¹¹⁵, T. Sfiligoi⁷⁸, F. Sforza³², A. Sfyrla⁵¹, E. Shabalina⁵⁶, N. W. Shaikh^{150a,150b}, L. Y. Shan^{35a}, R. Shang¹⁶⁹, J. T. Shank²⁴, M. Shapiro¹⁶, P. B. Shatalov⁹⁹, K. Shaw^{167a,167b}, S. M. Shaw⁸⁷, A. Shcherbakova^{150a,150b}, C. Y. Shehu¹⁵³, P. Sherwood⁸¹, L. Shi^{155,al}, S. Shimizu⁷⁰, C. O. Shimmin¹⁶⁶, M. Shimojima¹⁰⁴, M. Shiyakova^{68,am}, A. Shmeleva⁹⁸, D. Shoaleh Saadi⁹⁷, M. J. Shochet³³, S. Shojaii^{94a,94b}, S. Shrestha¹¹³, E. Shulga¹⁰⁰, M. A. Shupe⁷, P. Sicho¹²⁹, A. M. Sickles¹⁶⁹, P. E. Sidebo¹⁵¹, O. Sidiropoulou¹⁷⁷, D. Sidorov¹¹⁶, A. Sidoti^{22a,22b}, F. Siegert⁴⁶, Dj. Sijacki¹⁴, J. Silva^{128a,128d}, S. B. Silverstein^{150a}, V. Simak¹³⁰, O. Simard⁵, Lj. Simic¹⁴, S. Simion¹¹⁹, E. Simioni⁸⁶, B. Simmons⁸¹, D. Simon³⁶, M. Simon⁸⁶, P. Sinervo¹⁶², N. B. Sinev¹¹⁸, M. Sioli^{22a,22b}, G. Siragusa¹⁷⁷, S. Yu. Sivoklov¹⁰¹, J. Sjölin^{150a,150b}, M. B. Skinner⁷⁵, H. P. Skottowe⁵⁹, P. Skubic¹¹⁵, M. Slater¹⁹, T. Slavicek¹³⁰, M. Slawinska¹⁰⁹, K. Sliwa¹⁶⁵, R. Slovak¹³¹, V. Smakhtin¹⁷⁵, B. H. Smart⁵, L. Smestad¹⁵, J. Smiesko^{148a}, S. Yu. Smirnov¹⁰⁰, Y. Smirnov¹⁰⁰, L. N. Smirnova^{101,an}, O. Smirnova⁸⁴, M. N. K. Smith³⁷, R. W. Smith³⁷, M. Smizanska⁷⁵, K. Smolek¹³⁰, A. A. Snesarev⁹⁸, S. Snyder²⁷, R. Sobie^{172,m}, F. Socher⁴⁶, A. Soffer¹⁵⁷, D. A. Soh¹⁵⁵, G. Sokhrannyi⁷⁸, C. A. Solans Sanchez³², M. Solar¹³⁰, E. Yu. Soldatov¹⁰⁰, U. Soldevila¹⁷⁰, A. A. Solodkov¹³², A. Soloshenko⁶⁸, O. V. Solovyanov¹³², V. Solovyev¹²⁵, P. Sommer⁵⁰, H. Son¹⁶⁵, H. Y. Song^{60,ao}, A. Sood¹⁶, A. Sopczak¹³⁰, V. Sopko¹³⁰, V. Sorin¹³, D. Sosa^{61b}, C. L. Sotiropoulou^{126a,126b}, R. Soualah^{167a,167c}, A. M. Soukharev^{111,c}, D. South⁴⁴, B. C. Sowden⁸⁰, S. Spagnolo^{76a,76b}, M. Spalla^{126a,126b}, M. Spangenberg¹⁷³, F. Spanò⁸⁰, D. Sperlich¹⁷, F. Spettel¹⁰³, R. Spighi^{22a}, G. Spigo³², L. A. Spiller⁹¹, M. Spousta¹³¹, R. D. St. Denis^{55,*}, A. Stabile^{94a}, R. Stamen^{61a}, S. Stamm¹⁷, E. Stanecka⁴¹, R. W. Stanek⁶, C. Stancu^{136a}, M. Stancu-Bellu⁴⁴, M. M. Stanitzki⁴⁴, S. Stapnes¹²¹, E. A. Starchenko¹³², G. H. Stark³³, J. Stark⁵⁷, P. Staroba¹²⁹, P. Starovoitov^{61a}, S. Stärz³², R. Staszewski⁴¹, P. Steinberg²⁷, B. Stelzer¹⁴⁶, H. J. Stelzer³², O. Stelzer-Chilton^{163a}, H. Stenzel⁵⁴, G. A. Stewart⁵⁵, J. A. Stillings²³, M. C. Stockton⁹⁰, M. Stoebe⁹⁰, G. Stoica^{28b}, P. Stolte⁵⁶, S. Stonjek¹⁰³, A. R. Stradling⁸, A. Straessner⁴⁶, M. E. Stramaglia¹⁸, J. Strandberg¹⁵¹, S. Strandberg^{150a,150b}, A. Strandlie¹²¹, M. Strauss¹¹⁵, P. Strizenec^{148b}, R. Ströhmer¹⁷⁷, D. M. Strom¹¹⁸, R. Stroynowski⁴², A. Strubig¹⁰⁸, S. A. Stucci¹⁸, B. Stugu¹⁵, N. A. Styles⁴⁴, D. Su¹⁴⁷, J. Su¹²⁷, R. Subramaniam⁸², S. Suchek^{61a}, Y. Sugaya¹²⁰, M. Suk¹³⁰, V. V. Sulin⁹⁸, S. Sultansoy^{4c}, T. Sumida⁷¹, S. Sun⁵⁹, X. Sun^{35a}, J. E. Sundermann⁵⁰, K. Suruliz¹⁵³, G. Susinno^{39a,39b}, M. R. Sutton¹⁵³, S. Suzuki⁶⁹, M. Svatos¹²⁹, M. Swiatlowski³³, I. Sykora^{148a}, T. Sykora¹³¹, D. Ta⁵⁰, C. Taccini^{136a,136b}, K. Tackmann⁴⁴, J. Taenzer¹⁶², A. Taffard¹⁶⁶, R. Tafirout^{163a}, N. Taiblum¹⁵⁷, H. Takai²⁷, R. Takashima⁷², T. Takeshita¹⁴⁴, Y. Takubo⁶⁹, M. Talby⁸⁸, A. A. Talyshev^{111,c}, K. G. Tan⁹¹, J. Tanaka¹⁵⁹, R. Tanaka¹¹⁹, S. Tanaka⁶⁹, B. B. Tannenwald¹¹³, S. Tapia Araya^{34b}, S. Tapprogge⁸⁶, S. Tarem¹⁵⁶, G. F. Tartarelli^{94a}, P. Tas¹³¹, M. Tasevsky¹²⁹, T. Tashiro⁷¹, E. Tassi^{39a,39b}, A. Tavares Delgado^{128a,128b},

Y. Tayalati^{137d}, A. C. Taylor¹⁰⁷, G. N. Taylor⁹¹, P. T. E. Taylor⁹¹, W. Taylor^{163b}, F. A. Teischinger³², P. Teixeira-Dias⁸⁰, K. K. Temming⁵⁰, D. Temple¹⁴⁶, H. Ten Kate³², P. K. Teng¹⁵⁵, J. J. Teoh¹²⁰, F. Tepel¹⁷⁸, S. Terada⁶⁹, K. Terashi¹⁵⁹, J. Terron⁸⁵, S. Terzo¹⁰³, M. Testa⁴⁹, R. J. Teuscher^{162,m}, T. Theveneaux-Pelzer⁸⁸, J. P. Thomas¹⁹, J. Thomas-Wilsker⁸⁰, E. N. Thompson³⁷, P. D. Thompson¹⁹, A. S. Thompson⁵⁵, L. A. Thomsen¹⁷⁹, E. Thomson¹²⁴, M. Thomson³⁰, M. J. Tibbetts¹⁶, R. E. Ticse Torres⁸⁸, V. O. Tikhomirov^{98,ap}, Yu. A. Tikhonov^{111,c}, S. Timoshenko¹⁰⁰, P. Tipton¹⁷⁹, S. Tisserant⁸⁸, K. Todome¹⁶¹, T. Todorov^{5,*}, S. Todorova-Nova¹³¹, J. Tojo⁷³, S. Tokár^{148a}, K. Tokushuku⁶⁹, E. Tolley⁵⁹, L. Tomlinson⁸⁷, M. Tomoto¹⁰⁵, L. Tompkins^{147,aq}, K. Toms¹⁰⁷, B. Tong⁵⁹, E. Torrence¹¹⁸, H. Torres¹⁴⁶, E. Torró Pastor¹⁴⁰, J. Toth^{88,ar}, F. Touchard⁸⁸, D. R. Tovey¹⁴³, T. Trefzger¹⁷⁷, A. Tricoli²⁷, I. M. Trigger^{163a}, S. Trincas-Duvoid⁸³, M. F. Tripiana¹³, W. Trischuk¹⁶², B. Trocmé⁵⁷, A. Trofymov⁴⁴, C. Troncon^{94a}, M. Trotter-McDonald¹⁶, M. Trovatelli¹⁷², L. Truong^{167a,167c}, M. Trzebinski⁴¹, A. Trzupek⁴¹, J. C.-L. Tseng¹²², P. V. Tsiarehka⁹⁵, G. Tsipolitis¹⁰, N. Tsirintanis⁹, S. Tsiskaridze¹³, V. Tsiskaridze⁵⁰, E. G. Tskhadadze^{53a}, K. M. Tsui^{63a}, I. I. Tsukerman⁹⁹, V. Tsulaia¹⁶, S. Tsuno⁶⁹, D. Tsybychev¹⁵², A. Tudorache^{28b}, V. Tudorache^{28b}, A. N. Tuna⁵⁹, S. A. Tupputi^{22a,22b}, S. Turchikhin^{101,an}, D. Turecek¹³⁰, D. Turgeman¹⁷⁵, R. Turra^{94a,94b}, A. J. Turvey⁴², P. M. Tuts³⁷, M. Tyndel¹³³, G. Uccchielli^{22a,22b}, I. Ueda¹⁵⁹, M. Ughetto^{150a,150b}, F. Ukegawa¹⁶⁴, G. Unal³², A. Undrus²⁷, G. Unel¹⁶⁶, F. C. Ungaro⁹¹, Y. Unno⁶⁹, C. Unverdorben¹⁰², J. Urban^{148b}, P. Urquijo⁹¹, P. Urrejola⁸⁶, G. Usai⁸, A. Usanova⁶⁵, L. Vacavant⁸⁸, V. Vacek¹³⁰, B. Vachon⁹⁰, C. Valderanis¹⁰², E. Valdes Santurio^{150a,150b}, N. Valencic¹⁰⁹, S. Valentinetti^{22a,22b}, A. Valero¹⁷⁰, L. Valery¹³, S. Valkar¹³¹, S. Vallecorsa⁵¹, J. A. Valls Ferrer¹⁷⁰, W. Van Den Wollenberg¹⁰⁹, P. C. Van Der Deijl¹⁰⁹, R. van der Geer¹⁰⁹, H. van der Graaf¹⁰⁹, N. van Eldik¹⁵⁶, P. van Gemmeren⁶, J. Van Nieuwkoop¹⁴⁶, I. van Vulpen¹⁰⁹, M. C. van Woerden³², M. Vanadia^{134a,134b}, W. Vandelli³², R. Vanguri¹²⁴, A. Vaniachine^{6,k}, P. Vankov¹⁰⁹, G. Vardanyan¹⁸⁰, R. Vari^{134a}, E. W. Varnes⁷, T. Varol⁴², D. Varouchas⁸³, A. Vartapetian⁸, K. E. Varvell¹⁵⁴, J. G. Vasquez¹⁷⁹, F. Vazeille³⁶, T. Vazquez Schroeder⁹⁰, J. Veatch⁵⁶, L. M. Veloce¹⁶², F. Veloso^{128a,128c}, S. Veneziano^{134a}, A. Ventura^{76a,76b}, M. Venturi¹⁷², N. Venturi¹⁶², A. Venturini²⁵, V. Vercesi^{123a}, M. Verducci^{134a,134b}, W. Verkerke¹⁰⁹, J. C. Vermeulen¹⁰⁹, A. Vest^{46,as}, M. C. Vetterli^{146,d}, O. Viazlo⁸⁴, I. Vichou^{169,*}, T. Vickey¹⁴³, O. E. Vickey Boeriu¹⁴³, G. H. A. Viehhauser¹²², S. Viel¹⁶, L. Vigani¹²², R. Vigne⁶⁵, M. Villa^{22a,22b}, M. Villaplana Perez^{94a,94b}, E. Vilucchi⁴⁹, M. G. Vincet³¹, V. B. Vinogradov⁶⁸, C. Vittori^{22a,22b}, I. Vivarelli¹⁵³, S. Vlachos¹⁰, M. Vlasak¹³⁰, M. Vogel¹⁷⁸, P. Vokac¹³⁰, G. Volpi^{126a,126b}, M. Volpi⁹¹, H. von der Schmitt¹⁰³, E. von Toerne²³, V. Vorobel¹³¹, K. Vorobev¹⁰⁰, M. Vos¹⁷⁰, R. Voss³², J. H. Vosseveld⁷⁷, N. Vranjes¹⁴, M. Vranjes Milosavljevic¹⁴, V. Vrba¹²⁹, M. Vreeswijk¹⁰⁹, R. Vuillermet³², I. Vukotic³³, Z. Vykydal¹³⁰, P. Wagner²³, W. Wagner¹⁷⁸, H. Wahlberg⁷⁴, S. Wahrmund⁴⁶, J. Wakabayashi¹⁰⁵, J. Walder⁷⁵, R. Walker¹⁰², W. Walkowiak¹⁴⁵, V. Wallangen^{150a,150b}, C. Wang^{35b}, C. Wang^{141,88}, F. Wang¹⁷⁶, H. Wang¹⁶, H. Wang⁴², J. Wang⁴⁴, J. Wang¹⁵⁴, K. Wang⁹⁰, R. Wang⁶, S. M. Wang¹⁵⁵, T. Wang²³, T. Wang³⁷, W. Wang⁶⁰, X. Wang¹⁷⁹, C. Wanotayaroj¹¹⁸, A. Warburton⁹⁰, C. P. Ward³⁰, D. R. Wardrope⁸¹, A. Washbrook⁴⁸, P. M. Watkins¹⁹, A. T. Watson¹⁹, M. F. Watson¹⁹, G. Watts¹⁴⁰, S. Watts⁸⁷, B. M. Waugh⁸¹, S. Webb⁸⁶, M. S. Weber¹⁸, S. W. Weber¹⁷⁷, J. S. Webster⁶, A. R. Weidberg¹²², B. Weinert⁶⁴, J. Weingarten⁵⁶, C. Weiser⁵⁰, H. Weits¹⁰⁹, P. S. Wells³², T. Wenaus²⁷, T. Wengler³², S. Wenig³², N. Vermes²³, M. Werner⁵⁰, M. D. Werner⁶⁷, P. Werner³², M. Wessels^{61a}, J. Wetter¹⁶⁵, K. Whalen¹¹⁸, N. L. Whallon¹⁴⁰, A. M. Wharton⁷⁵, A. White⁸, M. J. White¹, R. White^{34b}, D. Whiteson¹⁶⁶, F. J. Wickens¹³³, W. Wiedenmann¹⁷⁶, M. WIELERS¹³³, P. Wienemann²³, C. Wiglesworth³⁸, L. A. M. Wiik-Fuchs²³, A. Wildauer¹⁰³, F. Wilk⁸⁷, H. G. Wilkens³², H. H. Williams¹²⁴, S. Williams¹⁰⁹, C. Willis⁹³, S. Willocq⁸⁹, J. A. Wilson¹⁹, I. Wingerter-Seez⁵, F. Winklmeier¹¹⁸, O. J. Winston¹⁵³, B. T. Winter²³, M. Wittgen¹⁴⁷, J. Wittkowski¹⁰², M. W. Wolter⁴¹, H. Wolters^{128a,128c}, S. D. Worm¹³³, B. K. Wosiek⁴¹, J. Wotschack³², M. J. Woudstra⁸⁷, K. W. Wozniak⁴¹, M. Wu⁵⁷, M. Wu³³, S. L. Wu¹⁷⁶, X. Wu⁵¹, Y. Wu⁹², T. R. Wyatt⁸⁷, B. M. Wynne⁴⁸, S. Xella³⁸, D. Xu^{35a}, L. Xu²⁷, B. Yabsley¹⁵⁴, S. Yacoub^{149a}, R. Yakabe⁷⁰, D. Yamaguchi¹⁶¹, Y. Yamaguchi¹²⁰, A. Yamamoto⁶⁹, S. Yamamoto¹⁵⁹, T. Yamanaka¹⁵⁹, K. Yamauchi¹⁰⁵, Y. Yamazaki⁷⁰, Z. Yan²⁴, H. Yang¹⁴², H. Yang¹⁷⁶, Y. Yang¹⁵⁵, Z. Yang¹⁵, W.-M. Yao¹⁶, Y. C. Yap⁸³, Y. Yasu⁶⁹, E. Yatsenko⁵, K. H. Yau Wong²³, J. Ye⁴², S. Ye²⁷, I. Yeletsikh⁶⁸, A. L. Yen⁵⁹, E. Yildirim⁸⁶, K. Yorita¹⁷⁴, R. Yoshida⁶, K. Yoshihara¹²⁴, C. Young¹⁴⁷, C. J. S. Young³², S. Youssef²⁴, D. R. Yu¹⁶, J. Yu⁸, J. M. Yu⁹², J. Yu⁶⁷, L. Yuan⁷⁰, S. P. Y. Yuen²³, I. Yusuff^{30,at}, B. Zabinski⁴¹, R. Zaidan¹⁴¹, A. M. Zaitsev^{132,af}, N. Zakharuk⁴⁴, J. Zalieckas¹⁵, A. Zaman¹⁵², S. Zambito⁵⁹, L. Zanello^{134a,134b}, D. Zanzi⁹¹, C. Zeitnitz¹⁷⁸, M. Zeman¹³⁰, A. Zemla^{40a}, J. C. Zeng¹⁶⁹, Q. Zeng¹⁴⁷, K. Zengel²⁵, O. Zenin¹³², T. Ženiš^{148a}, D. Zerwas¹¹⁹, D. Zhang⁹², F. Zhang¹⁷⁶, G. Zhang^{60,ao}, H. Zhang^{35b}, J. Zhang⁶, L. Zhang⁵⁰, R. Zhang²³, R. Zhang^{60,au}, X. Zhang¹⁴¹, Z. Zhang¹¹⁹, X. Zhao⁴², Y. Zhao¹⁴¹, Z. Zhao⁶⁰, A. Zhemchugov⁶⁸, J. Zhong¹²², B. Zhou⁹², C. Zhou⁴⁷, L. Zhou³⁷, L. Zhou⁴², M. Zhou¹⁵², N. Zhou^{35c}, C. G. Zhu¹⁴¹, H. Zhu^{35a}, J. Zhu⁹², Y. Zhu⁶⁰, X. Zhuang^{35a}, K. Zhukov⁹⁸, A. Zibell¹⁷⁷, D. Zieminska⁶⁴, N. I. Zimine⁶⁸, C. Zimmermann⁸⁶, S. Zimmermann⁵⁰, Z. Zinonos⁵⁶, M. Zinser⁸⁶, M. Ziolkowski¹⁴⁵, L. Živković¹⁴, G. Zobernig¹⁷⁶, A. Zoccoli^{22a,22b}, M. zur Nedden¹⁷, L. Zwalinski³²

- ¹ Department of Physics, University of Adelaide, Adelaide, SA, Australia
- ² Physics Department, SUNY Albany, Albany, NY, USA
- ³ Department of Physics, University of Alberta, Edmonton, AB, Canada
- ⁴ (a) Department of Physics, Ankara University, Ankara, Turkey; (b) Istanbul Aydin University, Istanbul, Turkey; (c) Division of Physics, TOBB University of Economics and Technology, Ankara, Turkey
- ⁵ LAPP, CNRS/IN2P3 and Université Savoie Mont Blanc, Annecy-le-Vieux, France
- ⁶ High Energy Physics Division, Argonne National Laboratory, Argonne, IL, USA
- ⁷ Department of Physics, University of Arizona, Tucson, AZ, USA
- ⁸ Department of Physics, The University of Texas at Arlington, Arlington, TX, USA
- ⁹ Physics Department, University of Athens, Athens, Greece
- ¹⁰ Physics Department, National Technical University of Athens, Zografou, Greece
- ¹¹ Department of Physics, The University of Texas at Austin, Austin, TX, USA
- ¹² Institute of Physics, Azerbaijan Academy of Sciences, Baku, Azerbaijan
- ¹³ Institut de Física d'Altes Energies (IFAE), The Barcelona Institute of Science and Technology, Barcelona, Spain
- ¹⁴ Institute of Physics, University of Belgrade, Belgrade, Serbia
- ¹⁵ Department for Physics and Technology, University of Bergen, Bergen, Norway
- ¹⁶ Physics Division, Lawrence Berkeley National Laboratory and University of California, Berkeley, CA, USA
- ¹⁷ Department of Physics, Humboldt University, Berlin, Germany
- ¹⁸ Albert Einstein Center for Fundamental Physics and Laboratory for High Energy Physics, University of Bern, Bern, Switzerland
- ¹⁹ School of Physics and Astronomy, University of Birmingham, Birmingham, UK
- ²⁰ (a) Department of Physics, Bogazici University, Istanbul, Turkey; (b) Department of Physics Engineering, Gaziantep University, Gaziantep, Turkey; (c) Istanbul Bilgi University, Faculty of Engineering and Natural Sciences, Istanbul, Turkey; (d) Bahcesehir University, Faculty of Engineering and Natural Sciences, Istanbul, Turkey
- ²¹ Centro de Investigaciones, Universidad Antonio Narino, Bogota, Colombia
- ²² (a) INFN Sezione di Bologna, Bologna, Italy; (b) Dipartimento di Fisica e Astronomia, Università di Bologna, Bologna, Italy
- ²³ Physikalisches Institut, University of Bonn, Bonn, Germany
- ²⁴ Department of Physics, Boston University, Boston, MA, USA
- ²⁵ Department of Physics, Brandeis University, Waltham, MA, USA
- ²⁶ (a) Universidade Federal do Rio De Janeiro COPPE/EE/IF, Rio de Janeiro, Brazil; (b) Electrical Circuits Department, Federal University of Juiz de Fora (UFJF), Juiz de Fora, Brazil; (c) Federal University of Sao Joao del Rei (UFSJ), Sao Joao del Rei, Brazil; (d) Instituto de Fisica, Universidade de Sao Paulo, Sao Paulo, Brazil
- ²⁷ Physics Department, Brookhaven National Laboratory, Upton, NY, USA
- ²⁸ (a) Transilvania University of Brasov, Brasov, Romania; (b) National Institute of Physics and Nuclear Engineering, Bucharest, Romania; (c) Physics Department, National Institute for Research and Development of Isotopic and Molecular Technologies, Cluj Napoca, Romania; (d) University Politehnica Bucharest, Bucharest, Romania; (e) West University in Timisoara, Timisoara, Romania
- ²⁹ Departamento de Física, Universidad de Buenos Aires, Buenos Aires, Argentina
- ³⁰ Cavendish Laboratory, University of Cambridge, Cambridge, UK
- ³¹ Department of Physics, Carleton University, Ottawa, ON, Canada
- ³² CERN, Geneva, Switzerland
- ³³ Enrico Fermi Institute, University of Chicago, Chicago, IL, USA
- ³⁴ (a) Departamento de Física, Pontificia Universidad Católica de Chile, Santiago, Chile; (b) Departamento de Física, Universidad Técnica Federico Santa María, Valparaiso, Chile
- ³⁵ (a) Institute of High Energy Physics, Chinese Academy of Sciences, Beijing, China; (b) Department of Physics, Nanjing University, Jiangsu, China; (c) Physics Department, Tsinghua University, Beijing 100084, China
- ³⁶ Laboratoire de Physique Corpusculaire, Clermont Université and Université Blaise Pascal and CNRS/IN2P3, Clermont-Ferrand, France
- ³⁷ Nevis Laboratory, Columbia University, Irvington, NY, USA
- ³⁸ Niels Bohr Institute, University of Copenhagen, Copenhagen, Denmark
- ³⁹ (a) INFN Gruppo Collegato di Cosenza, Laboratori Nazionali di Frascati, Frascati, Italy; (b) Dipartimento di Fisica, Università della Calabria, Rende, Italy

- 40 (a) Faculty of Physics and Applied Computer Science, AGH University of Science and Technology, Krakow, Poland; (b) Marian Smoluchowski Institute of Physics, Jagiellonian University, Krakow, Poland
- 41 Institute of Nuclear Physics, Polish Academy of Sciences, Krakow, Poland
- 42 Physics Department, Southern Methodist University, Dallas, TX, USA
- 43 Physics Department, University of Texas at Dallas, Richardson, TX, USA
- 44 DESY, Hamburg and Zeuthen, Germany
- 45 Lehrstuhl für Experimentelle Physik IV, Technische Universität Dortmund, Dortmund, Germany
- 46 Institut für Kern- und Teilchenphysik, Technische Universität Dresden, Dresden, Germany
- 47 Department of Physics, Duke University, Durham, NC, USA
- 48 SUPA-School of Physics and Astronomy, University of Edinburgh, Edinburgh, UK
- 49 INFN Laboratori Nazionali di Frascati, Frascati, Italy
- 50 Fakultät für Mathematik und Physik, Albert-Ludwigs-Universität, Freiburg, Germany
- 51 Section de Physique, Université de Genève, Geneva, Switzerland
- 52 (a) INFN Sezione di Genova, Genoa, Italy; (b) Dipartimento di Fisica, Università di Genova, Genoa, Italy
- 53 (a) E. Andronikashvili Institute of Physics, Iv. Javakhishvili Tbilisi State University, Tbilisi, Georgia; (b) High Energy Physics Institute, Tbilisi State University, Tbilisi, Georgia
- 54 II Physikalisches Institut, Justus-Liebig-Universität Giessen, Giessen, Germany
- 55 SUPA-School of Physics and Astronomy, University of Glasgow, Glasgow, UK
- 56 II Physikalisches Institut, Georg-August-Universität, Göttingen, Germany
- 57 Laboratoire de Physique Subatomique et de Cosmologie, Université Grenoble-Alpes, CNRS/IN2P3, Grenoble, France
- 58 Department of Physics, Hampton University, Hampton, VA, USA
- 59 Laboratory for Particle Physics and Cosmology, Harvard University, Cambridge, MA, USA
- 60 Department of Modern Physics, University of Science and Technology of China, Anhui, China
- 61 (a) Kirchhoff-Institut für Physik, Ruprecht-Karls-Universität Heidelberg, Heidelberg, Germany; (b) Physikalisches Institut, Ruprecht-Karls-Universität Heidelberg, Heidelberg, Germany; (c) ZITI Institut für technische Informatik, Ruprecht-Karls-Universität Heidelberg, Mannheim, Germany
- 62 Faculty of Applied Information Science, Hiroshima Institute of Technology, Hiroshima, Japan
- 63 (a) Department of Physics, The Chinese University of Hong Kong, Shatin, NT, Hong Kong; (b) Department of Physics, The University of Hong Kong, Hong Kong, China; (c) Department of Physics, The Hong Kong University of Science and Technology, Clear Water Bay, Kowloon, Hong Kong, China
- 64 Department of Physics, Indiana University, Bloomington, IN, USA
- 65 Institut für Astro- und Teilchenphysik, Leopold-Franzens-Universität, Innsbruck, Austria
- 66 University of Iowa, Iowa City, IA, USA
- 67 Department of Physics and Astronomy, Iowa State University, Ames, IA, USA
- 68 Joint Institute for Nuclear Research, JINR Dubna, Dubna, Russia
- 69 KEK, High Energy Accelerator Research Organization, Tsukuba, Japan
- 70 Graduate School of Science, Kobe University, Kobe, Japan
- 71 Faculty of Science, Kyoto University, Kyoto, Japan
- 72 Kyoto University of Education, Kyoto, Japan
- 73 Department of Physics, Kyushu University, Fukuoka, Japan
- 74 Instituto de Física La Plata, Universidad Nacional de La Plata and CONICET, La Plata, Argentina
- 75 Physics Department, Lancaster University, Lancaster, UK
- 76 (a) INFN Sezione di Lecce, Lecce, Italy; (b) Dipartimento di Matematica e Fisica, Università del Salento, Lecce, Italy
- 77 Oliver Lodge Laboratory, University of Liverpool, Liverpool, UK
- 78 Department of Physics, Jožef Stefan Institute and University of Ljubljana, Ljubljana, Slovenia
- 79 School of Physics and Astronomy, Queen Mary University of London, London, UK
- 80 Department of Physics, Royal Holloway University of London, Surrey, UK
- 81 Department of Physics and Astronomy, University College London, London, UK
- 82 Louisiana Tech University, Ruston, LA, USA
- 83 Laboratoire de Physique Nucléaire et de Hautes Energies, UPMC and Université Paris-Diderot and CNRS/IN2P3, Paris, France
- 84 Fysiska institutionen, Lunds universitet, Lund, Sweden
- 85 Departamento de Física Teórica C-15, Universidad Autónoma de Madrid, Madrid, Spain

- ⁸⁶ Institut für Physik, Universität Mainz, Mainz, Germany
- ⁸⁷ School of Physics and Astronomy, University of Manchester, Manchester, UK
- ⁸⁸ CPPM, Aix-Marseille Université and CNRS/IN2P3, Marseille, France
- ⁸⁹ Department of Physics, University of Massachusetts, Amherst, MA, USA
- ⁹⁰ Department of Physics, McGill University, Montreal, QC, Canada
- ⁹¹ School of Physics, University of Melbourne, Melbourne, VIC, Australia
- ⁹² Department of Physics, The University of Michigan, Ann Arbor, MI, USA
- ⁹³ Department of Physics and Astronomy, Michigan State University, East Lansing, MI, USA
- ⁹⁴ ^(a)INFN Sezione di Milano, Milan, Italy; ^(b)Dipartimento di Fisica, Università di Milano, Milan, Italy
- ⁹⁵ B.I. Stepanov Institute of Physics, National Academy of Sciences of Belarus, Minsk, Republic of Belarus
- ⁹⁶ National Scientific and Educational Centre for Particle and High Energy Physics, Minsk, Republic of Belarus
- ⁹⁷ Group of Particle Physics, University of Montreal, Montreal, QC, Canada
- ⁹⁸ P.N. Lebedev Physical Institute of the Russian Academy of Sciences, Moscow, Russia
- ⁹⁹ Institute for Theoretical and Experimental Physics (ITEP), Moscow, Russia
- ¹⁰⁰ National Research Nuclear University MEPhI, Moscow, Russia
- ¹⁰¹ D.V. Skobeltsyn Institute of Nuclear Physics, M.V. Lomonosov Moscow State University, Moscow, Russia
- ¹⁰² Fakultät für Physik, Ludwig-Maximilians-Universität München, München, Germany
- ¹⁰³ Max-Planck-Institut für Physik (Werner-Heisenberg-Institut), München, Germany
- ¹⁰⁴ Nagasaki Institute of Applied Science, Nagasaki, Japan
- ¹⁰⁵ Graduate School of Science and Kobayashi-Maskawa Institute, Nagoya University, Nagoya, Japan
- ¹⁰⁶ ^(a)INFN Sezione di Napoli, Naples, Italy; ^(b)Dipartimento di Fisica, Università di Napoli, Naples, Italy
- ¹⁰⁷ Department of Physics and Astronomy, University of New Mexico, Albuquerque, NM, USA
- ¹⁰⁸ Institute for Mathematics, Astrophysics and Particle Physics, Radboud University Nijmegen/Nikhef, Nijmegen, The Netherlands
- ¹⁰⁹ Nikhef National Institute for Subatomic Physics and University of Amsterdam, Amsterdam, The Netherlands
- ¹¹⁰ Department of Physics, Northern Illinois University, DeKalb, IL, USA
- ¹¹¹ Budker Institute of Nuclear Physics, SB RAS, Novosibirsk, Russia
- ¹¹² Department of Physics, New York University, New York, NY, USA
- ¹¹³ Ohio State University, Columbus, OH, USA
- ¹¹⁴ Faculty of Science, Okayama University, Okayama, Japan
- ¹¹⁵ Homer L. Dodge Department of Physics and Astronomy, University of Oklahoma, Norman, OK, USA
- ¹¹⁶ Department of Physics, Oklahoma State University, Stillwater, OK, USA
- ¹¹⁷ Palacký University, RCPTM, Olomouc, Czech Republic
- ¹¹⁸ Center for High Energy Physics, University of Oregon, Eugene, OR, USA
- ¹¹⁹ LAL, Univ. Paris-Sud, CNRS/IN2P3, Université Paris-Saclay, Orsay, France
- ¹²⁰ Graduate School of Science, Osaka University, Osaka, Japan
- ¹²¹ Department of Physics, University of Oslo, Oslo, Norway
- ¹²² Department of Physics, Oxford University, Oxford, UK
- ¹²³ ^(a)INFN Sezione di Pavia, Pavia, Italy; ^(b)Dipartimento di Fisica, Università di Pavia, Pavia, Italy
- ¹²⁴ Department of Physics, University of Pennsylvania, Philadelphia, PA, USA
- ¹²⁵ National Research Centre “Kurchatov Institute” B.P.Konstantinov Petersburg Nuclear Physics Institute, St. Petersburg, Russia
- ¹²⁶ ^(a)INFN Sezione di Pisa, Pisa, Italy; ^(b)Dipartimento di Fisica E. Fermi, Università di Pisa, Pisa, Italy
- ¹²⁷ Department of Physics and Astronomy, University of Pittsburgh, Pittsburgh, PA, USA
- ¹²⁸ ^(a)Laboratório de Instrumentação e Física Experimental de Partículas -LIP, Lisbon, Portugal; ^(b)Faculdade de Ciências, Universidade de Lisboa, Lisbon, Portugal; ^(c)Department of Physics, University of Coimbra, Coimbra, Portugal; ^(d)Centro de Física Nuclear da Universidade de Lisboa, Lisbon, Portugal; ^(e)Departamento de Física, Universidade do Minho, Braga, Portugal; ^(f)Departamento de Física Teórica y del Cosmos and CAFPE, Universidad de Granada, Granada, Spain; ^(g)Dep Física and CEFITEC of Faculdade de Ciências e Tecnologia, Universidade Nova de Lisboa, Caparica, Portugal
- ¹²⁹ Institute of Physics, Academy of Sciences of the Czech Republic, Prague, Czech Republic
- ¹³⁰ Czech Technical University in Prague, Prague, Czech Republic
- ¹³¹ Faculty of Mathematics and Physics, Charles University in Prague, Prague, Czech Republic

- 132 State Research Center Institute for High Energy Physics (Protvino), NRC KI, Russia
- 133 Particle Physics Department, Rutherford Appleton Laboratory, Didcot, UK
- 134 (a) INFN Sezione di Roma, Rome, Italy; (b) Dipartimento di Fisica, Sapienza Università di Roma, Rome, Italy
- 135 (a) INFN Sezione di Roma Tor Vergata, Rome, Italy; (b) Dipartimento di Fisica, Università di Roma Tor Vergata, Rome, Italy
- 136 (a) INFN Sezione di Roma Tre, Rome, Italy; (b) Dipartimento di Matematica e Fisica, Università Roma Tre, Rome, Italy
- 137 (a) Faculté des Sciences Ain Chock, Réseau Universitaire de Physique des Hautes Energies-Université Hassan II, Casablanca, Morocco; (b) Centre National de l'Energie des Sciences Techniques Nucleaires, Rabat, Morocco; (c) Faculté des Sciences Semlalia, Université Cadi Ayyad, LPHEA-Marrakech, Marrakech, Morocco; (d) Faculté des Sciences, Université Mohamed Premier and LPTPM, Oujda, Morocco; (e) Faculté des Sciences, Université Mohammed V, Rabat, Morocco
- 138 DSM/IRFU (Institut de Recherches sur les Lois Fondamentales de l'Univers), CEA Saclay (Commissariat à l'Energie Atomique et aux Energies Alternatives), Gif-sur-Yvette, France
- 139 Santa Cruz Institute for Particle Physics, University of California Santa Cruz, Santa Cruz, CA, USA
- 140 Department of Physics, University of Washington, Seattle, WA, USA
- 141 School of Physics, Shandong University, Shandong, China
- 142 Department of Physics and Astronomy, Shanghai Key Laboratory for Particle Physics and Cosmology, Shanghai Jiao Tong University, (also affiliated with PKU-CHEP), Shanghai, China
- 143 Department of Physics and Astronomy, University of Sheffield, Sheffield, UK
- 144 Department of Physics, Shinshu University, Nagano, Japan
- 145 Fachbereich Physik, Universität Siegen, Siegen, Germany
- 146 Department of Physics, Simon Fraser University, Burnaby, BC, Canada
- 147 SLAC National Accelerator Laboratory, Stanford, CA, USA
- 148 (a) Faculty of Mathematics, Physics and Informatics, Comenius University, Bratislava, Slovak Republic; (b) Department of Subnuclear Physics, Institute of Experimental Physics of the Slovak Academy of Sciences, Kosice, Slovak Republic
- 149 (a) Department of Physics, University of Cape Town, Cape Town, South Africa; (b) Department of Physics, University of Johannesburg, Johannesburg, South Africa; (c) School of Physics, University of the Witwatersrand, Johannesburg, South Africa
- 150 (a) Department of Physics, Stockholm University, Stockholm, Sweden; (b) The Oskar Klein Centre, Stockholm, Sweden
- 151 Physics Department, Royal Institute of Technology, Stockholm, Sweden
- 152 Departments of Physics and Astronomy and Chemistry, Stony Brook University, Stony Brook, NY, USA
- 153 Department of Physics and Astronomy, University of Sussex, Brighton, UK
- 154 School of Physics, University of Sydney, Sydney, NSW, Australia
- 155 Institute of Physics, Academia Sinica, Taipei, Taiwan
- 156 Department of Physics, Technion: Israel Institute of Technology, Haifa, Israel
- 157 Raymond and Beverly Sackler School of Physics and Astronomy, Tel Aviv University, Tel Aviv, Israel
- 158 Department of Physics, Aristotle University of Thessaloniki, Thessaloniki, Greece
- 159 International Center for Elementary Particle Physics and Department of Physics, The University of Tokyo, Tokyo, Japan
- 160 Graduate School of Science and Technology, Tokyo Metropolitan University, Tokyo, Japan
- 161 Department of Physics, Tokyo Institute of Technology, Tokyo, Japan
- 162 Department of Physics, University of Toronto, Toronto, ON, Canada
- 163 (a) TRIUMF, Vancouver, BC, Canada; (b) Department of Physics and Astronomy, York University, Toronto, ON, Canada
- 164 Faculty of Pure and Applied Sciences, and Center for Integrated Research in Fundamental Science and Engineering, University of Tsukuba, Tsukuba, Japan
- 165 Department of Physics and Astronomy, Tufts University, Medford, MA, USA
- 166 Department of Physics and Astronomy, University of California Irvine, Irvine, CA, USA
- 167 (a) INFN Gruppo Collegato di Udine, Sezione di Trieste, Udine, Italy; (b) ICTP, Trieste, Italy; (c) Dipartimento di Chimica Fisica e Ambiente, Università di Udine, Udine, Italy
- 168 Department of Physics and Astronomy, University of Uppsala, Uppsala, Sweden
- 169 Department of Physics, University of Illinois, Urbana, IL, USA
- 170 Instituto de Física Corpuscular (IFIC) and Departamento de Física Atomica, Molecular y Nuclear and Departamento de Ingeniería Electrónica and Instituto de Microelectrónica de Barcelona (IMB-CNM), University of Valencia and CSIC, Valencia, Spain

- 171 Department of Physics, University of British Columbia, Vancouver, BC, Canada
 - 172 Department of Physics and Astronomy, University of Victoria, Victoria, BC, Canada
 - 173 Department of Physics, University of Warwick, Coventry, UK
 - 174 Waseda University, Tokyo, Japan
 - 175 Department of Particle Physics, The Weizmann Institute of Science, Rehovot, Israel
 - 176 Department of Physics, University of Wisconsin, Madison, WI, USA
 - 177 Fakultät für Physik und Astronomie, Julius-Maximilians-Universität, Würzburg, Germany
 - 178 Fakultät für Mathematik und Naturwissenschaften, Fachgruppe Physik, Bergische Universität Wuppertal, Wuppertal, Germany
 - 179 Department of Physics, Yale University, New Haven, CT, USA
 - 180 Yerevan Physics Institute, Yerevan, Armenia
 - 181 Centre de Calcul de l'Institut National de Physique Nucléaire et de Physique des Particules (IN2P3), Villeurbanne, France
- ^a Also at Department of Physics, King's College London, London, United Kingdom
- ^b Also at Institute of Physics, Azerbaijan Academy of Sciences, Baku, Azerbaijan
- ^c Also at Novosibirsk State University, Novosibirsk, Russia
- ^d Also at TRIUMF, Vancouver BC, Canada
- ^e Also at Department of Physics and Astronomy, University of Louisville, Louisville, KY, USA
- ^f Also at Physics Department, An-Najah National University, Nablus, Palestine
- ^g Also at Department of Physics, California State University, Fresno, CA, USA
- ^h Also at Department of Physics, University of Fribourg, Fribourg, Switzerland
- ⁱ Also at Departament de Física de la Universitat Autònoma de Barcelona, Barcelona, Spain
- ^j Also at Departamento de Física e Astronomia, Faculdade de Ciências, Universidade do Porto, Porto, Portugal
- ^k Also at Tomsk State University, Tomsk, Russia
- ^l Also at Università di Napoli Parthenope, Napoli, Italy
- ^m Also at Institute of Particle Physics (IPP), Victoria, BC, Canada
- ⁿ Also at National Institute of Physics and Nuclear Engineering, Bucharest, Romania
- ^o Also at Department of Physics, St. Petersburg State Polytechnical University, St. Petersburg, Russia
- ^p Also at Department of Physics, The University of Michigan, Ann Arbor, MI, USA
- ^q Also at Centre for High Performance Computing, CSIR Campus, Rosebank, Cape Town, South Africa
- ^r Also at Louisiana Tech University, Ruston, LA, USA
- ^s Also at Institutio Catalana de Recerca i Estudis Avancats, ICREA, Barcelona, Spain
- ^t Also at Graduate School of Science, Osaka University, Osaka, Japan
- ^u Also at Department of Physics, National Tsing Hua University, Hsinchu, Taiwan
- ^v Also at Institute for Mathematics, Astrophysics and Particle Physics, Radboud University Nijmegen/Nikhef, Nijmegen, Netherlands
- ^w Also at Department of Physics, The University of Texas at Austin, Austin TX, USA
- ^x Also at CERN, Geneva, Switzerland
- ^y Also at Georgian Technical University (GTU), Tbilisi, Georgia
- ^z Also at Ochadai Academic Production, Ochanomizu University, Tokyo, Japan
- ^{aa} Also at Manhattan College, New York NY, USA
- ^{ab} Also at Hellenic Open University, Patras, Greece
- ^{ac} Also at Academia Sinica Grid Computing, Institute of Physics, Academia Sinica, Taipei, Taiwan
- ^{ad} Also at School of Physics, Shandong University, Shandong, China
- ^{ae} Also at Department of Physics, California State University, Sacramento CA, USA
- ^{af} Also at Moscow Institute of Physics and Technology State University, Dolgoprudny, Russia
- ^{ag} Also at Section de Physique, Université de Genève, Geneva, Switzerland
- ^{ah} Also at Eotvos Lorand University, Budapest, Hungary
- ^{ai} Also at Departments of Physics and Astronomy and Chemistry, Stony Brook University, Stony Brook NY, USA
- ^{aj} Also at International School for Advanced Studies (SISSA), Trieste, Italy
- ^{ak} Also at Department of Physics and Astronomy, University of South Carolina, Columbia SC, USA
- ^{al} Also at School of Physics and Engineering, Sun Yat-sen University, Guangzhou, China

- ^{am} Also at Institute for Nuclear Research and Nuclear Energy (INRNE) of the Bulgarian Academy of Sciences, Sofia, Bulgaria
- ^{an} Also at Faculty of Physics, M.V.Lomonosov Moscow State University, Moscow, Russia
- ^{ao} Also at Institute of Physics, Academia Sinica, Taipei, Taiwan
- ^{ap} Also at National Research Nuclear University MEPhI, Moscow, Russia
- ^{aq} Also at Department of Physics, Stanford University, Stanford CA, USA
- ^{ar} Also at Institute for Particle and Nuclear Physics, Wigner Research Centre for Physics, Budapest, Hungary
- ^{as} Also at Flensburg University of Applied Sciences, Flensburg, Germany
- ^{at} Also at University of Malaya, Department of Physics, Kuala Lumpur, Malaysia
- ^{au} Also at CPPM, Aix-Marseille Université and CNRS/IN2P3, Marseille, France
- * Deceased